Evaluation of a botulinum neurotoxin chimera containing two SNAP-25 cleaving proteases for anti-nociceptive activity in rodent pain models

Thesis submitted for the degree

of

Master of Science by Research

By

John Nealon, B.Sc.

Supervised by

Prof. J. Oliver Dolly

Co-supervised by

Dr Tom Zurawski and Dr Gary Lawrence

International Centre for Neurotherapeutics
School of Biotechnology
Dublin City University Ireland

January 2019

Declaration:

I hereby certify that this material, which I now submit for assessment on the programme of study leading to the award of a Master of Science is entirely my own work, and that I have exercised reasonable care to ensure that the work is original, and does not to the best of my knowledge breach any law of copyright, and has not been taken from the work of others save and to the extent that such work has been cited and acknowledged within the text of my work.

Signed: _____ (John Nealon) ID No: 14212971

Date: _____

Acknowledgements:

I would like to thank my supervisor, Professor J. Oliver Dolly, for offering me this opportunity and his constant support throughout my research.

I want to especially thank my co-supervisors Drs Tom Zurawski and Gary Lawrence for their constant support throughout the research process.

I also wish to offer my sincere thanks to my colleagues at the ICNT including Drs Marc Nugent and Orla Moriarty for their advice and assistance in seeing my thesis through to the end.

I would like to thank all the members of the ICNT, past and present, who made my experience such a warm and memorable one, particular thanks to Drs Laura Casals, Seshu Kumar Kaza, Om Prakash Edupuganti, Jiafu Wang, Jianghui Meng, Minghong Tang, Antonios Dougalis, Chunxu Shan, Manuel Yamil Yusef Robles, Miss Ciara Larkin and Aoife Connelly.

To my parents, Sean and Mary Nealon, and my brothers, Mark and Adam who always believed in me and helped me see the light at the end of the tunnel.

Finally, I want to thank Science Foundation Ireland who funded my research project.

Abbreviations used

4-AP: 4-Aminopyridine

5-HT: Serotonin

AMPA: α-Amino-3-hydroxy-5-methyl-4-isoxazolepropionic acid

AMPAR: α-Amino-3-hydroxy-5-methyl-4-isoxazolepropionic acid receptor

ASIC: Acid sensing ion channel

ATP: Adenosine tri-phosphate

BoNT: Botulinum neurotoxin

BoNT/A: Botulinum neurotoxin serotype A

BoNT/E: Botulinum neurotoxin serotype E

BoTIM/A: BoNT/A with inactive light chain A

BSA: Bovine serum albumin

Ca^{2+}: Calcium

CFA: Complete Freund's adjuvant

CGRP: Calcitonin gene related peptide

CNS: Central nervous system

COX: Cyclooxygenase

DAS: Digit abduction score

DOR: Delta opioid receptors

DRG: Dorsal root ganglion

ECL: Enhanced chemiluminescence

GABA: γ-Aminobutyric acid

gp130: Glycoprotein 130

HC: Heavy chain

Hc: Binding domain

H_N: Translocation domain

HPRA: Health Products Regulatory Authority

HRP: Horseradish peroxidase

HSA: Human serum albumin

IASP: International Association for the Study of Pain

IgG: Immunoglobulin G

IL-1β: Interleukin 1 beta

IL-6: Interleukin 6

JAK: Janus kinase

L4/L5: Lumbar 4/5

LC: Light chain

LC/A: Light chain A

LC/E: Light chain E

LD_{50}: Lethal dose

LDCV: Large dense core vesicles

LDS: Lithium dodecyl sulfate

MAPK: Mitogen activated protein kinases

MaxTD: Maximum tolerated dose

MOR: μ opioid receptor

MRC-5: Medical Research Council cell strain 5

Na_V: Voltage gated sodium channel

NE: Norepinephrine

NGF: Nerve growth factor

NK1: Neurokinin 1

NMDA: N-Methyl-D-aspartate

NMDAR: N-Methyl-D-aspartate receptor

NPY: Neuropeptide Y

NRT: Nocifensive response threshold

NSAID: Non-steroidal anti-inflammatory drug

O.C.T: Optimal cutting temperature

PAM: Pressure application measurement

PGE2: Prostaglandin E2

PGI2: Prostaglandin I2

PHN: Post-herpetic neuralgia

PI3K: Phosphoinositide 3 kinase

PKC: Protein kinase C

PLC: Phospholipase C

PNS: Peripheral nervous system

PVDF: Polyvinylidene fluoride

PWT: Paw withdrawal threshold

SDS-PAGE: Sodium dodecyl sulfate – polyacrylamide gel electrophoresis

SNAP-25: Synaptosomal-associated protein 25

$SNAP\text{-}25_A$: LC/A cleaved synaptosomal-associated protein 25 (amino acid residues 1-197)

$SNAP\text{-}25_E$: LC/E cleaved synaptosomal-associated protein 25 (amino acid residues 1 – 180)

SNARE: Soluble N-ethylmaleimide-sensitive factor attachment protein receptor

SNI: Spared nerve injury

SP: Substance P

Src: Proto-oncogene tyrosine-protein kinase Src

SSNRI: Selective serotonin re-uptake inhibitor

STAT: Signal transducer and activator of transcription proteins

STT: Spinothalamic tract

SV2: Synaptic vesicle protein 2

TBS: Tris buffered saline

TCA: Tricyclic anti-depressant

TGN: Trigeminal ganglia

TNFα: Tumour necrosis factor alpha

TrkA: Tropomyosin receptor kinase A

TRPA1: Transient receptor potential ankyrin 1

TRPV1: Transient receptor potential vanilloid 1

TTX-R: Tetrodotoxin resistant receptor

VAMP: Vesicle-associated membrane protein

VIP: Vasoactive intestinal peptide

Vzv: Varicella zoster virus

WHO: World health organisation

Publications and presentations

Peer-reviewed article:

Jiafu Wang, Laura Casals-Diaz, Tomas Zurawski, Jianghui Meng, Orla Moriarty, John Nealon, Om Prakash Edupuganti, Oliver Dolly., A novel therapeutic with two SNAP-25 inactivating proteases shows long-lasting anti-hyperalgesic activity in a rat model of neuropathic pain, Neuropharmacology, Volume 118, 15 May 2017, Pages 223-232

Abstract:

J. Oliver Dolly, Jianghui Meng, Laura Casals-Diaz, Omprakash Edupuganti, Tomas Zurawski, Charles Metais, John Nealon, Gary Lawrence and Jiafu Wang. EnSNAREing transduction of chronic pain with botulinum neurotoxins. 9th Neuroscience Ireland conference, 2015. International Centre for Neurotherapeutics, Dublin City University, Dublin 9, Ireland.

Poster:

J. Nealon, L. Casals-Diaz, C. Metais, J. Meng, J. Wang, T. Zurawski, J. O. Dolly. Mechanical hyper-sensitivity in a rat model of neuropathic pain is alleviated by a bio-therapeutic derived from two botulinum neurotoxins. IASP 16th World congress on pain, 2016. International Centre for Neurotherapeutics, Dublin City University, Dublin 9, Ireland.

Table of Contents

Table of figures

List of tables

Abstract

Thesis title: Evaluation of a botulinum neurotoxin chimera containing two SNAP-25 cleaving proteases for anti-nociceptive activity in rodent neuropathic and inflammatory pain models

Author: John Nealon

Botulinum neurotoxin A (BoNT/A), a 150 kDa di-chain protein produced by *Clostridium botulinum,* is used to treat chronic pain. It inhibits neuronal exocytosis by cleaving synaptosomal-associated protein 25 (SNAP-25) with its light chain protease (LC/A). The LC of serotype BoNT/E (LC/E) cleaves 17 more residues from SNAP-25 than LC/A; *in vitro* results have shown that unlike LC/A, the more extensive cleavage of SNAP-25 by LC/E prevents capsaicin-induced release of the pain mediating neuropeptide calcitonin gene-related peptide (CGRP). By attaching LC/E to BoNT/A, the short half-life of LC/E is extended to match BoNT/A, resulting in a chimera with potentially greater anti-nociceptive capabilities than BoNT/A. In the rat spared nerve injury (SNI) model of neuropathic pain, injections of LC/E-BoNT/A showed greater alleviation of mechanical pain than BoNT/A or LC/E-BoTIM/A, a BoNT/A and LC/E chimera with an inactive LC/A. Unfortunately, intra-articular knee injections of LC/E-BoNT/A or BoNT/A induced confounding muscle paralysis, even at doses tolerated for intra-plantar injections; therefore, it was not feasible to inject enough neurotoxin to relieve symptoms of an inflammatory knee pain model. Injections of LC/E-BoNT/A prior to induction of nocifensive behaviours in the capsaicin or formalin models, resulted in more striking anti-nociceptive effects than BoNT/A pre-injections. LC/E-BoNT/A reduced formalin-induced phase I flinching behaviour and was comparable to sub-cutaneous buprenorphine treatment in relieving capsaicin-induced lifting/licking behaviours and heat hypersensitivity. However, these observations were inconsistent between batches of BoNTs produced; results from an *in vitro* substrate cleavage assay and *in vivo* dose escalation studies indicated activity loss of LC/E-BoNT/A over long-term storage, explaining some of the inconsistencies in anti-nociceptive effects. A fresh batch of LC/E-BoNT/A demonstrated anti-nociceptive effects in the capsaicin and SNI model, but further symptoms of systemic toxicity than the previous batch.

Chapter 1 - Introduction

Nociception and pain

Pain is a complex and subjective experience which can evoke unpleasant physical and emotional responses, and thus serves a protective role against injury. This is highlighted by its definition according to the International Association for the Study of Pain (IASP) as "an unpleasant sensory and emotional experience associated with actual or potential tissue damage or described in terms of such damage". These potentially/actually damaging tissue events are termed "noxious stimuli" and nociception is the "neural coding of noxious stimuli" (Loeser et al., 2011). The repercussions from a lack of pain sensation are best exemplified by the sufferers of congenital insensitivity to pain, a disease in which patients retain normal sensory responses (e.g. light touch perception and detection of differences in temperature) but feel no pain in response to noxious stimuli, and thus sustain unknown injuries. Complications of this condition include self-mutilation from the ages 0-4 from biting of the tongue and mouth, frequent bruises and cuts, and histories of unreported fractures (Drenth and Waxman, 2007). While pain normally serves a self-protective role and is necessary for one's well-being, it can become maladaptive and persist beyond recovery from the initial injury, despite the lack of a noxious stimulus. Chronic pain, generally defined as pain lasting or recurring for more than 3-6 months, is a worldwide problem that affects an estimated 20% of the general population (Merskey et al., 1994, Goldberg and McGee, 2011). Chronic pain is often associated with pathologies such as chronic inflammation (e.g. rheumatoid arthritis) but can also be neuropathic (e.g. diabetic neuropathy), or idiopathic in nature (e.g. chronic primary pain) (Treede et al., 2015). Symptoms of these conditions include spontaneously occurring pain and hypersensitisation to stimuli (Cervero and Laird, 1996), including hyperalgesia (heightened pain from a noxious stimuli) or allodynia (pain from a previously innocuous stimuli) (Loeser et al., 2011). Some chronic pain symptoms correlate directly with disease progression e.g. rheumatoid arthritis (Jansen et al., 2001), yet other chronic pain diseases show abnormal changes in the mechanisms of

physiological pain detection that persist past wound healing e.g. phantom limb pain (Vaso et al., 2014, Flor et al., 2006).

Physiological pain process

The process of physiological pain detection can be broadly summarised in the following stages: transduction of the noxious stimulus, transmission, modulation, projection and perception (Fig. 1.1 A). Noxious stimuli (mechanical, temperature or chemical) activate transducers such as transient receptor potential vanilloid 1 (TRPV1 – responds to temperatures of 43 °C) or transient receptor potential ankyrin 1, (TRPA1 – responds to mustard oil binding) on the terminals of high threshold sensory neurons termed nociceptors, found in the peripheral nervous system (PNS). Once activated, these receptors transduce the stimuli into action potentials which are transmitted by unmyelinated C- and/or thinly myelinated Aδ nociceptors to the cell body in the dorsal root ganglion (DRG), then continuing on the nociceptor's central axon to the dorsal horn of the spinal cord (Muir and Woolf, 2001). Heavily myelinated, low-threshold Aβ fibres were originally believed to transmit only non-noxious signals, but research has found a population of Aβ fibres which transmit nocifensive signals (Djouhri and Lawson, 2004). The generation and propagation of these action potentials relies heavily on voltage gated sodium channels (Na_v), which are highly expressed on nociceptors (Toledo-Aral et al., 1997, Djouhri et al., 2003). The C-fibres terminate in lamina I and II of the dorsal horn while the Aδ nociceptors terminate at lamina I and V, and Aβ fibres terminate in lamina III and IV (Fig. 1.1 B). Here, the central terminals of the nociceptors release glutamate, activating α-amino-3-hydroxy-5-methyl-4-isoxazolepropionic acid receptors (AMPAR) causing excitatory postsynaptic currents in the second order dorsal horn neurons which are modulated by interneurons and descending innervation as depicted in Fig. 1.1 C (Basbaum et al., 2009, Todd, 2010). Projection neurons carry these signals to the brain stem, then thalamus via ascending pathways such as the spinothalamic and spinoreticulothalamic tracts. It is believed that the thalamus is responsible for processing poorly localised pain. Nocifensive action potentials are propagated towards the cortical structures such as the somatosensory cortex and adjacent cortical

areas, for processing of the original location and intensity of the incoming pain signal (Basbaum et al., 2009, Muir and Woolf, 2001).

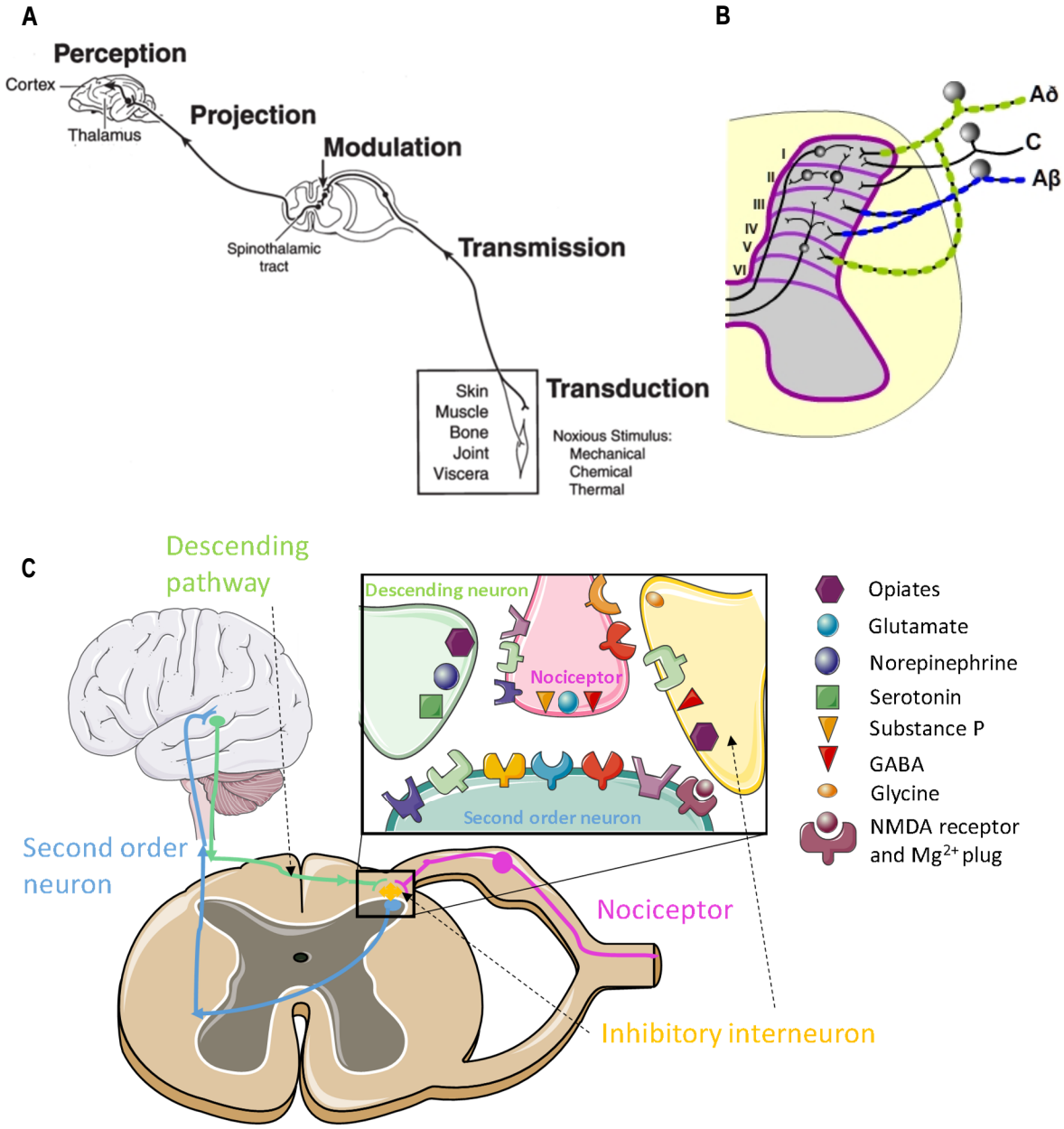

Fig. 1.1 Anatomical outline of physiological pain and spinal modulation of nociception (A) Noxious stimuli are transduced into action potentials by nociceptors and transmitted along axons, to the DRG and then dorsal horn for modulation. The modified signal is projected to the brain where it is perceived as pain (Muir and Woolf, 2001). **(B)** Thinly myelinated nociceptors called Aδ fibres terminate in lamina I and V of the dorsal horn. Unmyelinated C-fibres terminate in lamina I-II, both Aδ and C fibres respond to noxious stimuli and are nociceptors. Heavily myelinated non-nocifensive or nocifensive Aβ fibres pain terminate in lamina III-IV (Woolf and Mannion, 1999). **(C)** Incoming action potentials induce depolarisation of the presynaptic terminal and exocytosis of pain-inducing neurotransmitters such as glutamate or sensitising neuropeptides such as substance P. Release of endogenous opioids, monoamines (e.g. serotonin) or inhibitory neurotransmitters (e.g. glycine) from descending innervation and inhibitory interneurons can modulate the release of excitatory neurotransmitters in the dorsal horn, by binding to their respective receptors on the primary afferent, or second-order neurons which transport the nociceptive signal to the brain. **(A)** taken from (Muir and Woolf, 2001), **(B)** taken from (RnCeus.com), **(C)** adapted from (RnCeus.com).

Acute pain and the transition to chronic pain

Acute pain is typically defined as pain that is present for less than 3 months, with subacute pain being a subset of this that persists for more than 6 weeks but less than 3 months (King, 2013). These pain states differ from chronic pain in that they are expected to recover with the associated injury (Richardson and Vasko, 2002), while chronic pain is recognised as "pain that persists past normal healing time" (Treede et al., 2015). Interestingly, overlapping mechanisms (discussed below) have been identified in acute and chronic pain, exemplified by the fact that high levels of unmanageable acute and subacute pain after traumatic injuries or surgical procedures are risk factors for the development of chronic pain (Lavand'homme, 2011, Pozek et al., 2016). That said, the mechanisms behind the transition from acute to chronic pain, and how chronic pain is maintained in the absence of injury are not fully understood.

Peripheral sensitisation

Following tissue injury, nociceptors innervating the wound become more responsive and demonstrate reduced thresholds to stimuli, via a process called peripheral sensitisation (Loeser et al., 2011). As a result, the affected area becomes hypersensitive to both noxious and innocuous stimuli prompting guarded behaviour from the victim, thus allowing the wound to heal without further aggravation (Costigan et al., 2009). The release of pro-inflammatory and pro-algesic mediators (discussed in more detail below) by non-neuronal and damaged cells at the injury site (known as the "inflammatory soup"), drives peripheral sensitisation through excitation of nociceptors to cause spontaneous pain and/or by sensitising the neurons to noxious stimuli, via receptor augmentation or upregulation (Kidd and Urban, 2001).

Tissue injury results in the release of adenosine tri-phosphate (ATP), protons and glutamate from damaged cells into the extracellular space (Amaya et al., 2013), while kininogen present in the plasma is enzymatically activated to produce bradykinin (Tiffany and Burch, 1989). Mast cells located near primary afferent nociceptors degranulate and release histamine, serotonin (5-HT),

nerve growth factor (NGF) and pro-inflammatory cytokines, including tumour necrosis factor (TNFα), interleukin 6 (IL-6), and IL-1β (Raoof et al., 2018, Chatterjea and Martinov, 2015). Some of these molecules such as bradykinin bind to their receptor to depolarise the nociceptor and initiate a noxious action potential (Liu et al., 2010); other inflammatory soup components sensitise the nociceptor to stimuli. For example, injections of 5-HT induce profound hyperalgesia to heat. This is mediated by 5-HT binding to 5-HT2A, a G-protein coupled receptor found on TRPV1 expressing nociceptors, which activates the second messenger phospholipase C (PLC) and phosphokinase C (PKC) pathways causing phosphorylation, and thus augmentation of the TRPV1 receptor, mediating heat hyperalgesia (Loyd et al., 2011, Tokunaga et al., 1998, Sugiuar et al., 2004, Raymond et al., 2001). Many of these above-mentioned mediators can elicit both excitatory currents in the nociceptor via ionotropic receptors and initiate mechanisms of sensitisation via binding to metabotropic receptors. For a list of the different components of the inflammatory soup that target nociceptors and their mechanisms of action, please refer to Table 1.1 and Fig. 1.2.

A number of these molecules such as bradykinin and 5-HT further drive the inflammatory process. Bradykinin acts as a potent vasodilator and increases blood vessel permeability, thus promoting monocyte and neutrophil infiltration (Milner and Dohert, 2015). 5-HT can attract neutrophils to the injury via platelet aggregation (Duerschmied et al., 2013), while platelets also release 5-HT and histamine into the inflammatory soup (Li et al., 2007, Mannaioni et al., 1993, Cerrito et al., 1993). Monocytes and neutrophils are also attracted to the injury by the release of chemokines and complement components at the initial injury (Velnar et al., 2009). Recruited monocytes are converted to inflammatory macrophages, which release pro-inflammatory cytokines (TNFα, IL-1β, etc.) into the inflammatory soup, maintaining hypersensitisation (Table 1.1) (Lavin and Merad, 2013, Zhang and An, 2007).

IL-1β and bradykinin can induce synthesis of prostaglandins in several cell types (neurons, neutrophils and macrophages) (Pinho-Ribeiro et al., 2017, Supowit et al., 2011). Prostaglandins are derivatives of arachidonic acid and are synthesised by cyclooxygenase 1 and 2 (COX-1 and COX-2),

COX-2 is not expressed in peripheral tissues until upregulated by inflammatory cytokines such as IL-1β and TNFα (Bakhle and Botting, 1996, Lee et al., 2009, Ke et al., 2007). Prostaglandin E2 and I1 (PGE2 and PGI2) are the most studied prostaglandins in peripheral sensitisation (Milner and Dohert, 2015). PGE2 binding to EP1 or EP4 receptors can induce nociceptor hypersensitivity by modifying TRPV1, as summarised in Table 1.1.

Nearly all the pain/inflammatory mediators described thus far, can induce the release of neuropeptides calcitonin gene-related peptide (CGRP) or Substance P (SP), or augment the release of said peptides from nociceptors (Table 1.1, Fig. 1.2). CGRP and SP are pro-inflammatory neuropeptides, with peripheral release of CGRP causing vasodilation (Brain et al., 1985), and SP inducing plasma extravasation (Lembeck and Holzer, 1979), driving the inflammatory process at the injury. SP can also bind to mast cells, inducing release of histamine (Johnson and Erdos, 1973) and increased TNFα expression (Ansel et al., 1993). This release of inflammatory mediators from neurons is called “neurogenic inflammation”.

It is clear that the mechanisms of peripheral sensitisation can become a self-fulfilling cycle, if not managed through normal wound healing mechanisms or pharmacological interventions. Release of inflammatory mediators such as bradykinin at the initial insult drive inflammatory cell infiltration and hypersensitisation, while nociceptors release neuropeptides such as SP in response, promoting immune cell infiltration and upregulation of pro-inflammatory cytokines such as TNF in mast cells. Sustained activation of nociceptors along with augmentation and upregulation of ligand-gated and voltage-gated channels, result in increased firing of action potentials by nociceptors and their heightened sensitivity to stimuli (Pinho-Ribeiro et al., 2017). This increase of nocifensive signalling leads to the process of central sensitisation discussed below.

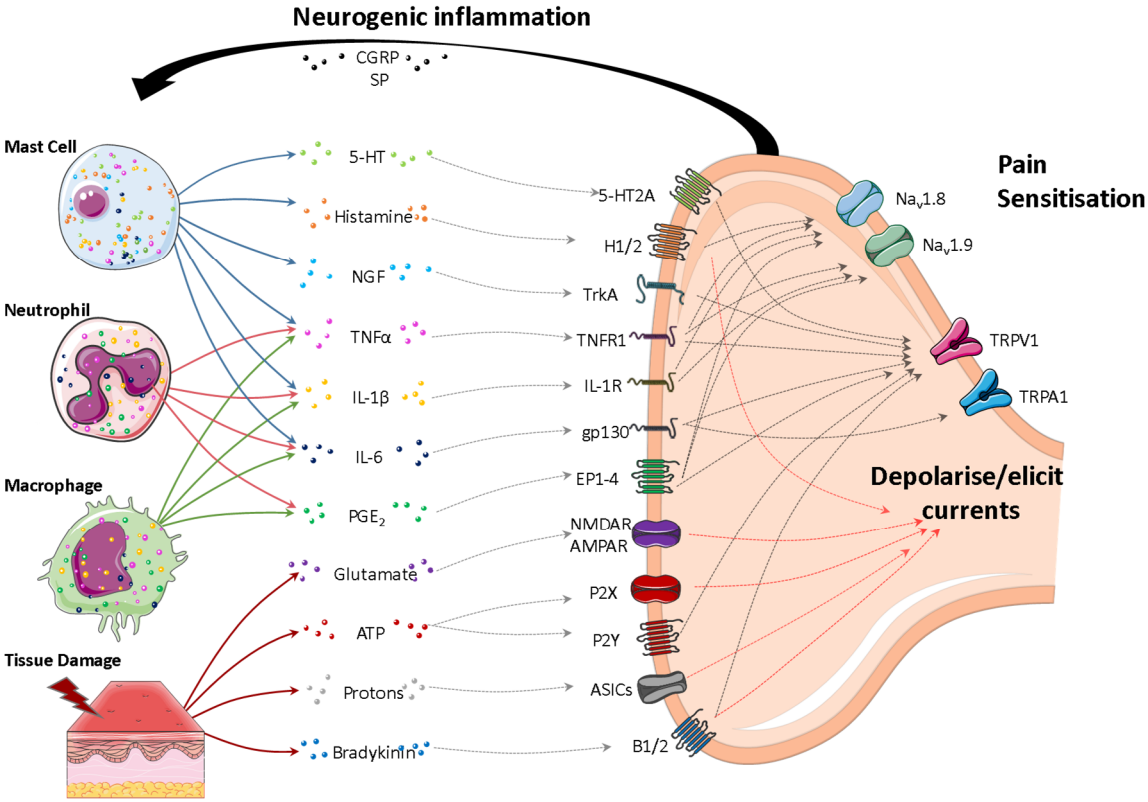

Fig. 1.2 Components of the inflammatory soup, source of their release and neuronal targets Pro-inflammatory and pro-algesic mediators activate and sensitise the nociceptor via voltage or ligand gated channel augmentation or upregulation, driving inflammation-induced pain. Activation of the nociceptor by the above mediators induces the release of neuropeptides CGRP and SP, which activate local inflammatory cells and recruit immune cell infiltration. Adapted from (Pinho-Ribeiro et al., 2017). H1/2 – Histamine receptors 1 & 2, TrkA - Tropomyosin receptor kinase A, TNFR1 – TNF receptor 1, IL-1R – IL-1β receptor, gp130 – glycoprotein 130, NMDAR - N-methyl-D-aspartate receptor, P2X/Y – ATP receptors, ASIC – acid-sensing ion channel, B1/2 – Bradykinin receptors 1 and 2.

MOLECULE	RECEPTOR	DEPOLARISE/ELICIT CURRENTS TOWARDS DRG	SENSITISE NOCICEPTOR (HYPERALGESIA, ALLODYNIA)	INDUCE OR AUGMENT RELEASE OF CGRP OR SP	REFERENCES
Bradykinin	B1 & B2	Yes	Activation of B2 receptors sensitises TRPV1 receptors heat and chemical stimuli via PKC and PLC pathways.	Direct release of neuropeptides and augments evoked release of neuropeptides	(Wang et al., 2006, Rohacs et al., 2008, Richardson and Vasko, 2002)
Serotonin	5-HT3 & 5-HT2A	Unclear	Induces heat hyperalgesia, most likely through phosphorylation of TRPV1 via PLC/PKC pathways post 5-HT2A activation.	Unclear	(Milner and Dohert, 2015, Loyd et al., 2013, Richardson and Vasko, 2002)
ATP	P2X and P2Y	Yes	Induces heat hyperalgesia, most likely through phosphorylation of TRPV1 via PLC/PKC pathways post P2Y activation.	Augments evoked release of neuropeptides	(Milner and Dohert, 2015, Tominaga et al., 2001, Richardson and Vasko, 2002)
Glutamate	AMPAR, NMDAR, Kainate receptor	Yes	Intra-plantar injections of glutamate induce symptoms of sensitisation, but mechanisms are unclear. Increased expression of glutamate receptors in inflamed rat hind-paws have been detected.	Unclear	(Amaya et al., 2013, Gold and Gebhart, 2010, Richardson and Vasko, 2002, Carlton and Coggeshall, 1999)
Protons	ASICs and TRPV1	Yes	Exposure to acidic environment allows for proton-induced TRPV1 activation at temperatures below 43 °C	Direct release of neuropeptides	(Tominaga et al., 1998, Richardson and Vasko, 2002)
Histamine	H1 & H2	Yes	Upregulates Na_V 1.8 expression post H2 activation.	No	(Pinho-Ribeiro et al., 2017, Gábor Jancsó, 2009)
TNFα	TNFR1 & TNFR2	No	TNFR1 activation modulates TTX-R via p38 MAPK. TRPV1 is upregulated and modulated in a p38/MAP kinase and PKC dependent fashion.	Augments evoked release of neuropeptides	(Pinho-Ribeiro et al., 2017, Jin and Gereau, 2006, Constantin et al., 2008, Richardson and Vasko, 2002)
IL-1β	IL1R	No	Sensitise TTX-R in a p38 MAPK dependent fashion	Augments evoked release of neuropeptides	(Pinho-Ribeiro et al., 2017, Binshtok et al., 2008, Richardson and Vasko, 2002)
IL-6	gp130	No	Activation of gp130 induces JAK/STAT dependent upregulation of TRPV1 and TRPA1	Augments evoked release of neuropeptides	(Pinho-Ribeiro et al., 2017, Fang et al., 2015, Malsch et al., 2014, Richardson and Vasko, 2002)
NGF	TrkA	No	TrkA activation causes p38 MAPK dependent upregulation of TRPV1 TrkA activates PI3K/Src kinase signalling, leading to phosphorylation and rapid membrane insertion of TRPV1	Augments evoked release of neuropeptides	(Amaya et al., 2013, Ji et al., 2002, Zhang et al., 2005, Richardson and Vasko, 2002)
PGE2	EP1,2 &4	No	Sensitise TRPV1 and TTX-R via PKA and PKC pathway, post activation of EP1, 2 or EP4 receptors.	Augments evoked release of neuropeptides	(Kawabata, 2011, Richardson and Vasko, 2002)

Table 1.1 Summary of mediators of the inflammatory soup and their actions on nociceptors p38 MAPK - p38 mitogen-activated protein kinases, JAK – Janus kinases, STAT – signal transducer and activator of transcription proteins, PI3K – phosphoinositide 3-kinase, TTX-R - Tetrodotoxin resistant sodium channels (Na_V 1.8 or 1.9 are most commonly affected in peripheral sensitisation).

Central sensitisation

Central sensitisation is the process by which neurons of the CNS become hyper-excitable, resulting in amplified processing of nociceptive signals, or nociceptive processing of sub-threshold signals (e.g. those from low-threshold Aβ fibres) (Basbaum et al., 2009, Loeser et al., 2011). The mechanisms of this are numerous, complex and not fully understood, and so this review will focus on the activity-dependent mechanisms of central sensitisation restricted to the spinal cord. Central sensitisation is initiated by intense and repetitive noxious signals to the CNS, typically originating from the increased activity of peripherally sensitised nociceptors (Milner and Dohert, 2015). Once a noxious action potential reaches the central terminal of the nociceptor in the dorsal horn, release of glutamate, SP and CGRP is induced. Glutamate binding to AMPAR evokes a fast (milliseconds) excitatory postsynaptic potential (EPSP) while SP binding to neurokinin 1 receptors (NK1) induces slow (seconds) depolarising currents (Millan, 1999, Murase and Randic, 1984). CGRP is often co-localised with SP (Schaible, 2007, Aline Boer et al., 2005, Ma et al., 2001, Ribeiro-da-Silva, 1995) and upon release binds to CGRP1 receptors; the release of CGRP seems to potentiate the action of SP (Oku et al., 1987) and inhibit its degradation (Le Greves et al., 1985). Greater release of SP and CGRP due to increased peripheral activity results in a cumulative depolarisation induced by temporal summation of NK1 and CGRP1 mediated slow synaptic potentials; this results in the phenomenon of action potential "wind-up" (Latremoliere and Woolf, 2009, Budai and Larson, 1996). This is characterised by gradual increases in action-potential discharges per each successive stimuli (Mendell and Wall, 1965). Wind-up facilitates the activation of NMDAR in the dorsal horn, which under normal conditions is inactive due to a Mg^{2+} plug in the channel pore; the increased depolarisation of the membrane mediated by wind-up forces the Mg^{2+} from the NMDAR pore, allowing its activation by glutamate released from nociceptor pre-synaptic terminals (Mayer et al., 1984, Thompson et al., 1990). This step is vital in initiating the process of central sensitisation (Woolf and Thompson, 1991).

The inward current of Ca^{2+} resulting from the opening of NMDARs increases the levels of intracellular Ca^{2+}, activating Ca^{2+} dependent kinases, which phosphorylate NMDARs and AMPARs. Phosphorylation of these receptors not only alters their sensitivity but their trafficking to plasma-membrane, increasing dorsal horn excitability to primary nocifensive input (Carvalho et al., 2000, Chen and Roche, 2007, Lau and Zukin, 2007, Latremoliere and Woolf, 2009). Activation of intracellular kinase pathways responsible for phosphorylation of glutamate receptors, such as the PKC pathway, is also mediated by postsynaptic CGRP1 activation (Sun et al., 2004) and tropomyosin receptor kinase B (TrkA) activation by brain derived neurotrophic factor (BDNF) release, which is increased by CGRP (Buldyrev et al., 2006). Inhibitory neurons at the spinal cord typically modulate nocifensive signals through the release of inhibitory neurotransmitters, gamma-Aminobutyric acid (GABA) and glycine. During central sensitisation, the activation of kinase pathways such as the PKC pathway prevents GABA and glycine mediated inhibition of nocifensive signals to spinothalamic tract (STT) neurons (Lin et al., 1996). This disinhibition results in increased excitation of dorsal horn neurons to non-nociceptive Aβ fibre input (Baba et al., 2003). Together these changes in dorsal horn excitability and inhibition result in ascending tracts propagating a greater degree of nocifensive signals from the hyper excitable dorsal horn neurons. These activity-dependent changes are induced rapidly (within seconds) and dissipate within minutes to hours of cessation of nociceptive input, depending on the length and intensity of the original stimulus (Latremoliere and Woolf, 2009). If heightened nociceptive activity is maintained, however, further transcription dependent mechanisms of central sensitisation serve to maintain long-lasting pathological forms of central sensitisation.

Inflammatory pain

Diseases of chronic inflammatory pain are strongly driven by peripheral sensitisation, with common treatment responses being based on the use of non-steroidal anti-inflammatory drugs (NSAID) which inhibit COX enzymes and the formation of prostaglandins (Kidd and Urban, 2001). Efforts to fully understand the peripheral disease mechanisms of arthritis have identified a strong neurogenic inflammatory component. The connective tissue and synovium of human joints are strongly innervated by peptidergic afferents expressing CGRP and SP, and autonomic fibres expressing vasodilatory neuropeptides such as vasoactive intestinal peptide (VIP) and neuropeptide Y (NPY) (Kidd et al., 1990, Milner and Dohert, 2015, Gronblad et al., 1988, Mapp et al., 1990). In conditions of chronic, unrelenting inflammation such as rheumatoid arthritis, peptidergic nociceptors and autonomic neurons receive constant noxious stimulation causing the release of these inflammatory neuropeptides, thus maintaining chronic swelling via neuronal stimulation. Levels of CGRP and SP are also raised in the joints of animal models of arthritis (Donaldson, 2009), and these symptoms can be reduced by intervention with CGRP receptor antagonists (Hirsch et al., 2013). The heat sensing receptor TRPV1 is shown to be highly up-regulated in rodent models of chronic inflammatory pain, both at the site of inflammation (hind-paw skin), the sciatic nerve and DRG (Ji et al., 2002). TRPV1 antagonists are effective at relieving symptoms in rodent models of arthritis but have been dismissed as potential therapies in humans due to side-effects such as hyperthermia (Wong and Gavva, 2009).

At the site of inflammation low-threshold, heavily-myelinated Aβ fibres are exposed to pro-inflammatory mediators such as NGF, which results in a phenotypic switch in these neurons. NGF stimulates large DRG neurons to begin expressing SP and BDNF, so that innocuous stimulation of the peripheral Aβ fibres induces a release of SP and BDNF in the dorsal horn (Neumann et al., 1996). This phenotypic switch aids in triggering central sensitisation in inflammatory based pain. Peripheral inflammation also alters the function and cytokine expression profiles of spinal microglia (Raghavendra et al., 2004), specifically resulting in activation of p38 MAPK (Svensson et al., 2003)

and subsequent synthesis and release of IL-1β (Samad et al., 2001) and TNFα (Kawasaki et al., 2008). These induce activation of COX-2 in the dorsal horn neurons, driving production of PGE2. Binding of PGE2 to its EP2 receptor can potentiate AMPAR and NMDAR currents (Kohno et al., 2008), while binding to presynaptic EP4 receptors enhances neurotransmitter release from central terminals (Vasko et al., 1994). Many treatments of inflammatory pain seek to inhibit the driving mechanisms of peripheral sensitisation and inflammation (e.g. NSAID treatment) (Kidd and Urban, 2001), and as a result the activity dependent mechanisms of central sensitisation are ablated. This differs from the central changes that occur in other chronic pain states, such as in neuropathic pain described below.

Neuropathic pain

The various diseases associated with neuropathic pain show diverse pathological mechanisms, including peripheral (trauma) or central nerve injury (stroke), infection-induced neuropathy (post-herpetic neuralgia) or chemically induced neuropathy (chemotherapy) (Campbell and Meyer, 2006). This overview will focus on peripheral and central mechanisms of peripheral nerve injury derived neuropathic pain. Following peripheral nerve injury, the aforementioned mechanisms of peripheral sensitisation occur, including macrophage infiltration of the damaged nerve and increased expression of pro-inflammatory cytokines by these cells. Peripheral sensitisation in neuropathic pain also shows unique features, with denervation of Schwann cells and the resulting inflammation being of particular importance. Following injury, Schwann cells can further recruit macrophages to the site by secretion of leukaemia inhibitory factor and monocyte chemoattractant protein-1 (Sugiura et al., 2000), and possibly signal nearby uninjured neurons, contributing to sensitisation of these adjacent afferents (Schafers et al., 2003, Campbell and Meyer, 2006). Another distinctive feature of neuropathic pain is the generation of ectopic activity by the injured nerve, nearby uninjured nerves and from the DRG (Amir et al., 2005, Wu et al., 2002). Ectopic action potentials (not derived from a stimulus) induce spontaneous pain (Bostock et al., 2005, Baron, 2006) and are driven by Na_V activity, as demonstrated by the ablation of peripheral nerve injury

pain by topical lidocaine application (a non-selective sodium channel blocker) (Meier et al., 2003). Interestingly, application of sub-anaesthetic doses of lidocaine (i.e. 20% of the normal spinal dose required for analgesia) into the DRG relieved spontaneous phantom limb pain (Vaso et al., 2014), indicating an important role for ectopic impulse generation from the DRG in maintaining neuropathic pain despite injury recovery.

The generation of ectopic action potentials plays a vital role in driving the central sensitisation mechanisms of nerve injury pain. During neuropathic pain, Aβ neurons undergo a similar phenotypic switch as seen in inflammatory pain conditions, with large DRG neurons now expressing SP and BDNF. However, the number of different transcriptional changes that occur in the DRG are approximately 100-fold greater than those observed in inflammatory pain conditions (Latremoliere and Woolf, 2009). Central neuron death resulting from the peripheral injury causes structural changes in the dorsal horn in the form of sprouting of Aβ fibres from lamina III-IV into lamina I-II, where they may contact nociceptors and possibly alter activity (Woolf et al., 1992, Shortland et al., 1997, Lekan et al., 1996). Neuronal death also seems to have a far greater effect in activating spinal glial cells than inflammatory pain conditions, with them releasing a number of cytokines, trophic factors and neurotransmitters to drive sensitisation of dorsal horn neurons (Romero-Sandoval et al., 2008, Watkins and Maier, 2002). These enhanced changes (compared to inflammatory pain) in the central processing of neuropathic pain may leave victims of nerve injury at particular risk of developing chronic pain after recovery, with chronic pain occurrence rates ranging from 5 – 60% depending on the severity of the injury (Costigan et al., 2009).

Treatment of chronic pain and societal impacts

Treatment of chronic pain typically follows a ladder of drug escalation according to the World Health Organisation (WHO) cancer pain relief guidelines (WHO, 1996), with drugs being prescribed based on the patient's symptoms (Schnitzer, 2006, Dworkin et al., 2007). The treatment of chronic pain is dominated by NSAIDs, weak and strong opioids, paracetamol and COX-2 inhibitors. Further drug options are available for chronic neuropathic pain (which tends to be less responsive to treatment) which include tricyclic antidepressants (TCAs), selective serotonin and norepinephrine reuptake inhibitors (SSNRIs), calcium channel α2-δ ligands and topical lidocaine (Dworkin et al., 2007). Despite the wide range of analgesics available, a pan European study revealed that 27-61% of chronic pain sufferers were unsatisfied with the treatment of their pain and that 31% reported that their pain was so severe they could not tolerate it anymore (Breivik et al., 2006).

Treatment discontinuation for chronic pain is high, reported at 26%, with 34% of these patients discontinuing their medication due to side effects, lack of efficacy or addiction risks (Breivik et al., 2006). As a result, treatments are tailored specifically based on each patient's response to the different drugs available. Therefore, clinicians are walking a fine line of reducing side effects and drug dependency while maintaining adequate pain relief. Examples of the adverse effects causing patients to discontinue treatment include higher risks of cardiovascular death and events caused by NSAIDs and COX-2 inhibitors (Schnitzer, 2006) as well as nausea, sedation and respiratory depression induced by opioids (Eisenberg et al., 2005, Furlan et al., 2006, Dahan et al., 2010). Due to the severe and long-lasting nature of chronic pain, patients prescribed opioids can become dependent on these medications and at risk of developing an opiate addiction. This risk was exemplified in a study where 49% of patients who discontinued opioid use cited fear of addiction or dependence as a motive, and 18% admitted to quitting due to difficulty in controlling their opioid use. Patients who remain on opioid treatment risk drug dependence, insufficient analgesia due to tolerance and developing opioid-induced hyperalgesia (developing hypersensitivity to specific pain stimuli from prolonged opioid exposure) (Varrassi et al., 2010, Lee et al., 2011a). These issues not

only come at a high cost to patients' well-being but also to the economy, with the cost of chronic non-cancer pain reaching €5.34 billion per year in Ireland (Raftery et al., 2012). These issues clearly show an unmet need for long-lasting effective pain treatment with minimal side effects and no risk of addiction.

SNARE-mediated exocytosis and its contributions to pain

Pre-synaptic, vesicular release of neurotransmitters is a vital mechanism in the physiological pain process, and Soluble N-ethylmaleimide-sensitive factor attachment protein receptor (SNARE) proteins are essential mediators of vesicle fusion. As shown in Fig. 1.3 A, these SNARE proteins form a complex which mediates the fusion of synaptic vesicles containing neurotransmitters, or large dense core vesicles (LDCVs) containing neuropeptides to the presynaptic membrane, thus resulting in exocytotic release of neurotransmitters and propagation of the pain signal. The SNARE complex is made up of the proteins syntaxin, vesicle-associated membrane protein (VAMP/synaptobrevin) and synaptosomal-associated protein Mr of 25 k (SNAP-25). Neuronal SNARE complexes are formed as these constituent parts assemble into a parallel four-α-helical bundle, with one α helix contributed by synaptobrevin, one by syntaxin 1 and two from SNAP-25 (Rizo, 2018, Gustavsson et al., 2012). As shown in Fig. 1.3 B, synaptobrevin is a vesicle bound protein while SNAP-25 and syntaxin are bound to the plasma membrane. This complex docks the vesicle to the plasma membrane; following an action potential the resultant influx of Ca^{2+} allows for binding of Ca^{2+} to vesicle bound synaptotagmin, triggering the fusion of the vesicle to the plasma membrane and exocytosis of its contents (Jahn and Fasshauer, 2012).

Stimulated release of the CGRP from cultured rat trigeminal ganglia neurons (TGNs) was found to be Ca^{2+} dependent and inhibited by proteolysis of SNAP-25 and VAMP/1 (Meng et al., 2007, Meng et al., 2009); furthermore, the trafficking and docking of TRPV1 and TRPA1 were also dependent on these same SNAREs (Meng et al., 2016), with TRPV1 and CGRP likely trafficked via the same LDCVs (Devesa et al., 2014). Targeting any one of these mediators would be advantageous in the treatment of chronic pain. Inhibition of CGRP release from peripheral nociceptors could inhibit the

neurogenic driving component of the inflammatory soup, while preventing TRPV1/TRPA1 membrane fusion would inhibit the peripheral upregulation of these receptors, and subsequent sensitisation of the nociceptor. This would reduce nocifensive signalling to the dorsal horn and inhibit induction of central sensitisation. The botulinum neurotoxins (BoNTs) are a group of neuroparalytic proteins that cleave specific SNARE proteins, thus inhibiting the formation of SNARE complexes (Pirazzini et al., 2017). By preventing SNARE complex formation in nociceptors these neurotoxins could inhibit multiple mechanisms of sensitisation such as CGRP release and TRP channel membrane fusion via inhibition of LDCV membrane fusion, along with preventing the membrane fusion of any other SNARE dependent pro-algesic or pro-inflammatory mediators.

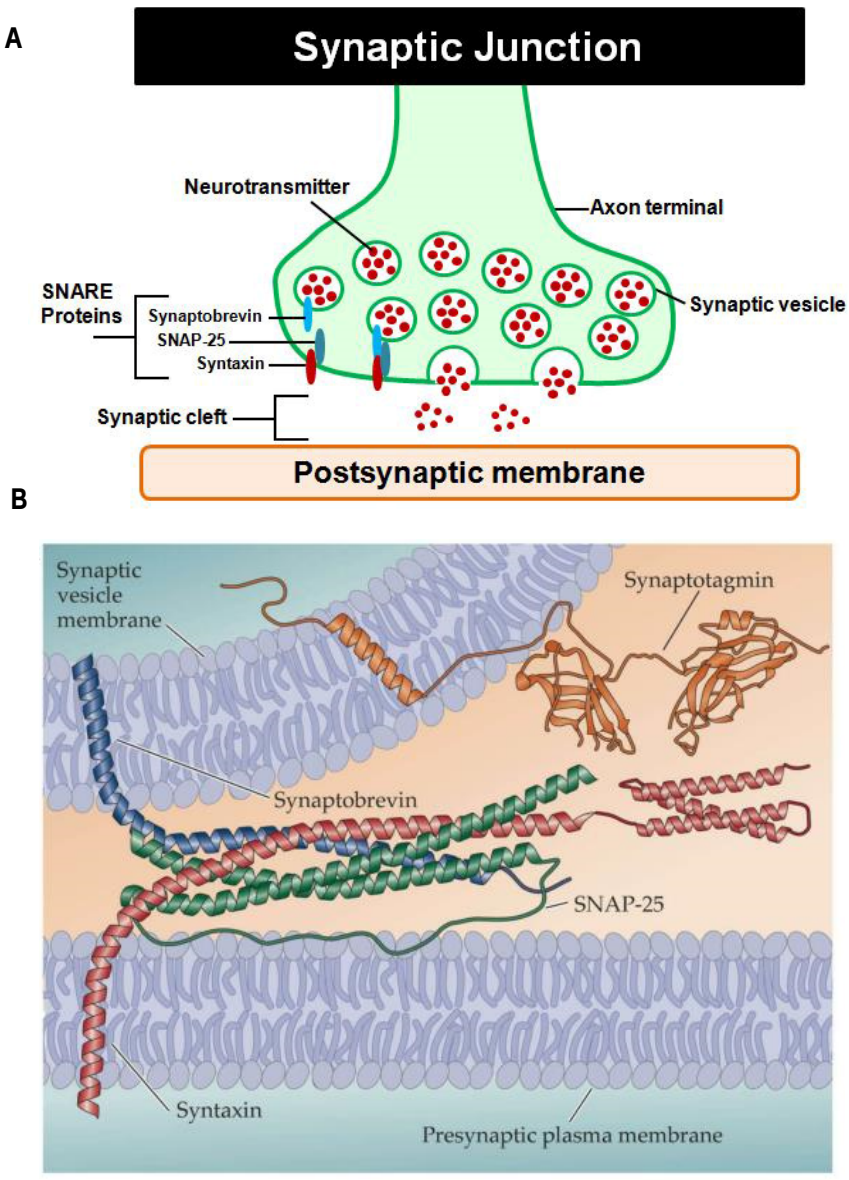

Fig. 1.3 SNARE-mediated vesicle fusion and neurotransmitter release **(A)** Vesicles containing neurotransmitters fuse to the presynaptic membrane via SNARE complex assembly, resulting in vesicular release. **(B)** Vesicle bound synaptobrevin forms a parallel alpha helix with a single syntaxin chain and two SNAP-25 chains. Following binding of Ca^{2+} to synaptotagmin, vesicle fusion with the presynaptic plasma membrane is triggered. Panel A taken from (Biolegend.com). Panel B taken from (Purves, 2004).

Botulinum neurotoxin structure and mechanism of action

BoNTs were originally discovered as the highly potent inhibitors of neuroexocytosis that cause the disease botulism. These neurotoxins are produced by *Clostridium botulinum* and target the synapses of cholinergic neurons, inhibiting membrane fusion of vesicles containing acetylcholine, resulting in a blockade of cholinergic transmission, and the flaccid paralysis characteristic of botulism. Seven naturally occurring serotypes of the neurotoxin have been identified (A-G); with BoNT serotypes A, B, E and F causing botulism (CDC, 1998). As shown in Fig. 1.4 A, BoNTs are homologous di-chain proteins with a molecular mass of ~150 kDa. This di-chain consists of a 50 kDa light chain (LC) and 100 kDa heavy chain (HC) linked together by a di-sulphide bridge. The HC is made up of the 50 kDa N terminal translocation domain (H_N) and 50 kDa C-terminal binding domain (H_C). The H_C contains two sub-domains, H_{CN} and H_{CC}, both of which are 25 kDa (Pirazzini et al., 2017). Intoxication of BoNT sensitive neurons is summarised in Fig. 1.4 B, and begins with binding of the H_{CC} to a ganglioside coreceptor, followed by binding to the luminal domain of a synaptic vesicle protein (see Table 1.2 for BoNT specific surface protein acceptors) (Binz and Rummel, 2009). The exact function of H_{CN} has not been fully elucidated but recent work indicates that the H_{CN} is required for binding and internalisation of the neurotoxin (Wang et al., 2017b). After binding, the toxin is internalised into the cell by receptor mediated endocytosis (Pirazzini et al., 2016). Acidification of the vesicle leads to protonation of the BoNT resulting in a conformational change of the H_N and LC allowing for interaction with the membrane lipids of the vesicle, opening a pore in the membrane and leading to translocation of the LC into the cytosol (Colasante et al., 2013). Reduction of the di-sulphide bond between the LC and H_N releases the LC into the cytosol to cleave a specific SNARE protein (Fischer and Montal, 2007) (see Table 1.2 for BoNT specific substrates).

A

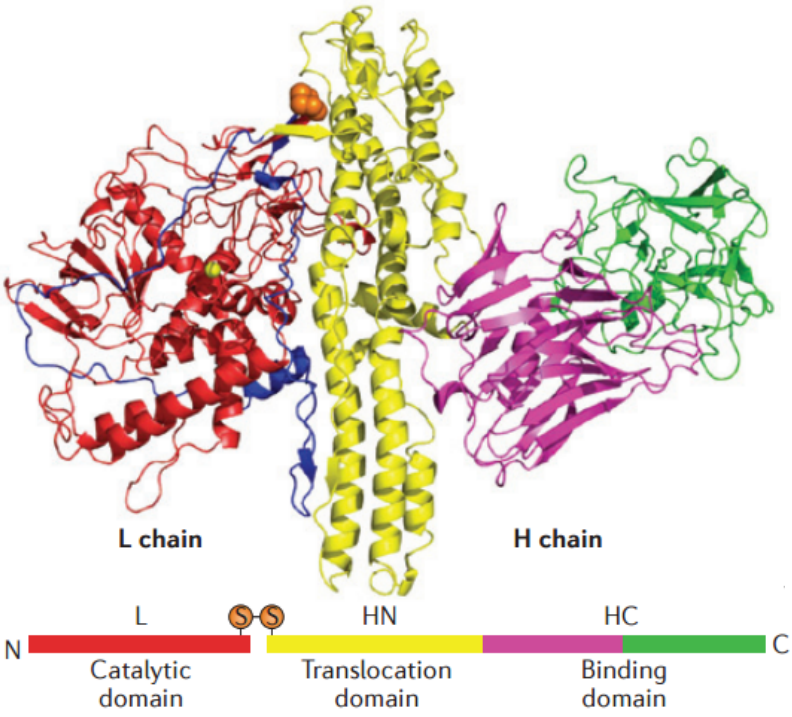

B

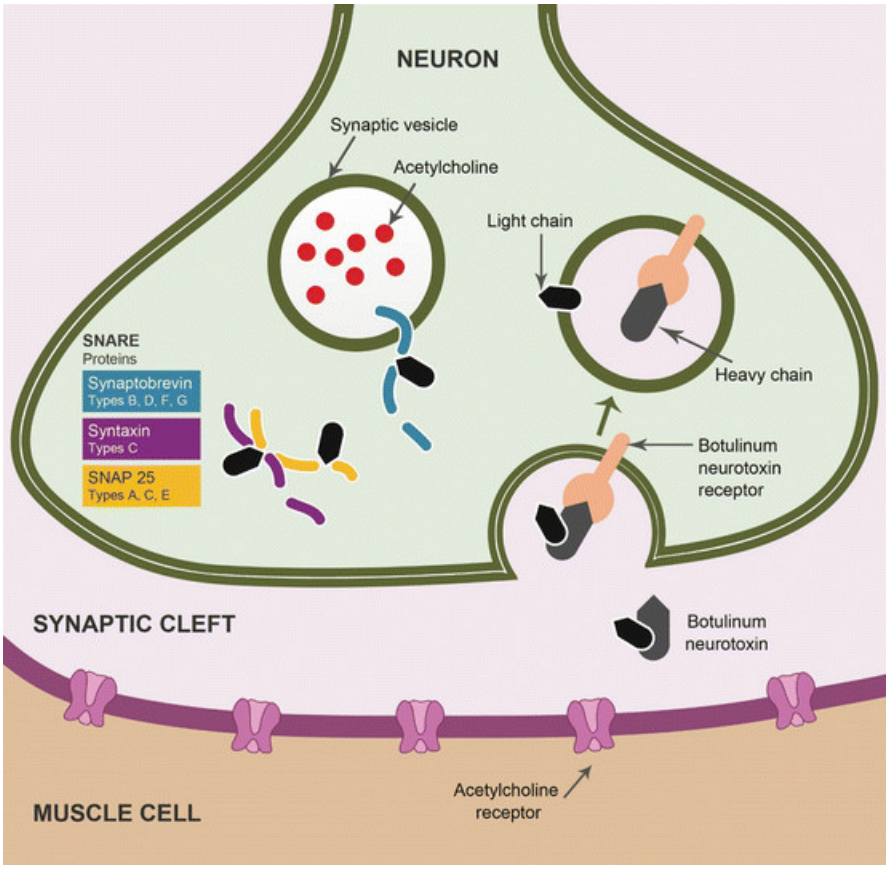

Fig. 1.4 BoNT di-chain structure and process of neuron intoxication (A) BoNTs are 150 kDa di-chains with a catalytic, 50 kDa light chain tethered to a 100 kDa heavy chain via a di-sulphide bridge. The heavy chain consists of the 50 kDa binding domain and the 50 kDa translocation domain. Graphic taken from (Rossetto et al., 2014, McCleane, 2008). **(B)** Botulinum neurotoxins, via the heavy chain binding domain, bind to the luminal domain of their respective protein receptors, which are exposed during vesicular release. The toxin is then internalised into the cell where the translocation domain plays a role in forming a pore in the vesicle, allowing the light chain to be released into the cytosol and cleave its target SNAREs. Graphic taken from (Saravanan et al., 2015)

SNARE cleavage results in either the inability to form SNARE complexes or the formation of functionally impaired, SDS-resistant SNARE complexes (caused by BoNT/A cleavage of SNAP-25) (Hayashi et al., 1994). Without fully functioning SNARE complexes vesicle fusion to the membrane is impaired, thus inhibiting exocytosis and causing neuroparalysis in the case of the neuromuscular junction (Humeau et al., 2000). These same paralytic properties resulted in patenting of clostridial produced BoNT/A multi-protein complex as a treatment of numerous disorders of muscle hyperexcitability. The BoNT/A protein complex BOTOX® is a 900 kDa complex consisting of the 150 kDa neurotoxin and several non-toxic proteins that serve to stabilise its entry into the body via ingestion (Gu and Jin, 2013, Frevert, 2010). These non-toxic proteins are disassociated from the neurotoxin after it crosses the intestinal wall into the bloodstream (Eisele et al., 2011). BOTOX® first received FDA approval for the treatment of strabismus, blepharospasm and hemifacial spasm in 1989, with numerous other clinical indications now approved (Chen, 2012). Studies have shown that BoNT/A purified neurotoxins demonstrate similar efficacy to BoNT/A multi-protein complexes in the treatment of cervical dystonia (Benecke et al., 2005) and are gradually receiving FDA approval similar to that of BoNT/A complexes (Pharmaceuticals, 2011).

BONT SEROTYPE	PROTEIN RECEPTOR	CATALYTIC TARGET
/A	SV2 A-C, fibroblast growth factor receptor 3	SNAP-25
/B	Synaptotagmin I and II	VAMP 1/2
/C	Unknown	SNAP-25 & syntaxin 1
/D	SV2 A, B and C	VAMP 1/2
/E	Glycosylated SV2 A and B	SNAP-25
/F	SV2 A, B and C	VAMP 1/2
/G	Synaptotagmin I and II	VAMP 1/2

Table 1.2 BoNT serotypes, protein receptors and catalytic targets in humans (Pirazzini et al., 2017)

Botulinum neurotoxins and the relief of chronic pain:

During clinical trials for the use of BoNT/A complex (BOTOX®, Allergan Inc.) to treat hyper-functional facial lines, patients treated with BOTOX® reported a reduction in migraine symptoms (Binder et al., 2000). This was eventually confirmed in a double blind, vehicle controlled study which demonstrated multiple site injections of BOTOX® into the peri-cranial muscles reduced the number and severity of migraines for up to three months after injections (Silberstein et al., 2000). In 2010, BOTOX® received FDA approval for the treatment of chronic migraine and is an attractive treatment option due to its long lasting prophylactic effects (potentially > 6 months) (Dodick et al., 2005). The observation that chronic migraine patients show greater levels of pain relief with each BOTOX® treatment is another attractive benefit, particularly compared to drug tolerance that can develop from current treatments for chronic pain mentioned above (Aurora et al., 2014).

BOTOX® has numerous off-label uses in different painful conditions, including (but not limited to) diabetic neuropathy, chronic musculoskeletal pain, temporomandibular joint disorder, post-herpetic neuralgia and trigeminal neuralgia (Yuan et al., 2009, Zhang et al., 2011b, Chen et al., 2015, Xiao et al., 2010, Morra et al., 2016). BoNT/A isn't the only serotype of BoNT to have potential in treatment of painful conditions, as the BoNT/B product Myobloc® is FDA approved for the treatment of pain arising from cervical dystonia (Chen, 2012, Solstice Neurosciences, 2009). Research on further uses of BoNT/B in chronic pain is lacking however (Pavone and Ueda, 2014). The long lasting anti-nociceptive effects of BoNT/A (ranging from 8 – 24 weeks) seem to be consistent in a number of different chronic pain conditions, including chronic refractory (treatment resistant) pain (Hu et al., 2013, Sandrini et al., 2017, Park and Park, 2017, Jabbari and Machado, 2011). These results indicate that BOTOX® has potential as a treatment for multiple forms of chronic pain, even those resistant to modern treatments, and has a low risk of tolerance or addiction. From here on "BoNT/A" will refer to the pure 150 kDa neurotoxin, while reports on the anti-nociceptive effects of BoNT/A complexes will be referred to by the specific brand of BoNT/A complex.

Peripheral anti-nociceptive mechanisms of BoNT/A in rodent models of pain

At first, the anti-nociceptive effects of BOTOX® were assumed to be the result of its effect on relaxing hyper-excitable skeletal muscle, but reports from patients with painful cervical dystonia showed reductions in pain scores after BOTOX® treatment without accompanying improvements in head posture (Tarsy and First, 1999). These findings implied that the neurotoxin could potentially act on nociceptors and not just at the neuromuscular junction. BoNT/A has been shown to gain access to these neurons *in vitro* and cleave SNAP-25 (Meng et al., 2007), indicating that BoNT/A could inhibit the release of pro-inflammatory neuropeptides from nociceptors at the site of injection, inhibiting neurogenic inflammation and peripheral sensitisation. BoNT/A and BOTOX® have been shown to inhibit the release of a number of different neurotransmitters *in vitro*, including CGRP, glutamate and substance P (Durham et al., 2004, McMahon et al., 1992, Welch et al., 2000). These three molecules are well known pain mediating neurotransmitters and neuropeptides, with their inhibition likely to play a role in the reduction of pain. Secondly, BoNT/A is reported to prevent induced upregulation of the receptor TRPV1 and TRPA1 to the plasmalemma in cultured sensory neurons (Meng et al., 2016). Both of these receptors are well characterised as nociceptive transducers (Julius, 2013) and are upregulated by TNFα and NGF in peripheral sensitisation (Ji et al., 2002, Meng et al., 2016) which is crucial in the development of chronic pain in inflammatory conditions such as rheumatoid arthritis. By potentially preventing the upregulation of these channels and inhibiting the release of pain mediators such as CGRP, it's no surprise that BoNT/A and BOTOX® are effective in relieving hypersensitisation in a number of animal models (Pavone and Luvisetto, 2010).

The first reports of BOTOX®-induced anti-nociceptive effects in a rodent pain model were reported by Cui *et al*. (2004) where they tested intra-plantar injections of the neurotoxin complex as a prophylactic intervention to reduce formalin-induced pain. Pre-injection of BOTOX® into the hind-paws of rats inhibited formalin-induced inflammatory pain behaviour (hind-paw lifting and licking behaviour), within 5 hours before injection of formalin into the same hind-paw. BOTOX® was found

to still inhibit formalin pain even when injected 12 days before injection of formalin. Pre-injection of BOTOX® also inhibited formalin-induced hind-paw oedema and levels of glutamate found in the hind-paw extracellular fluid (Cui et al., 2004). These results supported the hypothesis that BoNT/A could inhibit peripheral release of mediators of neurogenic inflammation (shown by reduced hind-paw swelling and inhibition of induced glutamate increases). The authors suggested that inhibition of peripheral sensitisation indirectly prevented mechanisms of central sensitisation, contributing to the decreases in formalin-induced pain behaviour. Importantly this study also showed that BOTOX® had no effect on baseline nocifensive thresholds and thus only affected pain induced by sensitisation. These results have been reproduced in rodent models of chronic inflammatory pain, particularly the Complete Freunds Adjuvant (CFA) model of knee and ankle pain. Intra-articular injections of Dysport® (BoNT/A complex - Ipsen Biopharm Ltd.) into inflamed knee joints was found to reduce CFA-induced swelling of the knee at one and two weeks post injection of toxin, and reduce CFA increased upregulation of IL-1β in the synovium of the articular cartilage (Yoo et al., 2014). Intra-articular injections of BOTOX® into CFA inflamed ankle joints inhibited CFA-induced hyperalgesia between 5 – 14 days after injection of toxin; the circumference of CFA inflamed joints was reduced at 7- and 14-days post toxin intervention. CFA increased levels of TNFα and IL-1β in the articular synovium were also reduced by injections of BOTOX® at these same time points (Wang et al., 2017c). Interestingly, while the anti-nociceptive effects of BoNT/A injections were reproduced in other rodent models of inflammatory pain (capsaicin-induced acute pain and Carrageenan sub-acute inflammatory pain), the anti-inflammatory effects were not (Bach-Rojecky and Lackovic, 2005). Furthermore, while inhibition of formalin-induced inflammation had been present using higher doses of BOTOX® (7 U/Kg), it was not induced by injections of 3.5 U/Kg, yet this lower dose was able to inhibit formalin-induced pain. These results suggest a disconnect between the anti-inflammatory effects and anti-nociceptive effects of BoNT/A, and possibly that inhibition of neurogenic inflammation is not the main mechanism of BoNT/A-induced analgesia.

Central anti-nociceptive mechanisms of BoNT/A in rodent models of pain

Substantial work has been performed exploring the effects of BoNT/A neurotoxin or complex interventions in other animal models of pain, to identify its anti-nociceptive potential and further explore the possible mechanisms of action. It has been suggested that the toxin/complex predominantly affects models of pain driven by mechanisms of central sensitisation (Matak and Lackovic, 2014), which is reflected in the number of chronic neuropathic pain models treatable by BoNT/A or BOTOX®. Intra-plantar injections of BoNT/A or BOTOX® have been found to relieve mechanical allodynia (measured by von Frey – refer to Methods, Behaviour assays of somatosensory function, von Frey test) in models of peripheral nerve injury, including the spinal nerve ligation model (Park et al., 2006), partial sciatic nerve transection (Bach-Rojecky et al., 2005) and the chronic constriction injury model (Luvisetto et al., 2007). In models of inflammatory pain BoNT/A complex had been injected into the site of inflammation and thus, could act to directly inhibit increased propagation of nocifensive signals to the dorsal horn, indirectly preventing central sensitisation. However, in rodent neuropathic pain models the toxin was injected distally to the site of neuro-inflammation. This means that BoNT/A is not at the origin sites of increased nocifensive signalling, which in neuropathic pain can be found at the injured nerve or the DRG, and so cannot inhibit the ectopic activity driving neuropathic pain leading to central sensitisation (Costigan et al., 2009, Campbell and Meyer, 2006, Amir et al., 2005). Despite this limitation, mechanical allodynia in these models is still reduced by intra-plantar injections of BoNT/A, distal to sciatic nerve injury or DRGs. Interestingly, following intra-plantar injections of BoNT/A in the CCI rodent model, immunohistochemical analysis revealed LC/A cleaved SNAP-25 ($SNAP\text{-}25_A$) in the plantar skin from the ipsilateral hind-paw, the sciatic nerve, DRG and L4/L5 dorsal horns of the spinal cord, indicating potential retrograde transport of BoNT/A (Marinelli et al., 2012). If BoNT/A activity is in fact not restricted to the injection site, it may inhibit neuro-inflammation from the injured nerve itself, prevent ectopic activity originating at the DRG, or even result in the blockade of neurotransmitter release from the central nociceptive terminals. Studies using rodent models of “mirror pain” (pain

induced in both hind-paws by injections of acidic saline into gastrocnemius muscle of one hind-limb) have reported the intriguing observation of a bilateral anti-nociceptive effect from a unilateral injection of BOTOX®. In the mirror pain model "ipsilateral" refers to the leg receiving injections of acidic saline which induce the model, resulting in hypersensitivity in both hind-paws (ipsilateral and contralateral). Injection of BOTOX® into the ipsilateral hind-paw of the mirror pain model reduced mechanical allodynia in both hind-paws, yet a contralateral injection of BOTOX® only relieved hypersensitivity in the contralateral hind-paw (Bach-Rojecky and Lackovic, 2009). The mechanisms of contralateral hypersensitivity are believed to mediated by central sensitisation, since this leg has not received injections of acidic saline (Da Silva et al., 2010, Sluka et al., 2001). Therefore, the effect of ipsilaterally injected BoNT/A on contralateral allodynia supports the hypothesis of a central action of BoNT/A. As contralateral injections of BoNT/A only relieved the contralateral hypersensitivity, this indicated the anti-nociceptive effects were not mediated by systemic spread of the toxin. The mechanisms in which BoNT/A can relieve symptoms of mirror pain are still unclear but the authors have suggested in follow up studies that it may be a result of transcytosis of the toxin from the nociceptor terminals in the ipsilateral dorsal horn to the central terminals of nociceptors in the contralateral dorsal horn (Bach-Rojecky et al., 2010).

The hypothesis that the anti-nociceptive effect of BoNT/A is mediated by retrograde transport remains a controversial one. While retrograde transport of BoNT/A has been observed in the past (Black and Dolly, 1986), it was assumed that this may be a mechanism of toxin degradation, due to lack of evidence showing toxin activity in the CNS (Hagenah et al., 1977, Habermann, 1974). Work using compartmentalised rat neuron cultures has shown that while SNAP-25_A can be detected in neuron cell bodies after application to neurites, indicating retrograde transport, this was only observed at exceptionally high doses (far greater than those used in animal or human studies). Furthermore, inhibition of evoked excitatory postsynaptic potentials was not inhibited by application of BoNT/A to the neurite compartment, unless exceeding doses 150,000-fold higher than those used in studies testing BoNT/A in rats (Lawrence et al., 2012). Experiments using a highly specific antibody for SNAP-25_A has shown that BoNT/A activity is only detected in the spinal cord at

high doses, likely resulting from systemic spread (Cai et al., 2017). The authors have challenged the detection of SNAP-25_A in sites distal to the injection site described above (Marinelli et al., 2012) on the basis that antibodies used may have lacked specificity. While the antinociceptive mechanisms of BoNT/A remained to be fully illuminated, the widespread anti-nociceptive effect across different animal and human models highlight its therapeutic importance.

Limitations of BoNT/A for the treatment of chronic pain

Although Botox has shown great promise in pain management, it is not free from side effects. These can include flu like symptoms, pain at the injection site and muscle weakness, but these occur infrequently and recover rapidly (Allergan, 2018). Despite the promising results in off label use of BOTOX®, most of these studies lack statistical power and the correct study design to satisfy FDA requirements (Pirazzini et al., 2017, Matak and Lackovic, 2014). Furthermore, not all patients suffering from chronic migraine respond to BOTOX® treatments and the reason for this is still unclear (Silberstein et al., 2015). Lastly, due to the extremely high potency of BoNT/A (lethal oral doses for humans can be as low as 30 ng) (Dhaked et al., 2010), the amount of BOTOX® that can be injected is very limited, reducing its potential as a treatment for chronic pain. Efforts are being made worldwide to improve this promising potential therapeutic by understanding its antinociceptive mechanism of action and how this can be altered to tailor BoNTs for better pain treatment.

Developing an improved BoNT chimera for the relief of pain

To overcome the limitations of BoNT/A for the treatment of chronic pain, efforts to improve the anti-nociceptive impact of SNAP-25 cleavage were explored. One constraint of LC/A cleavage of SNAP-25 is that it is unable to inhibit the release of CGRP from cultured TGNs induced by capsaicin stimulation, despite blocking CGRP release induced by bradykinin or K^+ depolarisation (Meng et al., 2007). The authors attributed this limitation to the known ability of increases in intracellular Ca^{2+} to reverse BoNT/A effects (Lundh et al., 1977). Considering the strong role increases in intra-cellular Ca^{2+} play in different pain states (Hagenacker et al., 2008, Latremoliere and Woolf, 2009), this could

mean that BoNT/A is unable to completely inhibit increased CGRP release in painful conditions. To overcome this, it was envisaged that BoNT/E, whose LC (LC/E) cleaves 26 terminal residues (cleaves at residues 180 – 181) from SNAP-25 compared to the 9 terminal residues cleaved by BoNT/A (LC/A cleaves at residues 197 - 198) (Chen and Barbieri, 2006), would induce a more stable blockade of CGRP release and provide greater antinociceptive benefits. However, BoNT/E lacks the long-lasting paralytic action of BoNT/A with patients recovering 4 weeks after injection (Eleopra et al., 1998); cultured sensory neurons were also found to be insensitive to BoNT/E (Meng et al., 2009). By developing an E/A chimera (BoNT/E di-chain with the /E H_C replaced with the H_C of BoNT/A) it was demonstrated that the LC/E could be redirected into BoNT/E insensitive sensory neurons via the H_C of BoNT/A. Furthermore, the LC/E that was re-targeted in this fashion also cleaved SNAP-25 (producing SNAP-25_E) and resulted in a blockade of capsaicin-induced CGRP release, unlike LC/A (Meng et al., 2009). Despite this progress in successfully re-targeting the superior LC/E into sensory neurons and preventing capsaicin-induced CGRP release, the E/A chimera retained the transient action of BoNT/E and so was not a suitable improvement over BoNT/A for development as treatment for chronic pain. To further develop an E/A chimera for the relief of pain, a method of increasing the half-life of LC/E was required. Research by Foran et al. (2003) using cultured sensory neurons showed that after co-incubation with both BoNT/A and BoNT/E, SNAP-25_E gradually diminished while levels of SNAP-25_A remained intact, indicating the longer half-life of BoNT/A over BoNT/E is not affected by turnover of SNAP-25 (Foran et al., 2003). The longer half-life of BoNT/A was eventually found to be a property of the LC/A (Wang et al., 2011a); thus by fusing the LC/E to the entire BoNT/A di-chain the longevity of LC/A was expected to be retained while allowing the LC/E access into nociceptors for the treatment of chronic pain. To test this hypothesis the chimeric protein LC/E-BoTIM/A was designed and produced. This consisted of the LC/E gene tethered to a BoNT/A mutant (BoTIM/A- see Fig. 1.5 A), which had a mutation in the gene for LC/A that rendered the LC/A inactive (mutation at active site H_{227} to Y). LC/E-BoTIM/A was found to successfully enter sensory neurons *in vitro*, cleave SNAP-25 and produce SNAP-25_E only and inhibit capsaicin-induced CGRP release. Unlike the E/A chimera, LC/E-BoTIM/A induced long-lasting paralysis in mice that

matched the half-life of BoNT/A yielding a potential therapeutic for chronic pain. LC/E-BoTIM/A could significantly reduce the symptoms of capsaicin-induced acute pain in rats, however while LC/E-BoTIM/A showed a trend towards further anti-nociceptive activity than BoNT/A, this did not reach statistical significance (Wang et al., 2011a).

To further improve the BoNT chimera for the treatment of chronic pain, it was hypothesised that retaining a fully active LC/A instead of a proteolytically inactive mutant such as BoTIM/A would preserve more analgesic potential. Thus, LC/E-BoNT/A was designed and produced, which consisted of a fully active BoNT/A di-chain with the LC/E tethered to the protein (Fig. 1.5 B). LC/E-BoNT/A, like LC/E-BoTIM/A could enter cultured sensory neurons and produced SNAP-25_E and inhibited the release of capsaicin-induced CGRP release, but also produced SNAP-25_A since it's LC/A retained proteolytic activity (Wang et al., 2017a). Next, LC/E-BoNT/A would need to be compared to LC/E-BoTIM/A and BoNT/A to determine if a chimera retaining an active LC/E and LC/A was a superior therapeutic than proteins consisting of a single active LC/E or LC/A only. The rodent pain models used to screen the BoNT chimeras are described below.

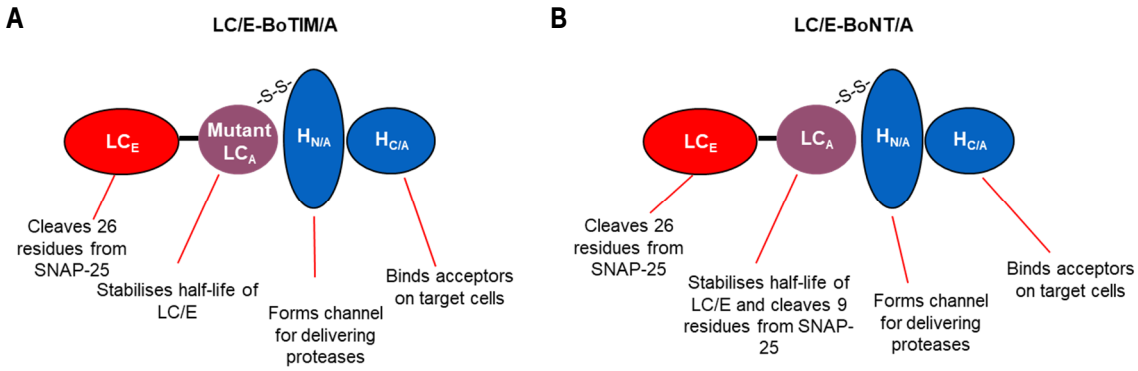

Fig. 1.5: Graphical depiction of BoNT chimeras, LC/E-BoNT/A and LC/E-BoTIM/A Schematics of **(A)** LC/E-BoTIM/A, **(B)** LC/E-BoNT/A structure. $H_{N/A}$ – translocation domain of BoNT/A. $H_{C/A}$ – binding domain of BoNT/A. BoTIM/A is a BoNT/A mutant with LC/A mutation at active site H227 to Y.

Selection of rodent pain models for testing of BoNT derived therapeutics

Rodent model of peripheral nerve injury pain

The spared nerve injury (SNI) model of neuropathic pain was first established in rats by Decosterd and Woolf (2000); it is induced by surgically revealing the point where the three terminal branches (sural, tibial and common peroneal nerves) of the sciatic nerve intersect, cutting and then ligating the tibial and peroneal nerves, "sparing" the sural nerve. This model was developed to investigate the roles that injured and nearby un-injured nerves play in the development of neuropathic pain (Decosterd and Woolf, 2000). Unlike models where all innervation of the hind-paw is axotomized (Wall et al., 1979), which are only reflective of conditions such as phantom-limb pain, the SNI model has the benefit of being a model of partial nerve injury, more reflective of clinical peripheral nerve injury cases. The SNI model has been found to be a more reproducible model of pain induced by peripheral nerve injury due to the relative ease of the surgery compared to other neuropathic pain models (Kumar et al., 2018). A rapid onset of prolonged mechanical and cold allodynia in the ipsilateral hind-paw regions innervated by the spared sural, and the saphenous nerves is another advantageous characteristic of the model. Based on the reliability of the model, the clinical relevance of it being a model of partial nerve injury and the long-lasting hypersensitivity induced, the SNI model was selected to test the therapeutic potential of BoNT derived therapeutics in neuropathic pain.

Rat model of Varicella zoster virus-induced neuropathic pain

As neuropathic pain can result from such a broad range of disease mechanisms such as infection, mechanical trauma, cancer, spinal cord injury etc. (Costigan et al., 2009), it was necessary to ascertain if BoNT chimeras proved effective in different neuropathic pain pathologies. Post-herpetic neuralgia (PHN) is a painful condition occurring after adult reactivation of the Varicella zoster virus (Vzv), which can develop into a chronic pain condition (Tontodonati et al., 2012). Reports have shown that BOTOX® can reduce visual analogue scale pain scores (patients score pain on a scale of 1-10), improve sleep quality and reduce opioid co-treatment in PHN patients, compared to patients

treated with lidocaine or saline (Xiao et al., 2010, Apalla et al., 2013). Therefore, it was decided to evaluate if BoNT variants could reduce the painful symptoms of the Vzv rat model of PHN. Injections of Vzv infected cells into the hind-paws of rats are reported to induce Vzv infection of the DRG (Sadzot-Delvaux et al., 1990) and results in mechanical and heat hypersensitivity, lasting in excess of 60 days (Dalziel et al., 2004, Jaggi et al., 2011); it is the only rodent model of PHN available. The symptoms of Vzv-induced mechanical hypersensitivity in rodents are relieved by several analgesics, including morphine, ibuprofen and the anti-convulsant gabapentin (a common treatment for neuropathic pain) (Hasnie et al., 2007).

Complete Freunds Adjuvant (CFA)-induced rat model of chronic, inflammatory, joint pain

It is hypothesised that the anti-nociceptive effect of BoNT/A could be mediated by its inhibition of the release of pro-algesic and pro-inflammatory mediators from peripheral nociceptors. This was first suggested by Cui et al. (2004) who demonstrated that intra-plantar pre-injection of BOTOX® could inhibit formalin-induced nocifensive behaviour and swelling. Interestingly, this anti-inflammatory effect was only present at a dose of 7 U/Kg while anti-nociceptive effects were observed at doses as low as 3.5 U/Kg, indicating that a greater amount of BOTOX® is required to have an anti-inflammatory effect (Cui et al., 2004). Unexpectedly, this anti-inflammatory effect is not present in other models of inflammatory pain as intra-plantar injections of BOTOX® do not reduce carrageenan or capsaicin-induced inflammation (Bach-Rojecky and Lackovic, 2005). These reports indicate that BOTOX® may have a potential anti-inflammatory effect in specific inflammatory pain conditions, although the mechanisms behind a differential anti-inflammatory effect between models is unclear. Pain from rheumatoid arthritis has been successfully treated with injections of BOTOX® (Mahowald et al., 2006, Singh et al., 2009, Mahowald et al., 2009), and an anti-inflammatory effect of Dysport® BoNT/A complex had also been shown in the CFA model of chronic inflammatory pain (Yoo et al., 2014). Since LC/E-BoNT/A and LC/E-BoTIM/A can induce a more stable block of capsaicin-induced release of CGRP from sensory neurons *in vitro* (Wang et al., 2011a, Wang et al., 2017a), it was hypothesised that these chimeras may show a more profound

anti-nociceptive and anti-inflammatory effect than BoNT/A in the CFA rat model. Intra-articular injections of CFA into the knee induce long-lasting inflammation, impaired weight-bearing ability of the injected joint (measured by the incapacitance test) (Wilson et al., 2006) and mechanical hyperalgesia measured by the pressure application method (PAM) (Barton et al., 2007). Importantly, treatment of the model with the NSAID rofexib can reduce CFA-induced hyper-sensitivity and CGRP up-regulation in the DRG (Staton et al., 2007). If BoNT/A can inhibit the release of up-regulated CGRP from peripheral neurons to reduce CFA-induced inflammation, then LC/E-BoNT/A should prove a more efficacious inhibitor of CFA-induced pain and inflammation.

Formalin rat model of acute, inflammatory pain

Injections of diluted formalin into the hind-paw of rodents induces a distinct bi-phasic behaviour profile. Phase 1 (0-5 min) is driven by direct activation of nociceptors by formalin, attributed to TRPA1 activation (Fischer et al., 2014, McNamara et al., 2007), which can be inhibited by centrally acting analgesics such as morphine or codeine (Hunskaar and Hole, 1987). Consistent with the inability of BoNT/A to block normal nociception, BoNT/A complex has no effect on phase 1 of the formalin test, unless injected centrally (Lee et al., 2011b). Following phase 1 there is a brief (5-15 min) phase of reduced nocifensive behaviour called the “interphase”, which is mechanistically still not understood (Fischer et al., 2014). Following the interphase is phase 2 of nocifensive behaviour, which is believed to be driven by increased peripheral nocifensive activity and central sensitisation (Fischer et al., 2014, Latremoliere and Woolf, 2009). The inflammatory reaction to formalin plays a role in driving peripheral sensitisation of neurons (Parada et al., 2001) and local application of lidocaine can inhibit both phase 1 and phase 2 nocifensive behaviours (Dallel et al., 1995), indicating that incoming peripheral activity is required to initiate and maintain both phase 1 and phase 2 behaviour. The relentless incoming nocifensive signals from the formalin tissue injury leads to phosphorylation of dorsal horn NMDA receptors mediated by Src kinase; when Src was decoupled from NMDA receptors, phase 2 behaviours were reduced while normal nocifensive behaviours were retained (Liu et al., 2008).

Capsaicin rat model of acute inflammatory pain

Intra-plantar injection of capsaicin induces short lasting nocifensive behaviour (most intense in first 3 minutes after injection) with longer lasting hypersensitivity to heat (~ 45 min) and mechanical stimuli (~ 4 hours) (Gilchrist et al., 1996). The model is driven by binding of capsaicin to TRPV1, directly activating nociceptors to induce the sensation of burning pain and the peripheral release of CGRP from the nociceptors, resulting in capsaicin-induced flare. The heat hyperalgesia is mediated by peripheral sensitisation of TRPV1 while secondary mechanical hyperalgesia surrounding the injection site is believed to be mediated by activity dependent central sensitisation (O'Neill et al., 2012). Centrally released SP can bind to NK1 resulting in long-lasting membrane depolarisation, contributing to temporal summation and unblocking the Mg^{2+} block on NMDA receptors (Latremoliere and Woolf, 2009, Murase et al., 1986, Sivilotti et al., 1993).

Project aims:

The overall aim of this project was to investigate if BoNT therapeutics including LC/E could relieve the symptoms of acute or chronic pain in rats. The LC/E was expected to have a superior anti-nociceptive effect over currently used BoNT/A, since LC/E can inhibit the release of CGRP from sensory neurons when stimulated with capsaicin. However, the half-life of LC/E was known to be far less than that of LC/A (Eleopra et al., 1998). To overcome this issue, the chimera LC/E-BoTIM/A was developed which tethered an active LC/E to a proteolytically inactive BoNT/A mutant, BoTIM/A. While this new toxin could inhibit the release of capsaicin-induced CGRP release from sensory neurons *in vitro*, and retained the longer activity of LC/A, it's anti-nociceptive effect on capsaicin-induced pain was not significantly greater than that of BoNT/A (Wang et al., 2011a). To further improve this chimera, the activity of LC/A was retained and the chimera LC/E-BoNT/A was produced. LC/E-BoNT/A also retained the longer paralytic action of BoNT/A while still inhibiting capsaicin-induced CGRP release *in vitro (Wang et al., 2017a)*. This was to be compared to LC/E-BoTIM/A in order to identify if the inclusion of two active LCs would increase anti-nociceptive potency.

To determine the most efficacious potential therapeutic for further screening in pain models, both LC/E-BoTIM/A and LC/E-BoNT/A were to be tested in a rodent chronic pain model. Since neuropathic pain represents patients more resistant to conventional analgesics (Dworkin et al., 2007), the SNI model of chronic neuropathic pain was selected to identify the more promising therapeutic candidate between LC/E-BoTIM/A and LC/E-BoNT/A. As BOTOX® and 150-kDa BoNT/A had been shown to have well documented effects in rodent models of neuropathic pain (Luvisetto et al., 2007, Park et al., 2006), it was expected that both chimeras would have superior effects due to the active LC/E. Furthermore, a comparison of the two chimeras would discern if the addition of an active LC/A provided any benefits over LC/E-BoTIM/A.

Once the top priority chimera between LC/E-BoNT/A or LC/E-BoTIM/A was selected for further testing, the second goal was to establish what effect the molecule would have in a virus-induced model chronic neuropathic pain, representing a different form of neuropathic pain. For this purpose, the Vzv model was to be tested to confirm its viability as a model of neuropathic pain and then used to screen the anti-nociceptive effects of LC/E-BoTIM/A or LC/E-BoNT/A. Following testing in the Vzv rat model, the candidate therapeutic was to be screened in the CFA model of chronic inflammatory pain. This was to compare the anti-nociceptive effects of the chimera in chronic neuropathic and inflammatory pain. Lastly, rat models of acute inflammatory pain (intra-plantar injections of formalin and capsaicin) would be used to investigate the prophylactic effects of the neurotoxin on acute pain induction and inflammation. Testing the chimera in all these different models would allow for a comprehensive investigation into the interventional and prophylactic effects on models of both neuropathic and inflammatory pain.

Chapter 2 - Materials & Methods

Materials

Buffers

0.1 M Phosphate buffer:

95 mL of 0.1 M $NaH_2PO_4H_2O$ mixed with 405 mL of 0.1 M $Na_2HPO_42H_2O$, made up to 1 L with dH_2O, pH 7.4

Homogenisation buffer:

50mM HEPES, 1mM EDTA, 150mM NaCl, 10% (v/v) glycerol, 1% (v/v) Igepal, 0.5% (w/v) sodium deoxycholate, pH to 7.5. Immediately before adding plantaris muscle to buffer, protease inhibitor cocktail (1:100), phosphatase inhibitor cocktail (1:100) and Benzonase® (endonuclease preparation 1:1000) were added to the buffer.

MOPS running buffer:

250 mM MOPS, 250 mM Tris, 5 mM EDTA,0.1% SDS, pH 7.0

TBS:

10 mM Tris-HCl, 100 mM NaCl, pH 7.4

TBS blocking/incubation buffer:

10mM Tris-HCL, 100 mM NaCl, 5% (w/v) BSA, pH 7.4

In vitro potency assay buffer:

20 mM HEPES, 100 mM NaCl, 10 µM $ZnCl_2$, 5 mM dithiothreitol, 10 µg/mL BSA, pH 7.4

Immunohistochemistry blocking buffer:

PBS with 0.3% (v/v) Triton X-100 and 5% (v/v) goat serum

Immunohistochemistry incubation buffer:

PBS with 0.1% (v/v) Triton X-100 and 1% (v/v) goat serum

Formaldehyde fixative solution:

4% (w/v) paraformaldehyde in 0.1 M phosphate buffer, pH 7.4

Normal saline:

0.9% (w/v) NaCl in water, pH 7.4

Heparinised saline:

5000 IU heparin in normal saline, pH 7.4

Injection vehicle 1:

0.5% (w/v) BSA, normal saline

Injection vehicle 2:

0.05% (w/v) HSA, 10 µM $ZnCl_2$, normal saline

Capsaicin:

0.1% (v/v) capsaicin, 5% (v/v) ethanol, 5% (v/v) Tween 80, normal saline

Formalin:

5% (v/v) formalin, normal saline

Equipment and chemicals

EQUIPMENT	SUPPLIER
INCAPACITANCE TESTER	Linton, UK
TISSUE HOMOGENISER, IKA®-T10	IKA, Germany
MICROSCOPE - OLYMPUS IX71	Olympus, Mason Technology Ltd. Ireland
OLYMPUS TH4-200 HALOGEN LAMP POWER SUPPLY UNIT	Olympus, Mason Technology Ltd. Ireland
OLYMPUS U-RFL-T REFLECTED FLUORESCENCE SYSTEM	Olympus, Mason Technology Ltd. Ireland
G: BOX CHEMI-16 GEL DOCUMENTATION SYSTEM	Syngene, Fisher-Scientific, Ireland
PIERCE™ POWER BLOTTER	Thermo-Fisher, Ireland
HARGREAVES APPARATUS	Ugo Basile, Italy
HOT/COLD PLATE	Ugo Basile, Italy
PRESSURE APPLICATION MEASUREMENT (PAM)	Ugo Basile, Italy
RANDALL SELITTO	Ugo Basile, Italy
ROTAROD	Ugo Basile, Italy
VON FREY APPARATUS	Ugo Basile, Italy
DIGITAL CALLIPERS	World Precision Instruments, UK

Table 2.1 Equipment & suppliers

COMPANY	Country	Web address
SIGMA ALDRICH	Ireland	www.sigmaaldrich.com/ireland
BIO-SCIENCES	Ireland	www.biosciences.ie
BOC	Ireland	www.boconline.ie
LENNOX	Ireland	www.lennox.ie
THERMO-FISHER	Ireland	www.fishersci.ie
VWR	Ireland	www.vwr.ie
ALOMONE	Israel	www.alomone.com
UGO BASILE	Italy	www.ugobasile.com
ATCC	UK	www.lgc-standards-atcc.org
ENVIGO	UK	www.Envigo.com
JACKSON IMMUNORESEARCH	UK	www.jieurope.com
MERCK MILLIPORE	UK	www.merckmillipore.com./ie
OLYMPUS	UK	www.olympus.co.uk
WPI	UK	www.wpi-europe.com/

Table 2.2 List of suppliers

REAGENTS/CHEMICALS	COMPANY	PRODUCT CODE
CAPSAICIN	Alomone, Israel	C-125
MRC-5 CELLS	ATCC, LGC, UK	CCL-171
VZV ELLEN STRAIN	ATCC, LGC, UK	VR-1367
HOECHST 33342	Biosciences, Ireland	H3570
MEDICAL OXYGEN 99%	BOC, Ireland	101-F
IMMOBILON WESTERN CHEMILUMINESCENT HRP SUBSTRATE	Fannin, Bio-Rad, UK	WBKLS0500
PRECISION PLUS PROTEIN™ ALL BLUE PRESTAINED PROTEIN STANDARDS	Fannin, Bio-Rad, UK	1610373
HUMAN SERUM ALBUMIN (HSA)	Irvine Scientific, Ireland	9988
ETHANOL	Lennox, Ireland	CC458600
BENZONASE®	Merck Millipore, Ireland	71205-3
BOVINE SERUM ALBUMIN (BSA)	Sigma Aldrich, Ireland	B8655
CFA	Sigma Aldrich, Ireland	F5881
DITHIOTHREITOL	Sigma Aldrich, Ireland	D0632
EDTA	Sigma Aldrich, Ireland	EDS
FLUOROMOUNT™	Sigma Aldrich, Ireland	F4680
FORMALDEHYDE 37% (W/W)	Sigma Aldrich, Ireland	252549
GLYCEROL	Sigma Aldrich, Ireland	G5516
GOAT SERUM	Sigma Aldrich, Ireland	G9023
HEPARIN	Sigma Aldrich, Ireland	H3393
HEPES	Sigma Aldrich, Ireland	H3375
IGEPAL	Sigma Aldrich, Ireland	I3021
MOPS	Sigma Aldrich, Ireland	M1254
NACL	Sigma Aldrich, Ireland	S3014
PARAFORMALDEHYDE	Sigma Aldrich, Ireland	P6148
PBS	Sigma Aldrich, Ireland	D8662
PHOSPHATASE INHIBITOR COCKTAIL	Sigma Aldrich, Ireland	P5726
PROTEASE INHIBITOR COCKTAIL	Sigma Aldrich, Ireland	P8340
SDS	Sigma Aldrich, Ireland	L3771
SODIUM DEOXYCHOLATE	Sigma Aldrich, Ireland	D6750
SODIUM PHOSPHATE MONOBASIC DIHYDRATE	Sigma Aldrich, Ireland	71500
SODIUM PHOSPHATE MONOBASIC MONOHYDRATE	Sigma Aldrich, Ireland	71507
SUCROSE	Sigma Aldrich, Ireland	S7903
TRIS	Sigma Aldrich, Ireland	T6066
TRIS-HCL	Sigma Aldrich, Ireland	T5941
TRITON X	Sigma Aldrich, Ireland	T8787
TWEEN-80	Sigma Aldrich, Ireland	P1754
ZNCL2	Sigma Aldrich, Ireland	208086
4X LITHIUM DODECYL SULPHATE SAMPLE BUFFER (LDS)	Thermo-Fisher, Ireland	B0007
TISSUE-TEK® OPTIMUM CUTTING TEMPERATURE COMPOUND (O.C.T)	VWR, Ireland	25608-930
BUPRENORPHINE	Veterinary prescription	
EUTHATAL (SODIUM PENTOBARBITAL 200 MG/ML)	Veterinary prescription	
ISOFLURANE	Veterinary prescription	

Table 2.3 Chemicals, reagents and suppliers

Antibodies

PRIMARY ANTIBODIES	DILUTION	SPECIES RAISED	COMPANY	PRODUCT CODE
ANTI C-FOS	1:5000	Rabbit	Merck Millipore	ABE457
ANTI-VARICELLA - ZOSTER VIRUS ANTIBODY, GLYCOPROTEIN I	1:100	Mouse	Merck Millipore	MAB8612
ANTI-SNAP 25	1:5000	Rabbit	Sigma-Aldrich	S9684
ANTI A-TUBULIN	1:5000	Mouse	Sigma-Aldrich	T5168

Table 2.4 Primary antibodies

SECONDARY ANTIBODIES	DILUTION	SPECIES RAISED IN	COMPANY	PRODUCT CODE	CONJUGATE
ANTI-RABBIT	1:500	Goat	Thermo-Fisher	A-11008	Alexa Fluor 488
ANTI-MOUSE	1:1000	Goat	Thermo-Fisher	A2114	Alexa Fluor 488
ANTI-MOUSE	1:5000	Donkey	Jackson Immunoresearch Europe	715035150	Horseradish peroxidase (HRP)
ANTI-RABBIT	1:10000	Donkey	Jackson Immunoresearch Europe	711035152	Horseradish peroxidase (HRP)

Table 2.5 Secondary antibodies

Methods

In vivo study design

Animals and study approval

Male Sprague Dawley rats and female Hsd: OLA TO mice were purchased from Envigo, UK (formerly Harlan) or bred in the Dublin City University (DCU) Bio-Resource Unit. Rats and mice were housed in an approved Specific Pathogen Free Bio-Resource Unit at DCU. Animals were group-housed (no more than 5 per cage) in Techniplast, double-decker, seal safe +, individually ventilated cages, with food and water available *ad libitum*. Bedding and environmental enrichment were provided, using sizzle-pet nesting material and gold chip sawdust supplied by LBS Biotechnology (UK) Room temperature was maintained between 19 and 22 °C and relative humidity from 45 to 65%, with a 12 h light/12 h dark schedule (lights on from 08:00–20:00) operated. All procedures were approved by the University Research Ethics Committee and authorised by the Health Products Regulatory Authority (HPRA), Ireland, thereby, fulfilling the requirements of Directive (2010)/63/EU and the National Statutory Instrument S.I. No 543 of 2012 (as amended by S.I. No. 434 of 2013 and S.I. No. 174 of 2014) on the protection of animals used for scientific purposes. Housing and regulatory details were the same for the entire report and will not be repeated for each section. Animal weights are detailed in relevant figure legends.

Randomisation and blinding

Age/weight-matched animals were randomly assigned to treatment groups by the random permuted blocks method. Experimenters carrying out injections and/or behavioural assessments were blinded to the treatment of each animal by coding of syringes by an independent researcher. Each cage housed rats with randomised treatments. Treatment codes were available to the researcher at the end of the study. Animals were identified by tail markings, each with a unique number written on the tail in permanent marker. It was not possible to blind the researcher to which animals were in a sham or pain model, due to the distinctive phenotypes of the different models (joint swelling, paw curling etc.). Final sample sizes are detailed in the figure legends.

Expression and characterisation of BoNTs

Production of BoNTs

Experimentation on recombinantly expressed BoNTs has been approved by the Environmental Protection Agency of Ireland and performed under containment level 2, according to a detailed and strictly enforced safety protocol. All toxins were produced by Drs Om Prakash Edupuganti, Gary Lawrence and Seshu Kazar (DCU); full details of toxin construction, expression and purification can be found in the following publications (Wang et al., 2017a, Wang et al., 2011a, Dolly et al., 2011, Wang et al., 2008). Briefly, synthesised genes for single chain BoNT/A, LC/E-BoTIM/A (mutation at active site H_{227} to Y) or LC/E-BoNTA were cloned into a prokaryotic expression vector, expressed in *E. coli* BL21 (DE3) strain and purified by Immobilized Metal Affinity Chromatography. Nicking of the single chain to an active di-chain was accomplished by incubation in thrombin (1 U/mg of toxin); this was monitored by SDS-PAGE and followed by Coomassie protein staining and Western blotting using antibodies for BoNT/A and LC/E. Three different batches of LC/E-BoNT/A, one batch of LC/E-BoTIM/A and BoNT/A were tested in the project. The three batches of LC/E-BoNT/A include an initial "lab sample" that was only used in Fig. 3.1. Consecutive experiments with LC/E-BoNT/A were performed with the refined "batch 1", which had been tested and found to have identical anti-nociceptive effects as the lab sample in the rat SNI model and an equivalent rat MaxTD dose (Wang et al., 2017a). Following observed decreases in toxin activity with batch 1, a further refined "batch 2" of LC/E-BoNT/A was used.

Potency testing of batch 2 of LC/E-BoNT/A

Study management was conducted by Dr Tom Zurawski and Dr Gary Lawrence (DCU). Non-lethal end-points have been suggested as a refinement for the mouse LD_{50} in efforts to replace it for potency testing of BoNT/A (NIEHS, 2008), and were required by the HPRA to conduct potency testing of BoNTs. The humane endpoints used included "severe indrawn scaphoid abdomen with respiratory distress, or weight loss of 20% versus pre-study weight", and were deemed suitable for research purposes to establish BoNT potency estimates. Intra-peritoneal injections of different

concentrations of batch #2 LC/E-BoNT/A, or vehicle (0.5% HSA, 0.9% NaCl), in a volume of 0.2 mL were administered to female Hsd: OLA TO mice. The mice were checked every 3 hours for signs of toxicity, then checked hourly after the first signs of distress (e.g. ocular/nasal discharge, rough coat, rapid breathing etc.) over four days. Animals were euthanised once they reached the endpoints listed above, or after four days. The number of mice reaching humane endpoints was used to calculate an estimated minimum lethal dose (LD_{50}).

Injections of BoNTs or buprenorphine

Intra-plantar injections of BoNTs or vehicle

Animals were briefly anaesthetised with 3% inhalable isoflurane in 99% medical oxygen at flow rate of 1 l/min (this anaesthesia protocol was used for all procedures requiring anaesthesia). Injections of 20 µl BoNTs or vehicle (0.5% BSA, normal saline or 0.05% HSA, 10µM $ZnCl_2$, normal saline) were conducted four-five days before formalin injection (Cui et al., 2004), four days before capsaicin or seven days after SNI. Vehicle details are noted in figure legends if they included BSA or HSA. LC/E-BoNT/A, LC/E-BoTIM/A, BoNT/A or vehicle were loaded into 0.3 mL disposable insulin syringes with a 29 G needle and injected intradermally into the plantar surface of the right hind paw. Animals were rehoused in their clean cages following injections and monitored daily for the first week after procedure and at least once a week after this.

Intra-articular injections of BoNTs or vehicle

Rats were briefly anaesthetised; the knee was flexed and the joint palpated until the patella tendon was felt to bend slightly under pressure. BoNTs/vehicle were administered using 0.3 mL syringes with a 29 G needle. The needle was then inserted 2mm into this space until resistance was noted, and BoNTs (50 µl) or vehicle (0.5% BSA, 0.9% NaCl) were delivered into the articular space. If injections were performed on CFA inflamed knees, then the needle was inserted until the first sign of resistance was noted. Animals were rehoused in their clean cages following injections and monitored daily for the first week after procedure and at least once a week after this.

Sub-cutaneous (systemic) administration of buprenorphine

Buprenorphine is an opioid modulator, which acts as an agonist for the μ-opioid receptor and an antagonist for the δ/κ-opioid receptors (Coe et al., 2019, Cox et al., 2015). It is an highly potent and consistent treatment for moderate to severe acute pain, such as immediate postoperative pain (Harcus et al., 1980) and sub-cutaneous injections of 0.1-0.5 mg/kg of Buprenorphine have successfully relieved capsaicin-induced pain in rats (Barrett et al., 2003). Buprenorphine at doses of 0.1-0.2 mg/Kg in 200 μl normal saline was loaded into a 1 mL syringe with a 25 G needle and injected sub-cutaneously into the nape of the conscious, restrained rat, 30 minutes before intra-plantar injection of capsaicin.

Determination of maximum tolerated dose (MaxTD) of all batches of BoNT/A and LC/E-BoNT/A

Rats used for dosing studies were tested (using the assays described below) before intra-plantar or intra-articular injections of BoNTs to establish baseline behaviour, and then up to 7 days after injections of BoNTs to record onset of paralysis, and the animal's recovery. MaxTD doses are required to identify the maximum amount of BoNTs that can be injected without inducing motor paralysis that would impair behavioural testing in models of pain, which rely on the rat's ability to withdraw the treated hind-paw/limb.

Rotarod test

The rotarod is a test to assess locomotor impairment in animals. The test consists of placing animals on a suspended, motorised cone. Rats walk to attempt to stay on the device as it rotates; impaired motor function is reflected by a reduction in the time it takes to fall during a testing period of a fixed length. Rats were trained at a fixed speed of 15 rpm until they could successfully complete three sequential trials of 180 s. On testing days, rats were placed on a rotarod running at a fixed speed of 15 rpm and the latency to fall was recorded, 180 s was used as a cut off. Rats were given a break of at least 3 minutes per trial. Each rat underwent three trials per testing session, which were averaged to give the mean latency to fall in seconds.

Digit abduction score (DAS)

The DAS is a measure of hind-paw paralysis following intra-plantar or intra-articular injection of BoNTs. Rats were restrained as depicted in Fig. 2.1 A, then a drop was simulated by flipping the rat 90 ° (head descending) to the final position in Fig. 2.1 B. This causes a digit abduction reflex as the rat prepares to land in response to the drop; muscle paralysis is quantified by the number of digits that can abduct. The DAS response was scored based on Fig. 2.1 C (Broide et al., 2013); for each digit that was unable to abduct after induction of the startle reflex, the DAS score increased. A score of 0 represented no paralysis while a value of 4 indicated maximum paralysis of the hind paw. Rats underwent three DAS trials with a break of 1 minute in between each trial and the responses were averaged to give a final score.

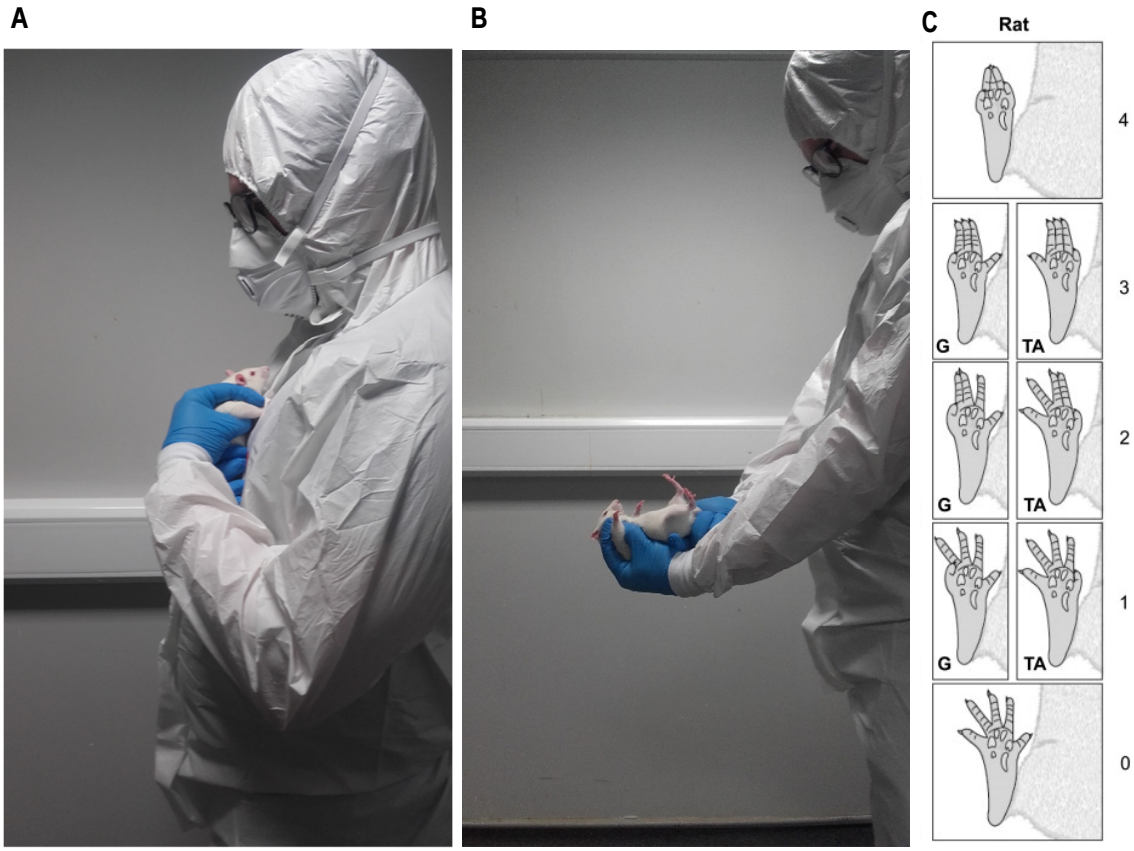

Fig. 2.1 Rat DAS scoring method (A) Starting position of DAS test, (**B)** Simulated drop that causes digit abduction reflex. **(C)** Scoring system for paralysis of digit abduction, onset of digit paralysis varies depending of site of injection of BoNT/A complex, injection sites noted in each image as G = Gastrocnemius or TA = Tibialis anterior muscles (Broide et al., 2013).

Kondziela inverted screen test

This test of grip strength is a laboratory standard for assessing fore-limb and hind-limb strength in rodents (Golli et al., 2016). Animals were placed on a wire screen mesh which was then rotated so the rat's head descended last. Bedding was placed under the rat to prevent injury after falling. The latency to fall from the screen mesh was recorded in seconds and each rat received 3 trials, with a break of at least 3 minutes between each trial.

Visual assessment score

Inspection of animal health was performed based on published scoring criteria (Hendriksen et al., 1999), to assess if the rats were suffering any adverse side effects from toxin injections. Briefly, animal monitoring sheets were used to record any potential adverse effects of procedures on animals and these were quantified as a health score using the scoring table below (Table 2.6). The scores were averaged to give an overall health score and plotted as a time course relative to toxin injection.

ANIMAL APPEARANCE	NOTES	SCORE
	Normal	0
	Rough coat	1
	Piloerection, ocular and/or nasal discharge	2
	Piloerection, hunched posture	3
	All of the above, orbital tightening.	4
ANIMAL BEHAVIOUR	NOTES	SCORE
	Normal	0
	Lack of exploratory/inquisitive behaviour	1
	Isolated, reduced mobility but alert	2
	Restless or immobile, unresponsive.	3

Table 2.6 Rat health score chart: Side effects induced by BoNTs were graded using a scoring system adapted from (Hendriksen et al., 1999). BoNT induced side effects are visible in the animal's appearance and behaviour. These can include patches of rough/unkempt fur in rats which are indicative of a lack of grooming, piloerection (raised fur/"goosebumps") over entire body indicative of stress, ocular and nasal discharge indicative of a lack of grooming, and an abnormal hunched posture which is a sign of discomfort and stress. Orbital tightening (narrowing of the eyes) is also indicative of discomfort in rats. Healthy rats typically demonstrate exploratory and inquisitive behaviour, reductions in this behaviour are signs of discomfort induced by BoNTs. Reductions in mobility and isolation from cage-mates indicate discomfort and potential weakness from injection of BoNTs. Restless behaviour (struggling during handling) is indicative of high stress while immobility and unresponsiveness would result from BoNT induced side effects.

Pain models

Preparation and injection of viral inoculum

The Ellen strain of Vzv (ATCC® VR-1367™) was selected to induce the model as it was the most readily available and major differences in inducing hypersensitivity when compared to the Dumas strain had not been reported (Hasnie et al., 2007). This standard laboratory strain was propagated on human primary embryonic lung fibroblast cells (MRC-5 cells, ATCC® CCL-171™) by Dr Tom Zurawski according to published methods (Hasnie et al., 2007). Briefly, MRC-5 cells were inoculated with Vzv and harvested once the cells displayed an 80% cytopathic effect (syncytial rounding and sloughing) after inspection by microscopy. The infected cells were scraped from the flasks and the cell suspension was centrifuged at 1000 X *g* for 5 mins at room temperature. The supernatant was discarded, and the pellet re-suspended in 4 °C sterile PBS to be used for injections.

Animals were briefly anaesthetised and intra-dermally injected with 50 µl of PBS containing 1×10^4 – 3.9×10^6 infected cells into the mid plantar area of the right hind paw. Sham animals received an injection of equal amounts of uninfected cells and all treated rats were returned to their housing cages after the procedure. Animals were monitored at least twice a week after injection of viral inoculum for any adverse health effects.

Intra-articular injections of CFA

Rats were briefly anaesthetised and CFA (Sigma Aldrich) was loaded into 1 mL syringes with 25 G needles. The right hind limb was shaved to reveal the skin of the right knee joint, the knee was flexed and the joint palpated until the patella tendon was felt to bend slightly under pressure. Before injection the knee was swabbed with a 70% isopropyl or ethanol alcohol wipe. The needle was then inserted 2mm into this space until resistance was noted, and 150 µl of CFA was slowly delivered into the joint cavity. BoNTs (50 µl) or vehicle (0.5% BSA, 0.9% NaCl) were administered 7 days after injection of CFA. Animals were monitored daily for the first week after procedure and at least once a week after this.

Formalin testing

Nocifensive behaviour induced by formalin was recorded on a raised Perspex platform above a video camera, with rats placed in a box with blacked out walls and a clear lid for a dimly lit environment (light intensity within testing chamber recorded as 57 lx). One day prior to testing, rats were acclimatised to the chamber for 20 minutes. On the testing day rats were placed into the recording chambers for 5 minutes before injections. Formalin was prepared by diluting 100% formalin (equal to 37% formaldehyde) in normal saline (0.9% NaCl) to a final concentration of 5%. Diluted formalin (50 µl) was loaded into 0.5 mL disposable insulin syringes with 29 G needles, then an intra-plantar injection administered to the right hind paw of lightly restrained conscious rats. Nocifensive behaviour was recorded for 60 minutes after injections and videos of the behaviour were scored by a single blinded investigator. Nocifensive behaviour was taken as the time spent licking and lifting the paw along with the number of flinches. These were recorded in 5-minute time bins and plotted.

Induction of capsaicin model

Nocifensive behaviour induced by capsaicin was recorded in the same chamber as the formalin test. Acclimatisation was conducted in the same fashion as the formalin test protocol. On the testing day, rats were placed into the recording chambers for 5 minutes before injections; 0.1% capsaicin was prepared in a vehicle consisting of 5% Tween-80, 5% ethanol and 0.9% NaCl and 20 µl loaded into 0.3 mL disposable insulin syringes with 29 G needles, then injected in the same manner as the formalin injections. Paw lifting, licking and flinching behaviour were recorded for 10 minutes after capsaicin injections, and videos of the behaviour were scored by a single blinded investigator.

Spared nerve injury model

These surgeries were performed by either Drs Laura Casals, Tom Zurawski or Orla Moriarty (DCU). Rats were briefly anaesthetised with 3% isoflurane. The fur was shaved from the right thigh and exposed skin cleaned with gauze soaked in surgical soap. The anaesthetised animal was placed on a pre-heated platform. A skin incision in the lateral surface of the thigh was made to expose the muscles, using a sterile scalpel blade. The skin around the cut was separated from its underlying loose connective tissue to expose the muscle layers, using blunt dissection. At approximately mid-thigh level, a portion of the sciatic nerve and its three terminal branches (the sural, common peroneal and tibial nerves) were exposed, using blunt dissection. Immediately distal to the trifurcation point, the common peroneal and tibial nerves were gently lifted using sterile forceps, tight-ligated and transected distal to the ligature. The wound was closed in layers, using sutures for the muscle; the overlaying skin was closed with wound clips/staples. Sham surgery was performed in the same manner, but the nerves were only exposed. Animals were monitored daily for the first week after procedure and at least once a week after this. Final sample sizes are described in figure legends.

Behaviour assays of somatosensory function

Hargreaves test

The Hargreaves test was used to measure behavioural responses to heat stimuli and establish a nocifensive threshold. The device consists of isolated testing chambers on top of a glass floor which the rats can freely move within, and an infra-red generator underneath which can heat the floor below the rat hind-paw. Rats were acclimatised in the Hargreaves testing chambers for 20 minutes, one day before testing began. The Hargreaves heat source was calibrated to induce a baseline nocifensive response in ~ 12 seconds, with a cut-off of 20 s to avoid sensitisation of the paw. On the day of testing, the rats were placed in the Hargreaves testing chamber 20 minutes before the test began. The Hargreaves probe was placed below the plantar surface of the left hind-paw and the test was started. Sudden flinching, raising, shaking or licking behaviours were recorded as

nocifensive responses. The left hind-paw of each rat was tested, and the test was then repeated for the right hind-paw. Rats were then given a 5-minute break before the left hind-paw was tested again. A total of three trials were recorded for each hind-paw and the average response was plotted for each paw per time point.

von Frey test

The von Frey test allows for measurement of tactile sensitivity. Rats are tested within isolated chambers on an elevated mesh floor; this allows application of nylon filaments to the paws. Each filament will bend under a different force, allowing for quantification of mechanical thresholds. Rats were acclimatised as per the Hargreaves test. On the day of testing the rats were placed in the von Frey testing chamber 20 minutes before the test began. The 4 g filament was applied to the plantar surface of the left hind-paw until it began to bend slightly, this was held for three seconds. Sudden flinching, raising, shaking or licking behaviours were recorded as nocifensive responses. If the filament produced a response, the next lower force filament was selected. Conversely, if the filament failed to produce a response, the next higher weight filament was used. Increasing or decreasing filaments were used until a change was recorded (e.g. increasing filaments eventually elicit a response), then four further trials were recorded, and the test concluded. The raw von Frey data were analysed using the Dixon method (Dixon, 1980) to calculate the 50% paw withdrawal thresholds (PWT).

Randall Selitto test

This allows measurement of mechanical pressure thresholds, which are larger than those elicited with the von Frey test, indicating that different aspects of mechanical sensitivity are being tested (Drew et al., 2007). The device consists of an automated, weighted lever that applies pressure through a blunt tip to the rat's paw. The test was terminated when the rats flinched, squeaked or attempted to escape restraint. A modified Randall Selitto device was used (Fig. 2.2) to allow for easier testing of the plantar surface of the hind-paw. This consisted of adhering a blunt soldering

iron tip to the device as depicted in Fig. 2.2. The rats were habituated to the device by daily handling and placing the paw into the testing position at the minimum setting, at four days before testing began. On the testing day rats were restrained and the hind-paw was placed in the test starting position. Only the ipsilateral hind-paw was tested due to the stressful nature of the test on the rats. The device was then activated so that a constant increase in mechanical pressure was applied to the rat hind-paw. Once the rat showed any one of the behaviours described above the test was terminated and the threshold recorded. A break of 5 minutes was provided to the animals between each test. Three trials were recorded per hind-paw, averaged, and converted to grams (using the formula supplied in the instruction manual). Baseline thresholds pre-Vzv injection were averaged and post-Vzv injection thresholds were converted into % changes from the average baseline.

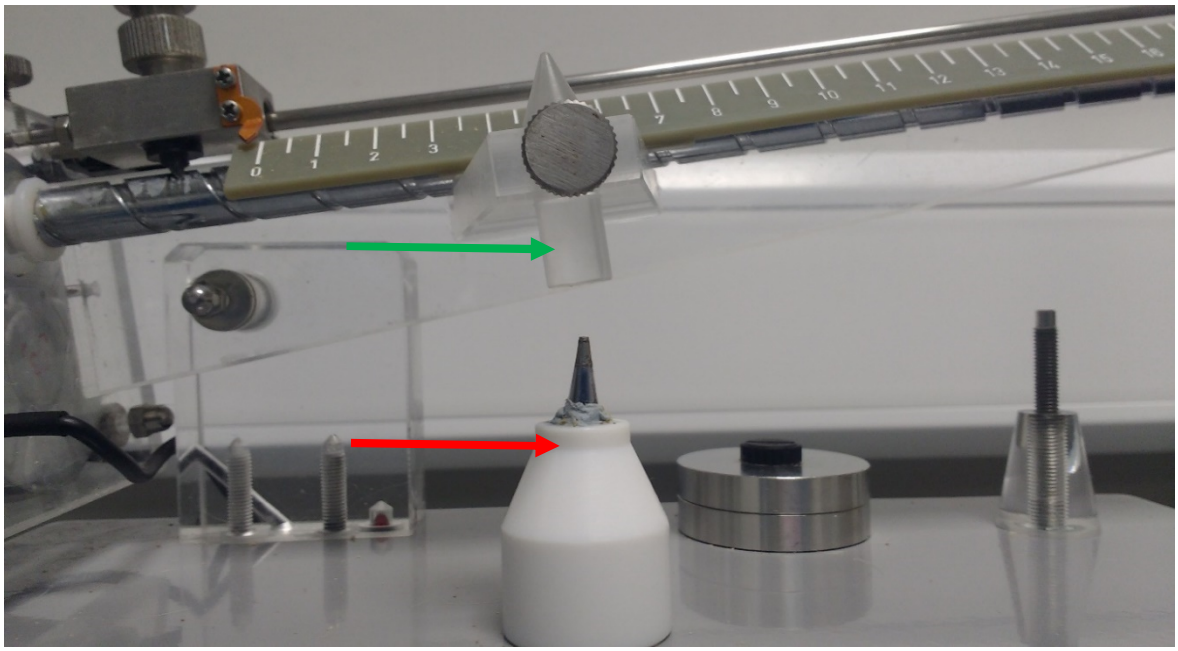

Fig. 2.2 Modified Randall Selitto test, a soldering iron tip was adhered to the white base (red arrow) for the plantar surface of the hind-paw to rest on. Pressure was applied to the dorsal side of the hind-paw from the flat surface above (green arrow).

Incapacitance test

This measures the weight bearing ability of the hindlimb. Since this is compromised in models of joint inflammation, it is a useful tool to measure potential recovery of limb function following administration of BoNT. The test was also used to measure limb paralysis induced by injecting high doses of BoNT, as the induced paralysis compromised weight bearing ability. The rats were restrained in a chamber with each hind-paw placed on a scale, which records the force applied to each scale and, therefore, shows how much bodyweight is distributed per hind limb. Rats were placed in the incapacitance tester for 5 minutes each day, in the four days leading up to the first testing day, to acclimatise them to the device. During testing rats were placed in the incapacitance meter; once the rat was stationary with both hind paws on the scales while facing straight forward (Fig. 2.3), the test was started and values (in grams) recorded. The rat was then returned to the home cage and the next animal tested. Each rat received four trials which were averaged to get the mean weight bearing values. These were converted into a % of the total body weight distributed to the ipsilateral hind limb.

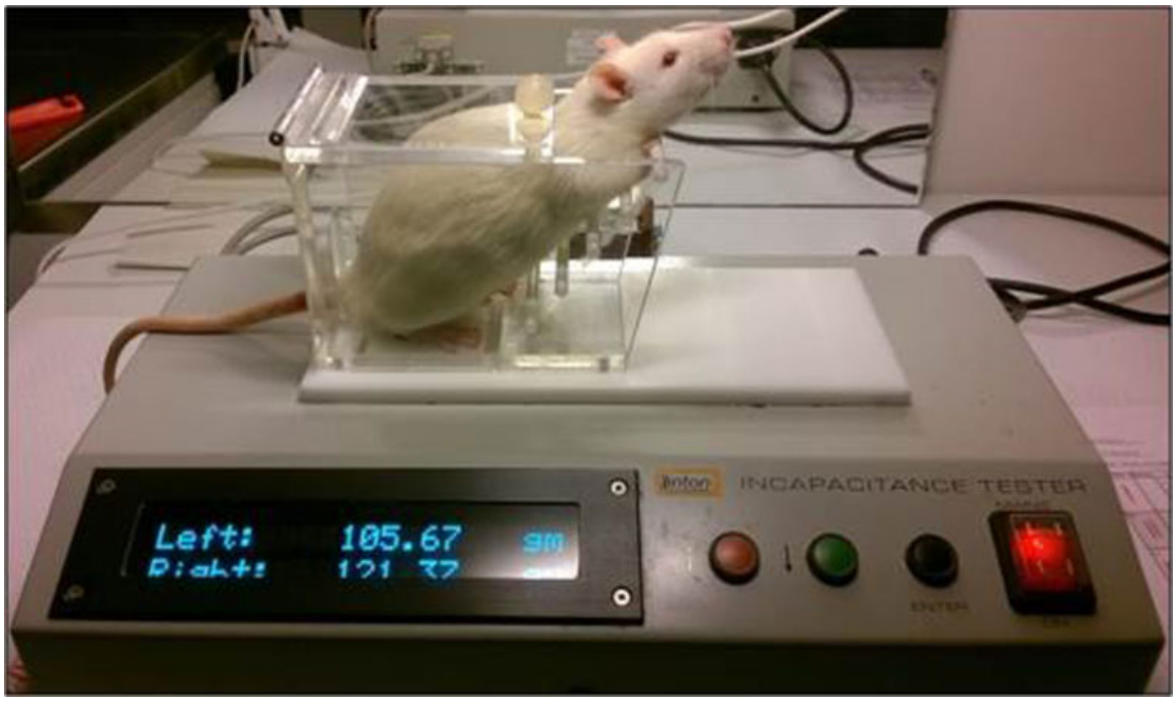

Fig. 2.3 Rat testing position for the incapacitance test, image taken from (Svard, 2016)

Pressure application method (PAM)

The PAM test is a measure of mechanical sensitivity, used specifically for joints. A pressure transducer is applied to the joint and force is gradually increased manually by the user until a nocifensive response is elicited (flinch, squeak, struggle behaviour etc.). Four days prior to testing, rats were restrained daily and held in a testing position for less than 1 minute, to acclimatise them to the testing position. On the test day, each rat was removed from the testing cage, restrained and the PAM sensor applied steadily to the knee joint, gradually increasing the pressure until a nocifensive response was noted. The peak force (measured in grams) was recorded from the PAM display. The animal was then returned to the cage. Rats received a 5-minute break in between trials and were tested three times per knee to get an average threshold. Both knees were tested, and the average values of each joint were plotted as a time-line.

Knee diameter

Rats were acclimatised to testing in the same manner as the PAM. Transverse knee diameters were measured using digital callipers and the rat returned to the home cage. Three measurements were taken per knee, averaged and plotted as a time-line; the animals were given a 5-minute break between each test.

Hot-plate/Cold-plate test

The hotplate provides a means to measure thresholds to heat stimuli. The rat is placed in a sealed chamber on a pre-heated plate. The latency for the animal to show a nocifensive response (licking of the hind-paw) is recorded. Animals were acclimatised to the hot-plate/cold-plate device at room temperature for 5 minutes one day before testing. At 50 minutes post capsaicin injection, rats were placed on the hotplate pre-set to either 54.5 or 51 °C (specified in the figure legends). The cut-off set for the hot-plate was 20 - 40 s to prevent tissue damage (20 s cut-off used for 54.5 °C test, 40 s for 51 °C test). Each rat received a single trial and latency to lick the injected hind paw was plotted. For cold-plate testing, the device was set to 5 °C and rats were tested throughout the SNI studies.

Behaviour was recorded before SNI surgeries, after surgeries and after injections of BoNTs. Rats were placed on the cold plate and the number of hind-paw raises and licks were recorded within 180 s.

Tissue harvesting and immunohistochemistry

Transcardial perfusion

Rats were sacrificed by overdose of anaesthetic (sodium pentobarbital, 200 mg/kg), 90 minutes after capsaicin injection. After confirming a deep plane of anaesthesia (lack of response to toe and tail pinch), the skin and body wall below the diaphragm were lifted using a blunt end forceps and abdominal muscles cut through, with body cavity opened and extended laterally. An incision was made along the border of the diaphragm muscle to expose the heart, which was held gently with blunt forceps. A blunt needle was inserted no more than ¼ inch into the left ventricle. The right atrium was then cut with an iridectomy scissors. Heparinised saline (5000 IU heparin/0.9% NaCl, pH 7.4) was perfused through the heart using 50 mL syringes attached to the needle inserted into the heart. This was done until the animal was completely exsanguinated. Between 200-500 mL (depending on the size of the rat) of 4% formaldehyde was perfused to fix the rat.

Tissue harvesting

Dissection to isolate tissue samples was performed on fixed or unfixed animals. To isolate plantaris muscles from unfixed animals, first the plantar skin was gently cut away using a scalpel blade to expose the plantaris muscle. This was raised using curved forceps and then excised from the hind-paw using a spring-loaded surgical scissors. Plantaris muscle samples were then stored at -80 °C. To isolate the spinal cord from fixed animals, the spinal cord was exposed by laminectomy. A bone cutter was used to cut the sides of the spinal cord, allowing the dorsal half of the spinal column to be lifted away using a forceps, revealing the spinal column. The hip bones were used as anatomical landmarks to identify the L4-L5 DRGs. The dorsal roots of the spinal nerves were traced back from the L4-L5 DRG to identify the L4-L5 region of the spinal cord. This was excised using a scalpel and forceps, then stored in 4% formaldehyde overnight at 4 °C.

Cryosectioning

The L4-L5 region of the spinal cord was stored in 30% sucrose solution (30% sucrose, 0.05%sodium azide, phosphate buffered saline - PBS) after an overnight fixation in 4% formaldehyde. After 24 hours in 30% sucrose, the ipsilateral and contralateral sides of the spinal cord were separated using a scalpel and frozen in optimal cutting temperature compound (OCT). The spinal cord was cut into 40 µm thick transverse sections using a cryostat (Leica – CM 3050S) and the L4-L5 regions stored in 30% sucrose at 4 °C.

Immunohistochemistry

Spinal cord sections were stained using a free-floating method, where they were washed 3 times with PBS and blocked in PBS with 0.3% Triton X-100 and 5% goat serum. The sections were then incubated over the weekend in an anti-c-fos primary antibody (rabbit polyclonal) at a 1:5000 dilution in PBS with 0.1% Triton X-100 and 1% goat serum at 4 °C. Sections were washed with PBS three times and incubated in a secondary fluorophore conjugated antibody (goat anti-rabbit IgG, Alexa Fluor 488) for 2 hours at room temperature. Sections were then mounted on microscopic slides and cover-slipped using Fluoromount™ mounting medium. Magnified images were captured on an Olympus IX71 microscope, U-RFL-T reflected fluorescence system and TH4-200 lamp. C-fos positive cells in the ipsilateral and contralateral LI-LII regions of the L4-L5 dorsal horns were counted using a manual Image J cell counter plug in. Immunostaining of Vzv infected cells was performed by Dr Tom Zurawski. MRC-5 cells were co-stained with anti-Vzv Glycoprotein I primary antibody and Hoechst 33342, and an anti-mouse fluorescent secondary antibody. Bright-field and fluorescent images were captured on the microscope system described above.

Detection of cleaved SNAP-25 *in vitro* and *ex vivo*

In vitro potency assay

The *in vitro* potency of BoNT/A and LC/E-BoNT/A was assessed using an established *in vitro* SNAP-25 cleavage assay (Wang et al., 2012). Toxins were diluted into the assay buffer and a C-terminus GFP-tagged, recombinant SNAP-25 fragment substrate (residues 134-206) was added to the diluted toxin, to a final concentration of 0.5 mg/mL. This was incubated at 37 °C for 30 min, then the reaction quenched by the addition of 4X LDS, to a final concentration of 1X LDS. To determine the % of intact SNAP-25, SNAP-25_A and SNAP-25_E, the samples were resolved on SDS-PAGE, Coomassie stained (see protein staining below), imaged and subjected to densitometric analysis using ImageJ software.

Tissue homogenisation

Frozen plantaris muscles were defrosted on ice and added to 200 µl of homogenisation buffer (see Materials). The tissue was cut in the buffer using spring-loaded surgical scissors, then blended using an electric tissue homogeniser (IKA® T-10) in short 3 second bursts, then homogenised by 3 second bursts with a battery powered mortar equipped with a polypropylene pestle. The homogenate was spun at 10,000 g for 15 minutes at 4 °C, the supernatant pipetted and then frozen at -20 °C.

Sodium dodecyl sulfate polyacrylamide gel electrophoresis (SDS-PAGE)

Protein samples were diluted in 4X LDS sample buffer (see materials) to a final concentration of 1X and heated at 95 °C for 10 minutes. The samples were loaded into pre-cast Bolt™ 12% Bis-Tris Plus Gels and run at 140 V at 4 °C, in MOPS running buffer (see Materials), until proteins were separated according to their molecular masses, indicated by pre-stained protein markers (10-250 kD, see materials).

Western-blotting

Following SDS-PAGE, proteins were electrophoretically transferred to a PVDF membrane by semi-dry transfer method, using a Pierce™ power blotter according to the prescribed protocol. Non-specific binding to membranes was inhibited by immediate incubation in blocking buffer (TBS containing 5% BSA). The membrane was then incubated in an anti-SNAP-25 primary antibody diluted in the same buffer, gently rocking at 4 °C overnight. This was then washed 3 times by gentle rocking in TBS buffer for 10 minutes, followed by incubation with a secondary antibody conjugated to HRP (diluted in TBS with BSA) for 90 minutes at room temperature. After a final 3 washes in TBS, the membrane was treated with an ECL kit to release a chemiluminescent signal which was captured G: BOX Chemi-16 gel documentation system.

Protein staining

Following SDS-PAGE gels were stained using the Pierce™ power blotter, according to the pre-programmed protein staining protocol. This allows for rapid Coomassie staining of the gel. Following staining, the gel was rinsed in deionized water and gently agitated at room temperature. Images of the gel were captured on the G: BOX Chemi-16 gel documentation system.

Data analysis and statistical procedures

All analysis was performed using GraphPad Prism 6 for Windows. Full details of statistical analyses are found in figure legends. Statistical analysis was not performed on dosing study assays used to determine the MaxTD, as the MaxTD is determined using cut-offs in these assays. In some cases, timelines were missing data-points (e.g. due to corruption of video recordings) which rendered them unsuitable for analysis by two-way ANOVA. These cases are noted in the relevant figure legends and the data also processed as the area under the curve for t-test or one-way ANOVA analysis.

Chapter 3 – Results

Testing of BoNT derived therapeutics in rodent models of pain

Neuropathic pain

Selection of prime candidate BoNT chimeras for screening as potential chronic pain therapeutics

As the overall aim of this project was assessment of novel therapeutics, the first goal was to select the most promising candidate for future investigation between LC/E-BoNT/A and LC/E-BoTIM/A. LC/E-BoTIM/A was shown to be effective on capsaicin-induced heat hypersensitivity in rats and showed a trend towards greater pain relief compared to BoNT/A (Wang et al., 2011a). As mentioned in the introduction, LC/E-BoNT/A was expected to be a superior therapeutic compared to LC/E-BoTIM/A as it retained two active LCs, whose SNARE cleaving capabilities were expected to underpin the neurotoxin's analgesic activity. In collaboration with Drs Laura Casals and Tom Zurawski, both novel molecules, and BoNT/A, were screened in the rat SNI model of neuropathic pain to compare the efficacy of these chimeras against BoNT/A and select the therapeutic candidate for further testing.

LC/E-BoNT/A reduced SNI-induced mechanical allodynia to a greater extent than either LC/E-BoTIM/A or BoNT/A

As mentioned in the methods, the MaxTD is the maximum amount of toxin that can be injected without inducing paralysis of the hind-limb which would interfere with behaviour testing. The MaxTD for intra-plantar injections of BoNT/A and LC/E-BoNT/A in the rat had previously been identified at 15 and 75 U/Kg, respectively (Wang et al., 2017a), and these doses were tested in the SNI model. To provide a direct comparison with LC/E-BoNT/A, LC/E-BoTIM/A was also tested at 75 U/Kg, thus, indicating the superior chimera for future therapeutic investigations. Rats underwent SNI surgeries and 7 days after surgery were given intra-plantar injections of either LC/E-BoNT/A, LC/E-BoTIM/A, BoNT/A or vehicle (0.5% BSA, 0.9% NaCl). Both LC/E-BoNT/A and LC/E-BoTIM/A were found to significantly reduce SNI-induced mechanical hypersensitivity, which was measured by the von Frey test as a quantification of tactile allodynia. Though BoNT/A showed a visible

increase in the mechanical thresholds, this did not reach statistical significance (Fig. 3.1 A-B). Furthermore, LC/E-BoNT/A proved to be significantly more effective than BoNT/A at relieving the induced mechanical allodynia on days 3-7 post injection (Fig. 3.1 A) and had a greater effect on tactile hypersensitivity overall, shown by the area under the curve (AUC) analysis (Fig. 3.1 B). LC/E-BoNT/A also reduced mechanical hypersensitivity to greater extent than LC/E-BoTIM/A, but only at days 3 and 7 post injection (Fig. 3.1 A) and did not have a significant effect in relieving sensitisation overall (measured by AUC) than LC/E-BoTIM/A (Fig. 3.1 B). Notably, LC/E-BoNT/A relieved mechanical allodynia to the point that it was no longer significantly different compared to the sham surgery group on days 3 and 7 post injection, indicating a temporary full recovery in neuropathic mechanical allodynia. As LC/E-BoNT/A showed a significant advantage over LC/E-BoTIM/A in relieving mechanical hypersensitivity, this molecule was prioritised for testing in a range of pain models as a potential novel pain therapeutic.

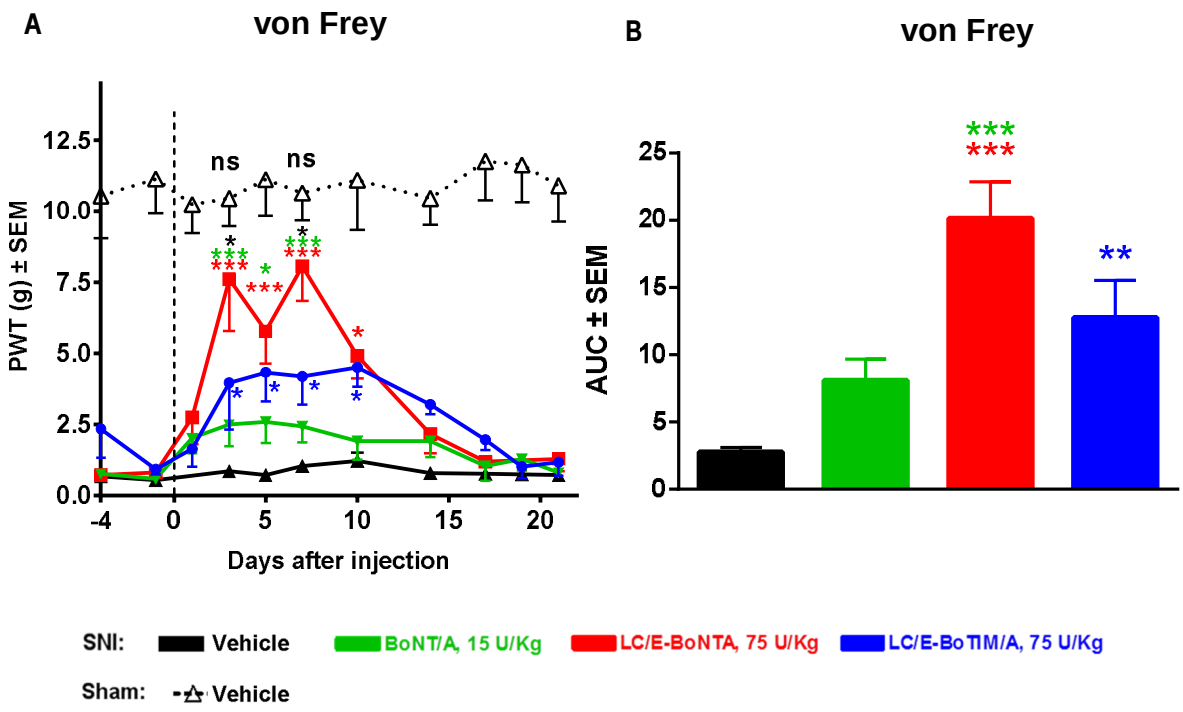

Fig. 3.1 LC/E-BoNT/A alleviates mechanical hypersensitivity following SNI surgery more effectively than LC/E-BoTIM/A at equal doses, and to a greater extent than the MaxTD of BoNT/A (A) Time course of the relief of mechanical hyperalgesia (measured as paw withdrawal threshold - PWT) by BoNT variants relative to days after toxin injection (vertical dotted line). **(B)** AUC analysis of SNI groups from panel **(A)**. Data represents means ± SEM; statistical analysis for **(A)** was performed using repeated measures two-way ANOVA and Bonferroni *post hoc* tests. As not all points aligned in the timeline, only data from days 3-10 post injection were analysed. There was a significant main effect of group ($F_{(3, 31)} = 33.0$, $p<0.001$). SNI was associated with a significant decrease in paw withdrawal threshold in vehicle-treated animals compared with sham controls and this effect was attenuated by LC/E-BoNT/A on days 3-10 post injection (*, $p<0.05$, ***$p<0.001$ vs. SNI vehicle). The SNI-induced hypersensitivity was also attenuated by LC/E-BoTIM/A on days 3-10 post injection (*$p<0.05$). Withdrawal thresholds were significantly higher in the SNI + LC/E-BoNT/A group than in the SNI + LC/E-BoTIM/A group on days 3 and 7 post injection (*$p<0.05$) and also the BoNT/A group (*, P<0.05, *** $P<0.001$). The time course data are summarised in a histogram of the AUC **(B)**, where an increase in the AUC is indicative of reduced sensitivity. SNI groups only were analysed by one-way ANOVA followed by Bonferroni *post hoc* tests. LC/E-BoNT/A- and LC/E-BoTIM/A-treated SNI rats showed reduced sensitivity compared with their vehicle-treated counterparts. Data are presented as means ± SEM, sham group: n ≥ 6, SNI groups: n ≥ 8. (*$p<0.05$, **$p<0.01$, ***$p<0.001$, red symbols: SNI + LC/E-BoNT/A vs SNI + vehicle, blue symbols: SNI + LC/E-BoTIM/A vs SNI + vehicle, green symbols SNI + LC/E-BoNT/A vs SNI + BoNT/A, black symbols SNI + LC/E-BoTIM/A vs. SNI + LC/E-BoNT/A, ns: not significant vs. sham control. Rats weighing 200-250 g at time of SNI surgery were used. Dr Casals tested the LC/E-BoNT/A, BoNT/A, saline and sham groups while John Nealon tested the LC/E-BoTIM/A group in the rat SNI model. Dr Tom Zurawski performed SNI surgeries. Injection vehicle consisted of 0.5% BSA and normal saline.

Testing of Vzv model of neuropathic pain for screening of BoNT derived therapeutics

The experiments presented below were to demonstrate that intra-plantar injection of Vzv-infected cells in rats would induce hypersensitivity to mechanical and heat stimuli as reported in the literature (Furlan et al., 2006, Hasnie et al., 2007). Consulting the literature indicated that injection of MRC-5 human diploid fibroblast cells infected with the Ellen Vzv strain would induce the model (Hasnie et al., 2007, Garry et al., 2005, Raftery et al., 2012). These reports showed that heat hypersensitivity was not consistent between research groups and so the Randall Selitto test for mechanical hyperalgesia was selected to test this model in place of the Hargreaves test of heat allodynia (refer to Methods, Behaviour assays of somatosensory function, Hargraves test/Randall Selitto test). First, confirmation of infection of MRC-5 cells with Vzv was demonstrated with immunohistochemical staining. Secondly, to identify an optimum number of virus infected MRC-5 cells required to induce plantar hypersensitivity, different virus titres were administered by intra-plantar injection into the right hind-paw of rats.

MRC5 cells showed signs of infection post Vzv application, confirmed by positive antibody staining for Vzv glycoprotein I

MRC5 cells cultured and infected with Vzv began to show signs of cell rounding from day one post inoculation as expected (Fig. 3.2 A) (Leske et al., 2012). By day 2 ~70% of the cells displayed rounding of the cell body, with sloughing of cells indicated by gaps that were previously populated. By day 3 post Vzv, the cells were no longer suitable for injection into rats as they had exceeded 80% cytopathic effect. The standard protocols for inducing the Vzv model stipulate that cell cultures must not exceed an 80% cytopathic effect (Hasnie et al., 2007, Dalziel et al., 2004). To confirm presence of the virus, infected MRC5 cells were stained with antibodies against Vzv Glycoprotein I, a glycoprotein expressed in Vzv infected cells (Cohen and Nguyen, 1997) (Fig. 3.2 B, green). Individual cells were identified with the nuclei marker, Hoechst 33342 (Fig. 3.2 B, blue). These images confirmed Vzv infection at dilutions of the virus as low as 10^{-6}, with higher concentrations of Vzv (10^{-1}-10^{-2}) proving toxic to the MRC-5 cells indicated by the sparse Hoechst staining.

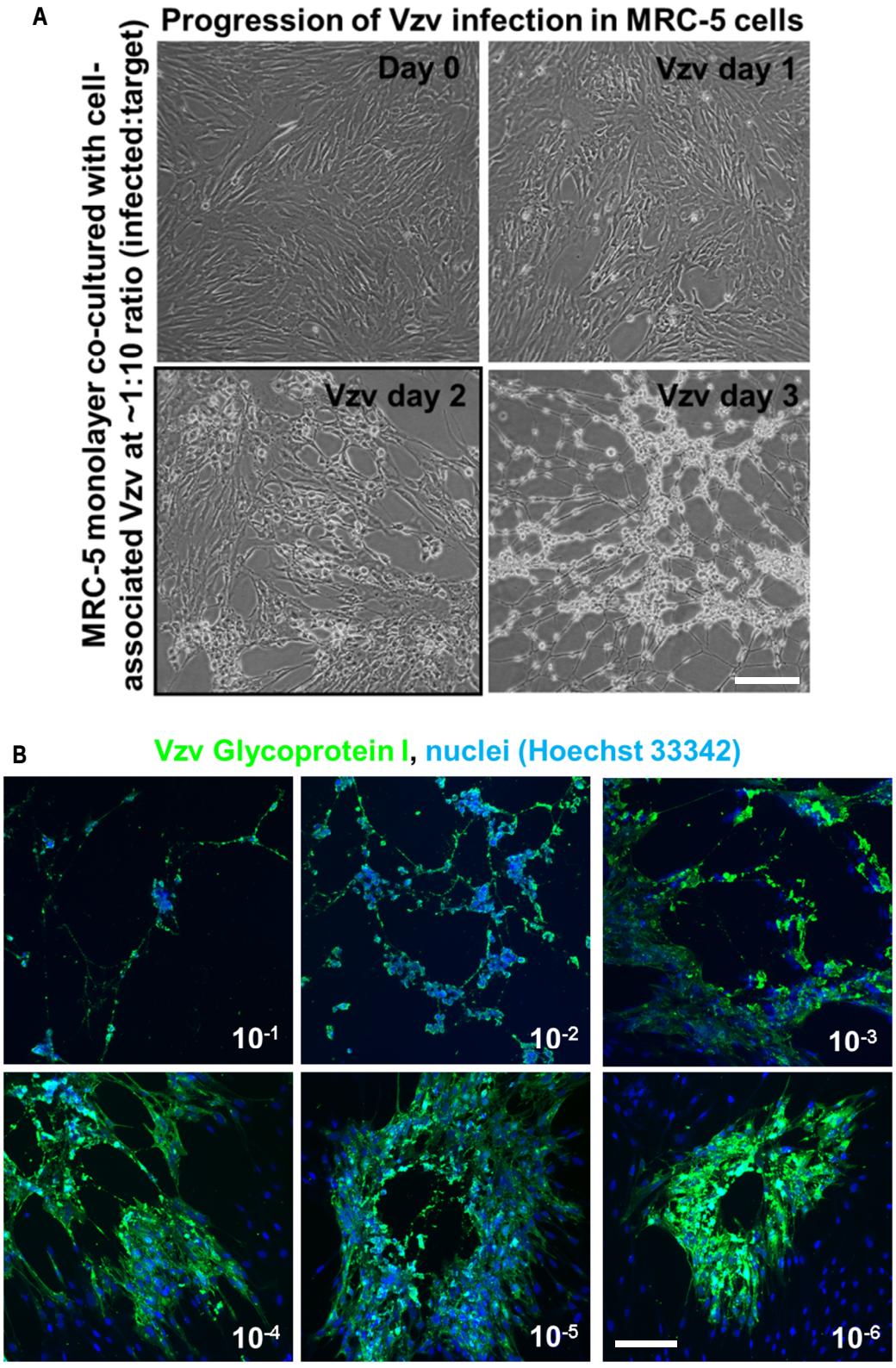

Fig. 3.2 Infection of MRC-5 cells confirmed by light microscopy and immunohistochemical staining (A) MRC-5 human lung fibroblast cells showed signs of Vzv infection (syncytial rounding and sloughing) at day 1 post infection. The cytopathic effect reaches ~ 80% by day 2 post inoculation and can be used for injections into animals. By day 3, the MRC-5 cells are no longer viable for inducing the model. **(B)** Presence of Vzv Glycoprotein I, 4 days after addition of serially diluted Vzv infected MRC-5 cells. Green fluorescent staining marks Vzv glycoprotein I present in cells, blue staining marks cell nuclei (Hoechst 33342). Infection of MRC-5 cells, antibody staining and imaging performed by Dr Tom Zurawski. Scale bar: 200 µm

Vzv-induced mechanical and heat hypersensitivity was insufficient for investigating BoNT mediated anti-nociceptive effects

To induce hypersensitivity in the hind-paw, rats received intra-plantar injections of 1×10^4, 2.8×10^6 or 3.9×10^6 Vzv-infected MRC-5 cells. These doses were based on reports on this model (Garry et al., 2005, Dalziel et al., 2004). Sham groups received injections of sham-infected cells, equal in number to their corresponding infected group. As there were no behavioural differences between the two tested sham groups (1×10^4 or 2.8×10^6 sham infected cells), they were merged into a single group of 15 animals. Decreases in mechanical thresholds (measured by von Frey and Randall Selitto tests) post administration of Vzv-infected cells were found to be inconsistent and not dose-dependent. The von Frey time course demonstrated that following Vzv injections all infected groups showed a trend towards decreased thresholds, but surprisingly, the greatest effect was induced by the lowest viral titre given (Fig. 3.3 A). This is also reflected in the Randall Selitto time course where only the 1×10^4 infected cells group showed obvious decreases in mechanical thresholds (Fig. 3.3 B). As the behaviour testing days for von Frey and Randall Selitto tests didn't fully synchronise, the time course data were not suitable for statistical analysis by repeated measures two-way ANOVA and is instead presented as AUC for analysis, as described in the figure legend (Fig. 3.4). One-way ANOVA of AUCs confirmed that only the lowest number of Vzv infected cells injected (1×10^4), induced significant mechanical allodynia as measured by the von Frey test, but not in the Randall Selitto test (Fig. 3.4 A-B). Since the Randall Selitto test showed no significant mechanical hyperalgesia, heat allodynia (measured by the Hargreaves test) was investigated in rats injected with 3.9×10^6 infected cells. These animals showed insignificant reductions in thresholds to heat stimuli (Fig. 3.3 C). The Hargreaves data were suitable for analysis by two-way repeated measures ANOVA as detailed in the figure legend and an AUC analysis was not necessary.

Together, these results showed striking inconsistencies in the magnitude and duration of reported Vzv-induced hypersensitivity and failed to demonstrate the previously described dose response of Vzv intervention on mechanical sensitivity (Hasnie et al., 2007). Thus, a more in-depth review of the literature was conducted. A lengthy investigation uncovered a thesis indicating a lack of

reproducibility in the model that could not be resolved by the authors despite multiple attempts and protocol variations (Medhurst, 2011). Herein, while some effect was observed from the lowest dose of Vzv administered (1×10^4 infected cells), the mechanical allodynia was too transient to effectively screen LC/E-BoNT/A. It is plausible that rat strains used in this case (Sprague Dawley) was resistant to the Ellen Vzv strain that we propagated on MRC-5 cells specifically, this is further explored in the Discussion chapter. As the published dose response of this model could not be reproduced and the sensitisation experienced by the rats was too transient, it was deemed an unethical use of animals to pursue this model further due to the lack of a consistent response.

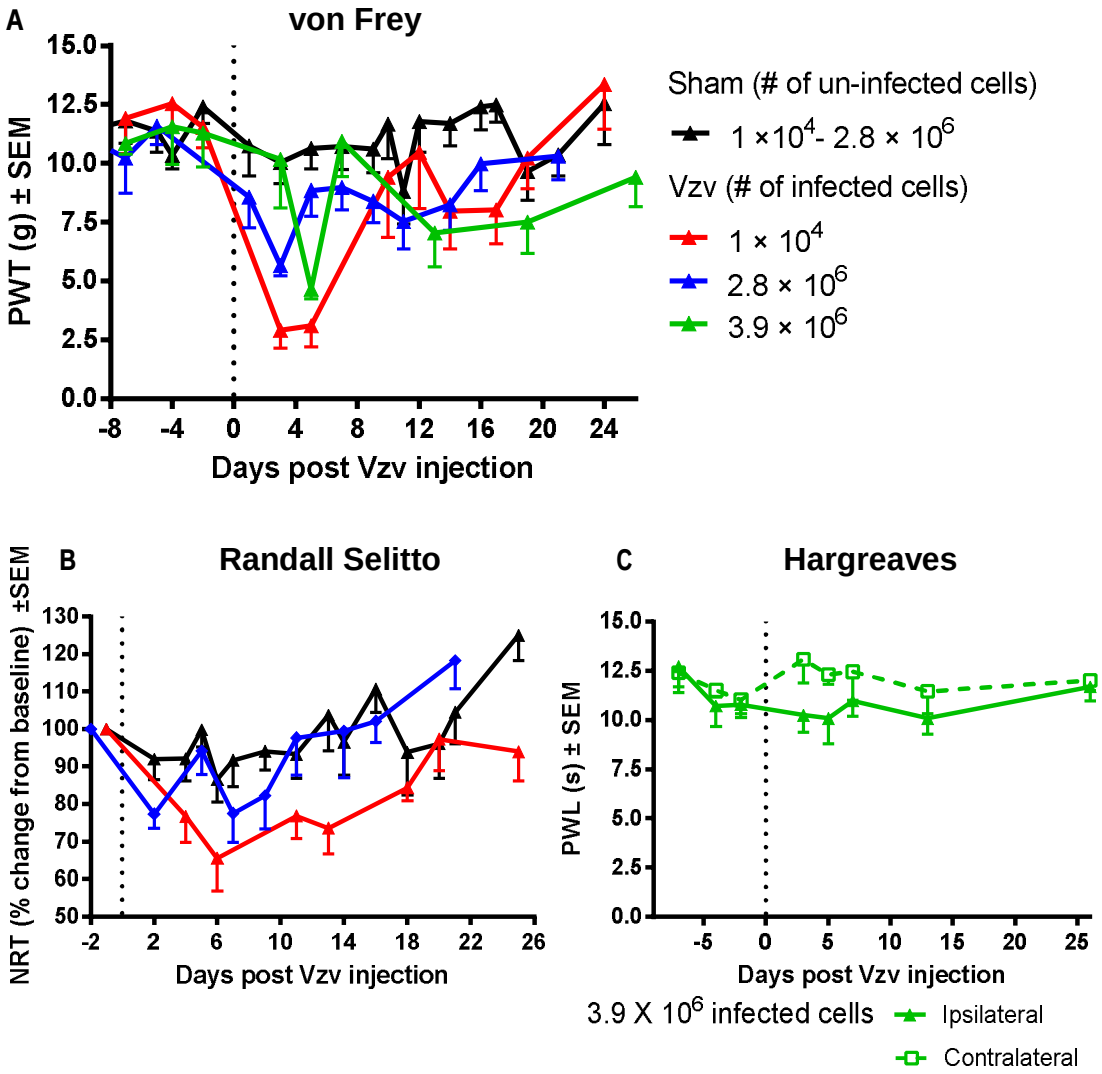

Fig. 3.3 Intra-plantar injections of Vzv infected MRC-5 cells induced transient tactile allodynia measured by von Frey peaking between 3-6 days after injection, minor reductions in Randall Selitto and Hargreaves test thresholds were observed (A) Von Frey and **(B)** Randall Selitto thresholds were recorded before and after Vzv injections (denoted by the dotted vertical lines). **(C)** Time course of heat thresholds in ipsilateral and contralateral hind-paws (measured by Hargreaves test) of 3.9 × 10^6 infected cells group. Data presented as means ± SEM; time course in **(C)** were analysed by repeated measures two-way ANOVA and Bonferroni *post hoc* tests. Sham group: n=15, Vzv (1 × 10^4): n=7, Vzv (2.8 × 10^6): n=7, Vzv (3.9 × 10^6): n=5. Rats weighed 200-300 g at the time of Vzv injections. Cells injected in PBS vehicle. NRT = Nocifensive response threshold, PWL = Paw withdrawal latency.

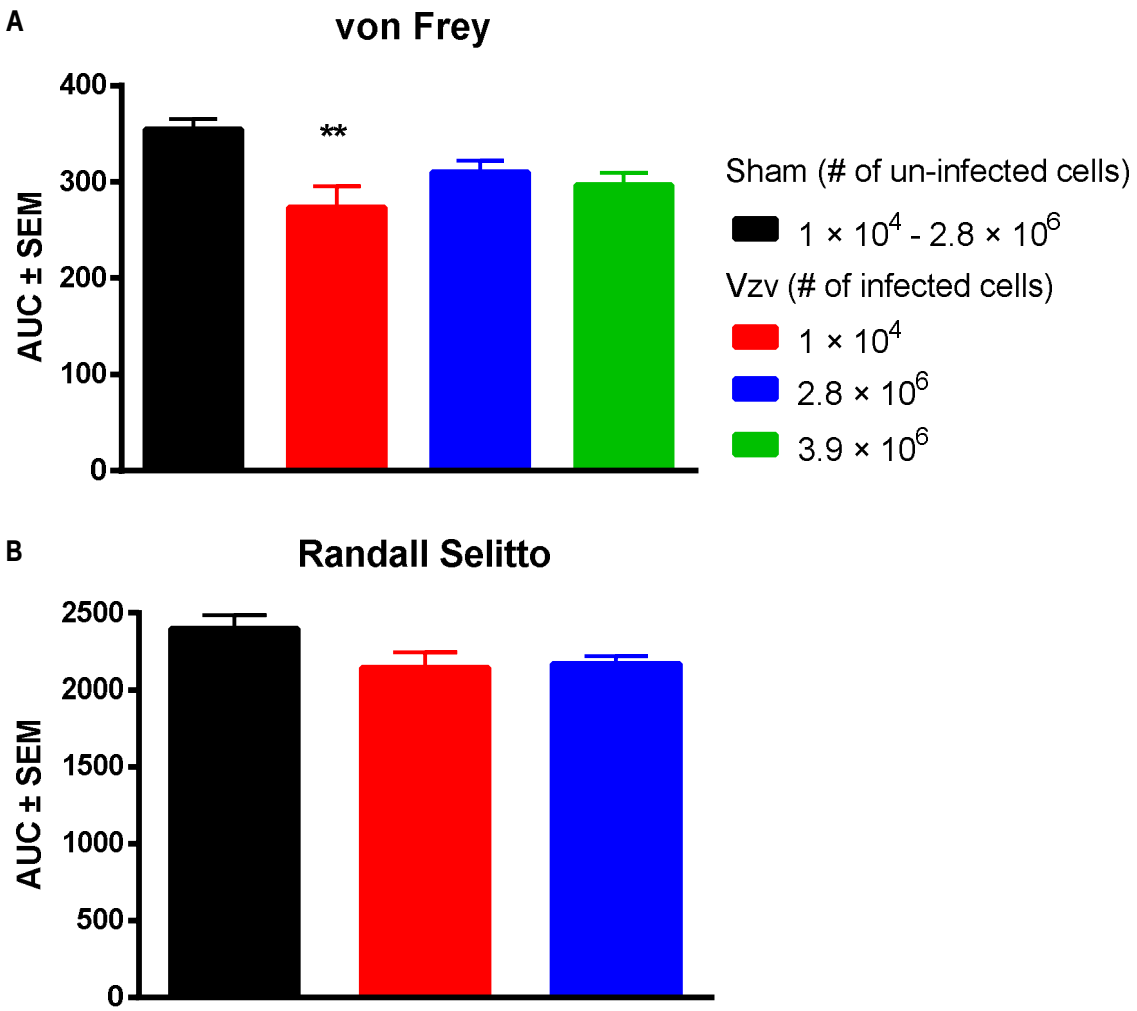

Fig. 3.4. Intra-plantar injections of Vzv infected MRC-5 cells induced transient tactile allodynia measured by von Frey with no dose response, insignificant reductions in Randall Selitto thresholds were observed (A) AUC summary of von Frey and **(B)** Randall Selitto time courses. Statistical analysis was conducted by one-way ANOVA followed by Bonferroni post hoc tests. Data presented as means ± SEM; **, P<0.01, 1×10^4 infected cells vs sham. Sham group: n=15, Vzv (1×10^4): n=7, Vzv (2.8×10^6): n=7, Vzv (3.9×10^6): n=5. Rats weighed 200-300 g at the time of Vzv injections. Cells injected in PBS vehicle.

Chronic inflammatory pain

Maximum intra-articular doses of BoNT injections into the rat knee were 1/3rd of the intra-plantar MaxTD

With the anti-nociceptive effects of LC/E-BoNT/A confirmed in the SNI model of neuropathic pain, the next step was to determine if its superior anti-nociceptive effect over BoNT/A would be reproduced in a rat model of chronic inflammatory joint pain. Dosing studies were first carried out to identify the MaxTD of LC/E-BoNT/A and BoNT/A for rat knee joint injections. Once the MaxTD of each toxin was set, these doses were tested in the CFA model of chronic inflammatory pain, to identify BoNT mediated reductions in joint swelling, mechanical hypersensitivity and functional recovery. An initial dose of 70 U/Kg for intra-articular injections of BoNT/A and LC/E-BoNT/A into the knee was selected, based on the dose of Dysport® used by Yoo et al., which was shown to reduce swelling around the knee joint in the rat CFA model (Yoo et al., 2014). Yoo et al. injected 20 U per rat, which was estimated to be 50 – 80 U/Kg based on the reported rat weights. To confirm paralysis from injection of BoNT/A or LC/E-BoNT/A into the knee (and therefore set an upper limit on what could be injected into the rat knee), 100 U/Kg of BoNT/A and 140 U/Kg of LC/E-BoNT/A were tested. A higher dose of LC/E-BoNT/A (140 U/Kg) was selected as it was shown to be better tolerated than BoNT/A when administered into the plantar skin of the hind-paw (Fig. 3.1) (Wang et al., 2017a).

As expected, 100 U/Kg of BoNT/A impaired locomotor ability from day one post injection but so did the 70 U/Kg dose by day 2 post injection, as measured by latency to fall from the rotarod (Fig. 3.5 A). LC/E-BoNT/A was observed to have less of an effect on motor function as only animals treated with 140 U/Kg showed a decrease in rotarod performance, while the LC/E-BoNT/A 70 U/Kg group were unaffected. Despite the lack of impact of 70 U/Kg of LC/E-BoNT/A on the rotarod, distinctive limping/dragging of the hind limb was noted in these animals, indicating that the rotarod test was not sensitive enough to detect hind limb paralysis following intra-articular injections in the knee joint. This limping behaviour was present in all groups in this study and so these doses were deemed unsuitable for analgesic assessment using the CFA model. While profound local paralysis associated

with all test groups in this study, the overall effects on animal welfare (measured by weight gain) were less severe. Fig. 3.5 B shows that all animals gained weight at an equal pace for 24 hours while rats injected with 100 U/Kg BoNT/A began to show impaired rotarod performance. No other treatment groups lost weight respective to the pre-injection values, although rats given 70 U/Kg of BoNT/A did show slowed weight gain 24 hours post toxin injection. Surprisingly, there were no obvious differences on animal weight gain between 70 U/Kg or 140 U/Kg of LC/E-BoNT/A. Since 140 U/Kg of LC/E-BoNT/A had less effect on both rotarod performance and weight gain than 70 U/Kg of BoNT/A, it is likely that LC/E-BoNT/A is better tolerated than BoNT/A when injected into the knee joint.

The doses of BoNT/A were decreased to 40 and 20 U/Kg while 60 and 40 U/Kg were selected for LC/E-BoNT/A. Increases in rat weight post toxin injection (Fig. 3.5 D) showed that 40 U/Kg of BoNT/A was the only dose which caused an obvious change in weight gain compared to the other test doses, further indicating that BoNT/A was less tolerable than LC/E-BoNT/A. Only the higher doses of each toxin reduced rotarod performance below the cut-off point of 80% of baseline fall latency (Fig. 3.5 C), yet all four doses of the toxins produced limping behaviours in the rats. This reveals an inconsistency in the previous experiment where 70 U/Kg of LC/E-BoNT/A hadn't caused a noticeable drop in rotarod performance in Fig. 3.5 A, yet a lower dose of 60 U/Kg had resulted in reduced fall latencies in Fig. 3.5 C, with both groups showing limping behaviour. This indicated that while limping was consistently induced by the intra-articular injections, this did not always result in reduced rotarod performance in the rats, most likely due to inter-animal variability resulting from the small sample sizes (n=2). To find a more sensitive method to quantify the motor effects of BoNTs following intra-articular injection, the incapacitance test was used to measure the % of the animal's total bodyweight being placed on the ipsilateral hind limb. Healthy, untreated rats equally distributed their bodyweight on each hind limb, therefore a cut-off of 40% of total bodyweight being placed on the ipsilateral limb was used to indicate detectable motor deficiency. All doses (except 40 U/Kg of LC/E-BoNT/A) reduced the weight placed on the ipsilateral hind limb below 40% of the total body weight, indicating a reduction of hind limb function (Fig. 3.5 E). While this seemed

a more sensitive test than the rotarod, it still wasn't acceptable as 40 U/Kg of LC/E-BoNT/A had induced limping behaviours. Since all doses induced noticeable limping of the ipsilateral hind limb they were deemed unsuitable to be tested for analgesic effects in the CFA model. As neither incapacitance nor rotarod testing could be used to quantify the paralytic effects of lower doses in the knee joint, a new assay was required. It was observed that the rats were unable to abduct the digits of the treated hind paws, possibly by spread of excess BoNT from the knee joint to nearby nerves innervating the extensor digitorum longus muscle responsible for digit abduction. Therefore, the rat digit abduction assay (Broide et al., 2013) was selected to identify the MaxTD in the final dosing study.

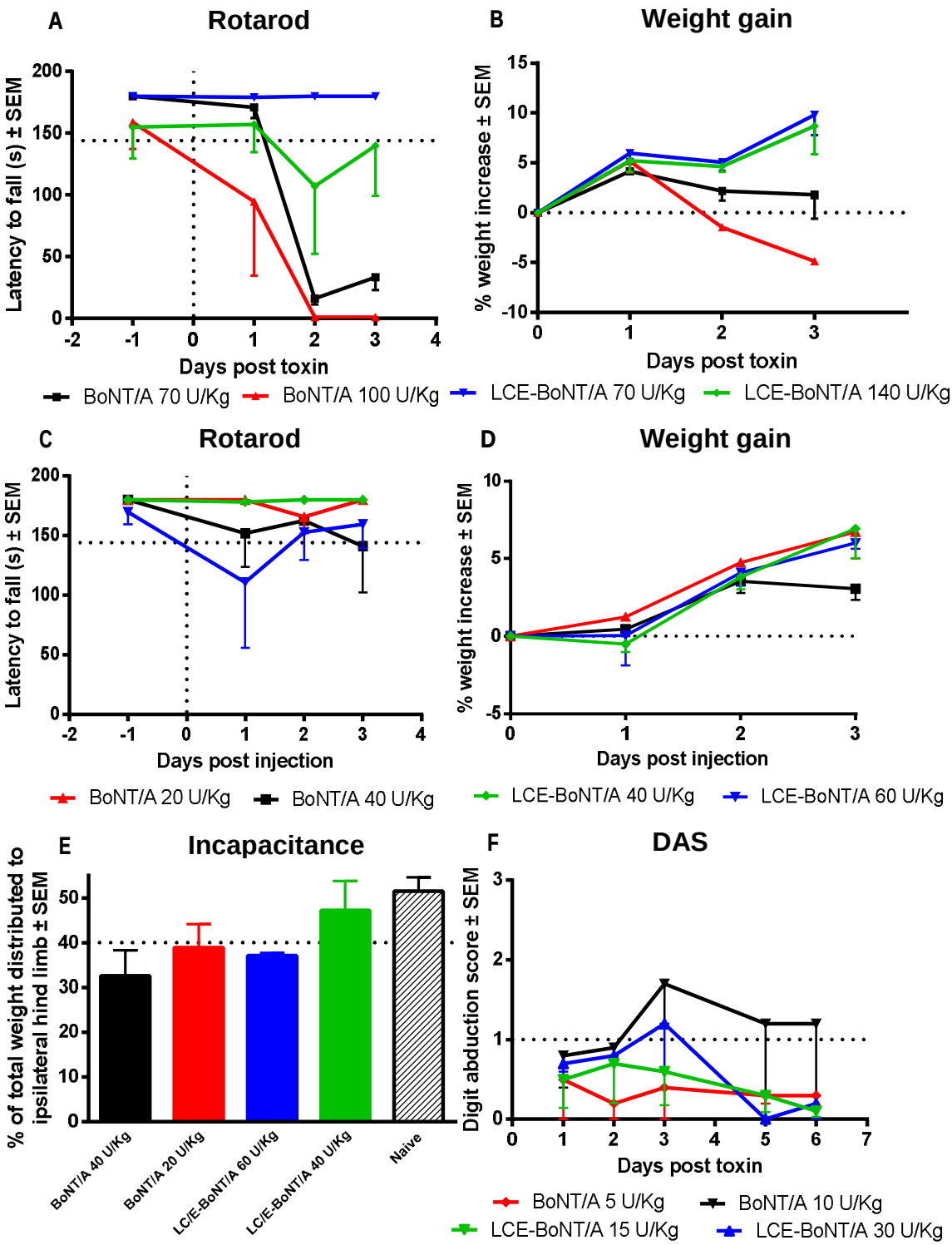

Fig. 3.5. Intra-articular injections of BoNT/A and LC/E-BoNT/A as low as 10 U/Kg and 30 U/Kg, respectively, caused motor impairment as measured by assays of locomotor function and digit abduction Time courses of rotarod tests are depicted in **(A)** and **(C)** with the corresponding weight gain data presented in **(B)** and **(D)**. Weight gain data are indicative of potential systemic toxicity from BoNT injections. Impaired weight bearing is presented in **(E)** and paralysis of the DAS reflex is presented in **(F)**. Vertical, dotted lines indicate injection date and horizontal dotted lines show cut-offs set for the dose effects on rats. Sample sizes for all groups was n=2 and all data presented as means ± SEM. 22 of the 24 rats used weighed 170 – 220 g at the time of BoNT injections, the remaining 2 rats weighed 320-365 g at the time of BoNT injections. This was due to a limited number of animals available at the time of this study. Vehicle: 0.5% BSA in normal saline.

Four final doses were screened using the DAS (a measure of digit abduction paralysis) post injection, namely 15 and 30 U/Kg LC/E-BoNT/A, 5 and 10 U/Kg of BoNT/A. Of these four doses, only 10 U/Kg of BoNT/A and 30 U/Kg of LC/E-BoNT/A showed limping behaviour in the treated hind limb. Furthermore, both these groups gave a DAS score greater than one by day three post injection, reaching the cut-off point for the MaxTD (Fig. 3.5 F). Hence, both doses were deemed unsuitable for testing in knee pain models. The MaxTD of BoNT/A was set at 5 U/Kg, as it showed no paralytic effects in the DAS test, nor did it induce obvious limping post injection. Since the 30 U/Kg dose of LC/E-BoNT/A only induced a mild and transient paralytic effect as measured by the DAS (1 day), it was expected that a 50% decrease to 15 U/Kg would be too great and not reflective of a MaxTD. Hence, the MaxTD of LC/E-BoNT/A was set at 25 U/Kg, a 16.67% decrease from 30 U/Kg.

MaxTD of BoNT/A and LC/E-BoNT/A had no anti-nociceptive or anti-inflammatory effect on the rat CFA model of chronic inflammatory pain

Baseline incapacitance performance and PAM thresholds were recorded two days before intra-articular injection of CFA into the knee joint. Transverse knee diameter was measured on the day of injection while the animals were anaesthetised, prior to induction of the model. Within one day after CFA injection, functional performance of the ipsilateral limb deteriorated as measured by incapacitance testing (Fig. 3.6 A), thresholds to mechanical pressure on the ipsilateral knee joint decreased (Fig. 3.6 B) and considerable swelling around the ipsilateral joint developed (Fig. 3.6 C). Both weight bearing, and mechanical thresholds were shown to gradually improve right up to the last testing day (31 days post CFA). Transverse knee diameter on the other hand decreased from peak swelling for up to 8 days after induction of the model but remained stable for the rest of the study. Seven days after model induction, rats were injected with either vehicle, 5 U/Kg of BoNT/A or 25 U/Kg of LC/E-BoNT/A. Neither toxin improved functional weight bearing, mechanical thresholds or transverse knee diameter in comparison to vehicle injections. It is possible that the doses injected into the knee were too low to have a significant anti-nociceptive effect. This is reflected in Fig. 3.6 D, where both toxins only slow the growth curves of the rats slightly. Based on previous experience the MaxTD dose of BoNTs would be expected to have a greater effect on

slowing rat weight gain. Furthermore, these doses were far lower than the analgesic dose of LC/E-BoNT/A (75 U/Kg) and the dose of BoNT/A that showed a statistically non-significant increase improvement in mechanical sensitivity in SNI model (15 U/Kg, refer to Fig. 3.1). Considering the persistent, painful inflammation of the knee joint (lasting 28+ days) the symptoms of this model were likely too severe to be effectively reduced by such low doses.

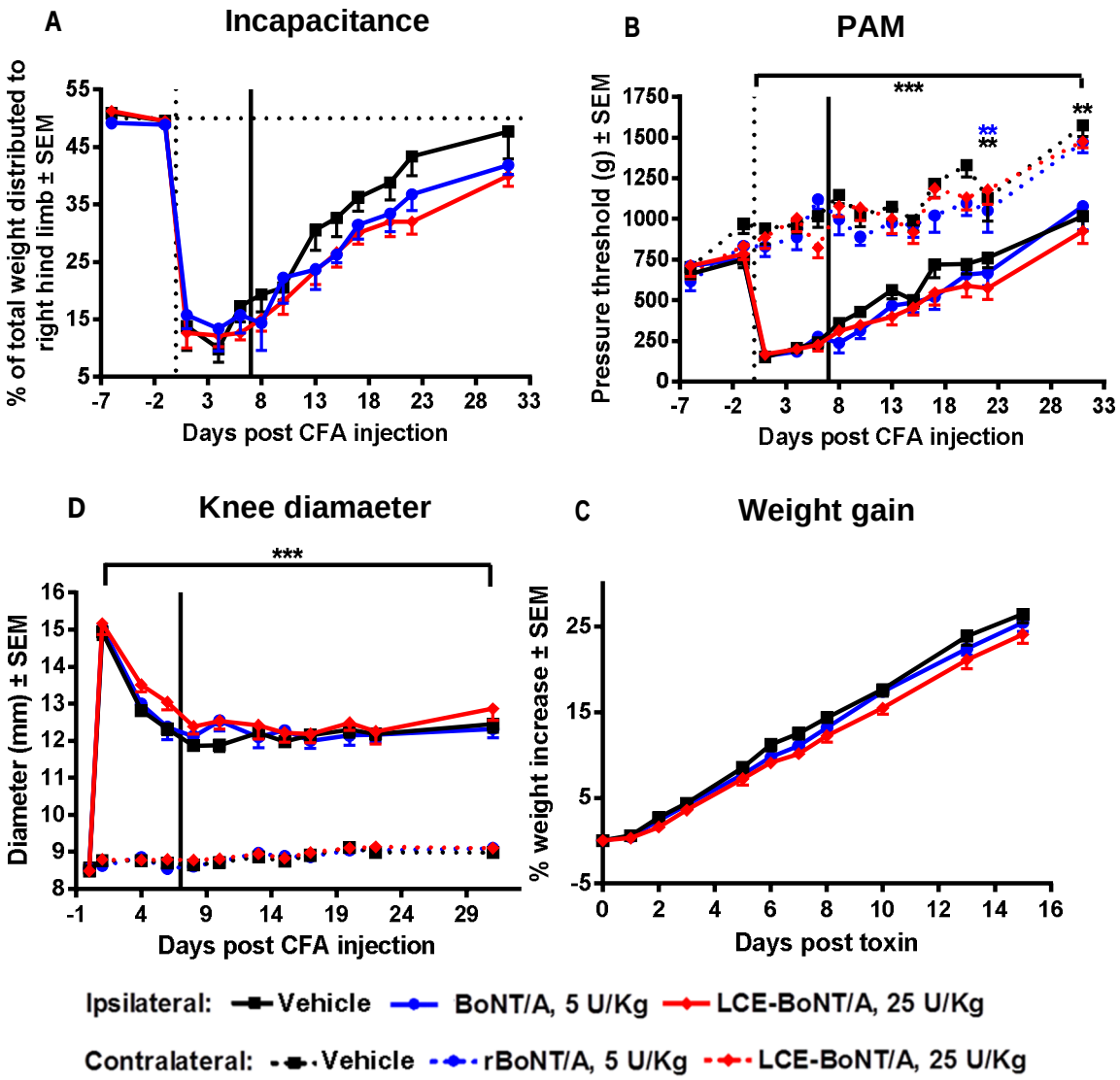

Fig. 3.6 Intra-articular injections of BoNTs MaxTD doses lacked an anti-nociceptive or anti-inflammatory effect in the CFA model of knee pain and inflammation Time courses of **(A)** functional weight bearing, **(B)** mechanical thresholds, **(C)** transverse knee diameter, and **(D)** weight gain. All data presented as means ± SEM. Vertical dotted line shows day of CFA injection; solid vertical line indicates toxin injection day. Statistical analysis was conducted by repeated measures two-way ANOVA and Bonferroni *post hoc* tests. No statistical significance was found between any of the three treatment groups at any time points post BoNT injection. **(B)** ***, P<0.001, All ipsilateral knees vs. all contralateral knees, ** P<0.01, Vehicle ipsi vs vehicle contra, **BoNT/A ipsi vs BoNT/A contra. **(C)** ***, P<0.001, All ipsilateral knees vs. all contralateral knees. Saline: n=8, BoNT/A: n=7, LC/E-BoNT/A: n=8. Rats weighing 250 – 300 g at the time of CFA injections were used. Vehicle: 0.5% BSA and normal saline.

Acute inflammatory pain

LC/E-BoNT/A reduces nocifensive behaviour in rats induced by intra-plantar injection of formalin

To further investigate the anti-nociceptive potential of LC/E-BoNT/A in relieving inflammatory based pain, the chimera was tested against vehicle in the formalin model of acute inflammatory pain. This model was selected as BOTOX® has previously been shown to reduce formalin-induced lifting and licking behaviour in phase 2 of the model but not phase 1 (Cui et al., 2004). Rats were pre-treated with LC/E-BoNT/A or vehicle by intra-plantar injection five days before receiving injections of formalin to the same hind-paw. The formalin-induced behaviours assessed were hind-paw flinching, lifting, licking and combined lifting/licking. After injection of formalin the characteristic bi-phasic response was observed; the animals initially spent up to 5 minutes displaying nocifensive behaviour (phase 1), followed by a longer period of nocifensive behaviour (phase 2) gradually decreasing over a total of 60 minutes after injection of formalin (Fig. 3.7 A-D). As some time-points in Fig. 3.7 were missing due to corrupted recordings of animal behaviour, the time-courses were not suitable for statistical analysis, and so this was performed by area under the curve analysis instead (Fig. 3.8). Animals pre-treated with LC/E-BoNT/A did not show a clear difference in flinching behaviour between 5 and 10 minutes after formalin (Fig. 3.7 A) which was likely due to an anti-nociceptive effect of LC/E-BoNT/A on flinching behaviour in phase 1 (Fig. 3.8 A); this was not observed in the other phase 1 behavioural parameters. Animals pre-treated with LC/E-BoNT/A showed reduced flinching behaviour in phase 2 (15-60 min) (Fig. 3.8 E) and reductions in lifting behaviour in phase 2 when compared to vehicle (Fig. 3.7 B, 3.8 F). Unexpectedly, rats treated with LC/E-BoNT/A showed some increase in phase 2 licking behaviour compared to those treated with vehicle, although this was not found to be statistically significant (Fig. 3.7 D, 3.8 H). When lifting and licking behaviour were combined, pre-treatment with LC/E-BoNT/A was found to reduce overall phase 2 nocifensive behaviour, but this did not achieve statistical significance (Fig. 3.7 C, 3.8 G). Although BOTOX has previously been demonstrated to cause a dose-dependent reduction in phase 2 lifting/licking scores, it has never been shown to affect phase 1 formalin-

induced flinching behaviour. Here, LC/E-BoNT/A was found to decrease phase 1+2 flinching and on phase 2 lifting, but not on phase 2 licking or combined lifting/licking behaviour. Together, these results indicate that pre-injection of LC/E-BoNT/A provides a moderate antinociceptive effect in the formalin model of acute inflammatory pain.

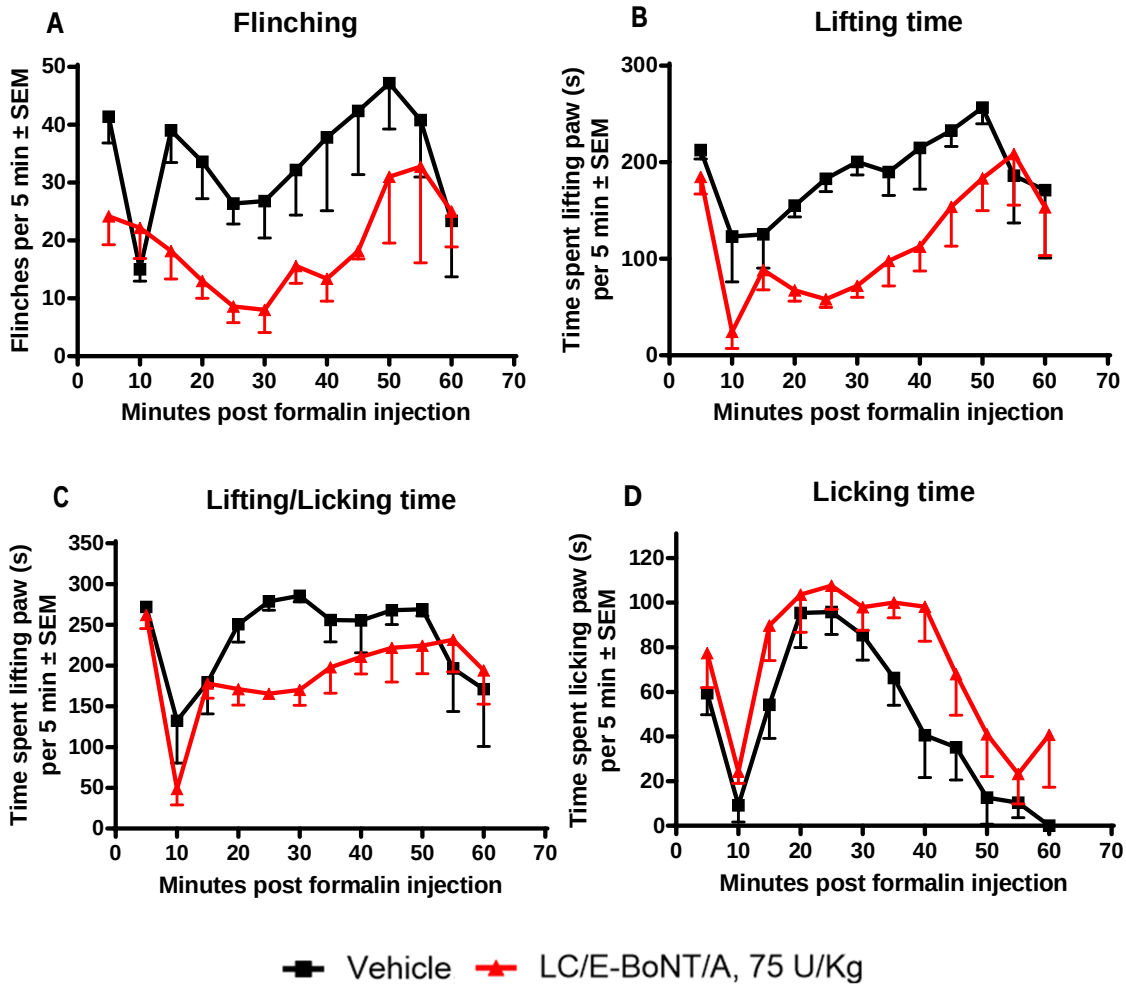

Fig. 3.7 Time courses show antinociceptive effects of LC/E-BoNT/A in the rat formalin model on phase 1 hind-paw flinching, phase 2 hind-paw flinching and lifting, but no effect on hind-paw licking Hind-paw flinching **(A)**, lifting time **(B)**, combined lifting and licking time **(C)** and licking time **(D)** were plotted as time courses relative to formalin injection. Time points represent total behaviour within a 5-minute block. Data plotted as means ± SEM. Rats weighing between 190 – 250 g at the time of BoNT/vehicle injections were used. LC/E-BoNT/A n=4-5, vehicle n=5. Vehicle: 0.5% BSA and normal saline.

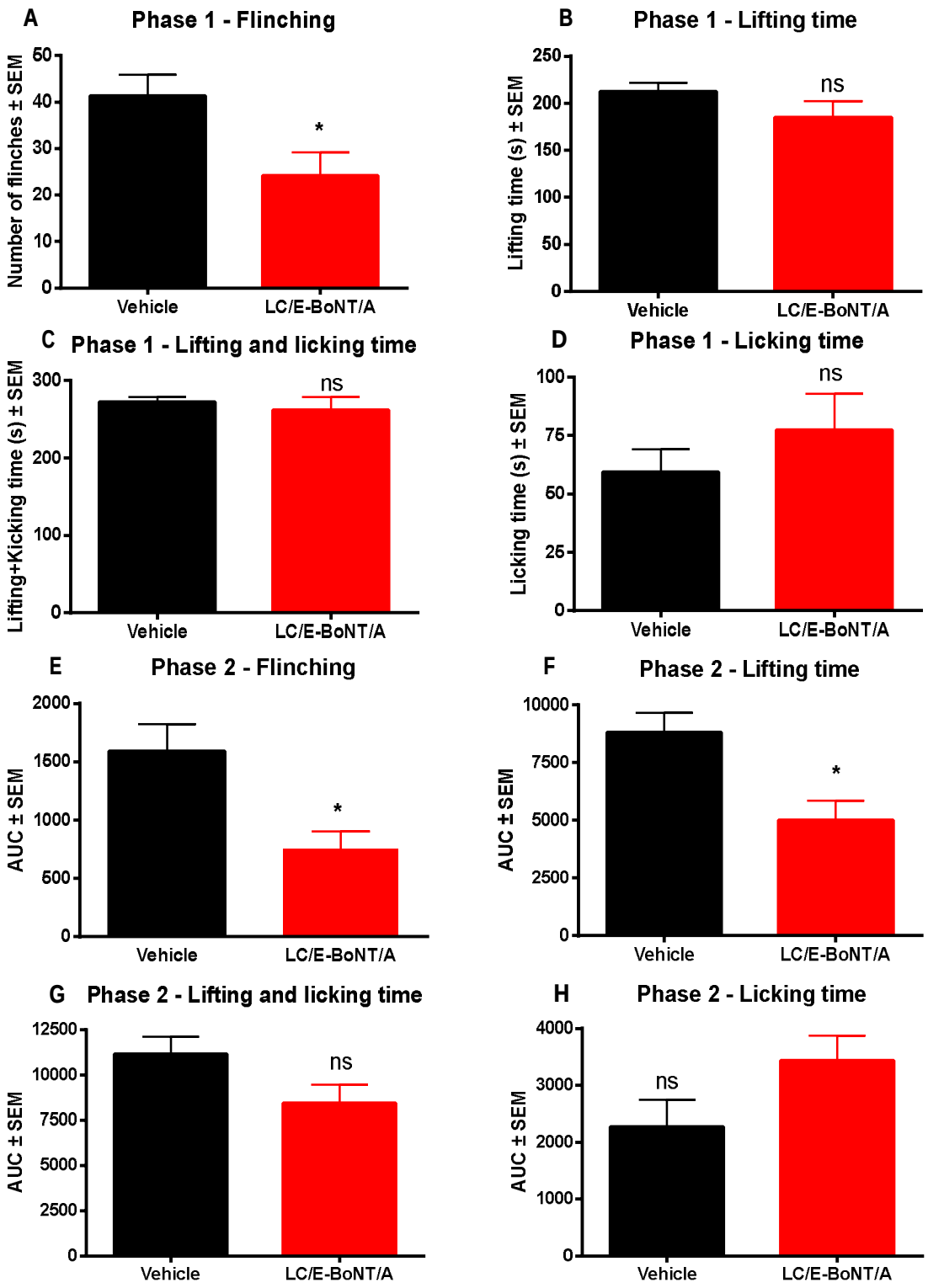

Fig. 3.8 AUC analysis of antinociceptive effects of LC/E-BoNT/A in the rat formalin model show significant effects on phase 1 hind-paw flinching, phase 2 hind-paw flinching and lifting Total hind-paw flinching **(A),** lifting time **(B),** combined lifting and licking time **(C)** and licking time **(D)** up to 5 minutes after formalin injection were plotted (phase 1). Total hind-paw flinching **(E),** lifting time **(F),** combined lifting and licking time **(G)** and licking time **(H)** from 15-60 minutes after formalin injection were plotted (phase 2). Data plotted as means ± SEM and analysed by unpaired t-tests. *, P<0.05, LC/E-BoNT/A vs. vehicle, ns, no significant difference LC/E-BoNT/A vs vehicle. Vehicle n=5, LC/E-BoNT/A n=4-5. Rats weighing between 190 – 250 g at the time of BoNT/vehicle injections were used. Vehicle: 0.5% BSA and normal saline.

LC/E-BoNT/A demonstrates further anti-nociceptive effects than BoNT/A on capsaicin-induced lifting and licking behaviours

As LC/E-BoTIM/A and BoNT/A have both been shown to reduce capsaicin-induced nocifensive behaviours and heat hyperalgesia (Wang et al., 2011a), the capsaicin model was selected to further explore the anti-nociceptive effects of LC/E-BoNT/A in acute, inflammatory pain. Buprenorphine, a μ-opioid receptor agonist as well as a κ-opioid receptor antagonist, has been shown to have an analgesic effect in the capsaicin rat model, thus it was used as the positive control (Kress, 2009, Barrett et al., 2003). LC/E-BoNT/A, BoNT/A and buprenorphine were all tested in the capsaicin model. Following completion of the behavioural analysis, spinal cords were dissected from euthanised rats and processed for immunostaining. Specifically, sections were analysed for c-fos expression, with c-fos upregulation being a common marker of pain signal induction to the dorsal horn (Hunt et al., 1987). Thus, it was tested if behavioural antinociceptive effects would correlate with a reduction in c-fos upregulation.

Four days before capsaicin injections, rats received intra-plantar injections of either 75 U/Kg of LC/E-BoNT/A, 15 U/Kg of BoNT/A or vehicle. On the testing day, animals then received injections of capsaicin into the same hind-paw. The rats assigned to the positive control group, were given a sub-cutaneous injection of 0.2 mg/kg of buprenorphine diluted in normal saline (Abbott and Bonder, 1997) 30 minutes before capsaicin injections. Following injections of capsaicin, nocifensive behaviour and hypersensitivity to noxious heat was observed at levels consistent with the literature (Wang et al., 2011a). Sub-cutaneous buprenorphine significantly reduced all nocifensive behaviours induced by capsaicin, as well as inhibiting heat hyperalgesia compared to rats pre-treated with vehicle four days before capsaicin injection (Fig. 3.9 A-D). Buprenorphine also significantly inhibited capsaicin-induced increased c-fos expression in the ipsilateral dorsal horn in comparison to vehicle, to the point where there was no significant increase in ipsilateral c-fos expression compared to contralateral dorsal horns (Fig. 3.10 D-E).

LC/E-BoNT/A injections 4 days prior to capsaicin significantly reduced the combined lifting + licking behaviour and lifting time in comparison to vehicle (Fig. 3.9 A-B) but had no effect on licking behaviour or latency to respond on the hotplate (Fig. 3.9 C-D). LC/E-BoNT/A did not significantly improve the affected parameters compared to BoNT/A pre-treatment, however BoNT/A was shown to only be effective on lifting behaviour and not significantly reduce lifting + licking time (Fig. 3.9 A-B). Unlike buprenorphine treated animals, capsaicin-induced ipsilateral c-fos counts for LC/E-BoNT/A or BoNT/A treated animals were not significantly different from vehicle treated rats (Fig. 3.10 E). Thus, although both BoNTs showed moderate antinociceptive behavioural effects, these were not correlated with a reduction in capsaicin-induced c-fos upregulation (Fig. 3.10 E).

While there were detectable anti-nocifensive effects of both toxins in the capsaicin model, those induced by BoNT/A were noticeably diminished in comparison with a previous study using BoNT/A produced by this lab, in the capsaicin pain model (Wang et al., 2011a). Furthermore, animals injected with 15 U/Kg of BoNT/A gained weight at the same rate as rats injected with vehicle, while animals injected with 75 U/Kg of LC/E-BoNT/A exhibited a slower growth curve (Fig. 3.9 E). This may indicate a drop in BoNT/A activity, explaining the reduced anti-nociceptive effect.

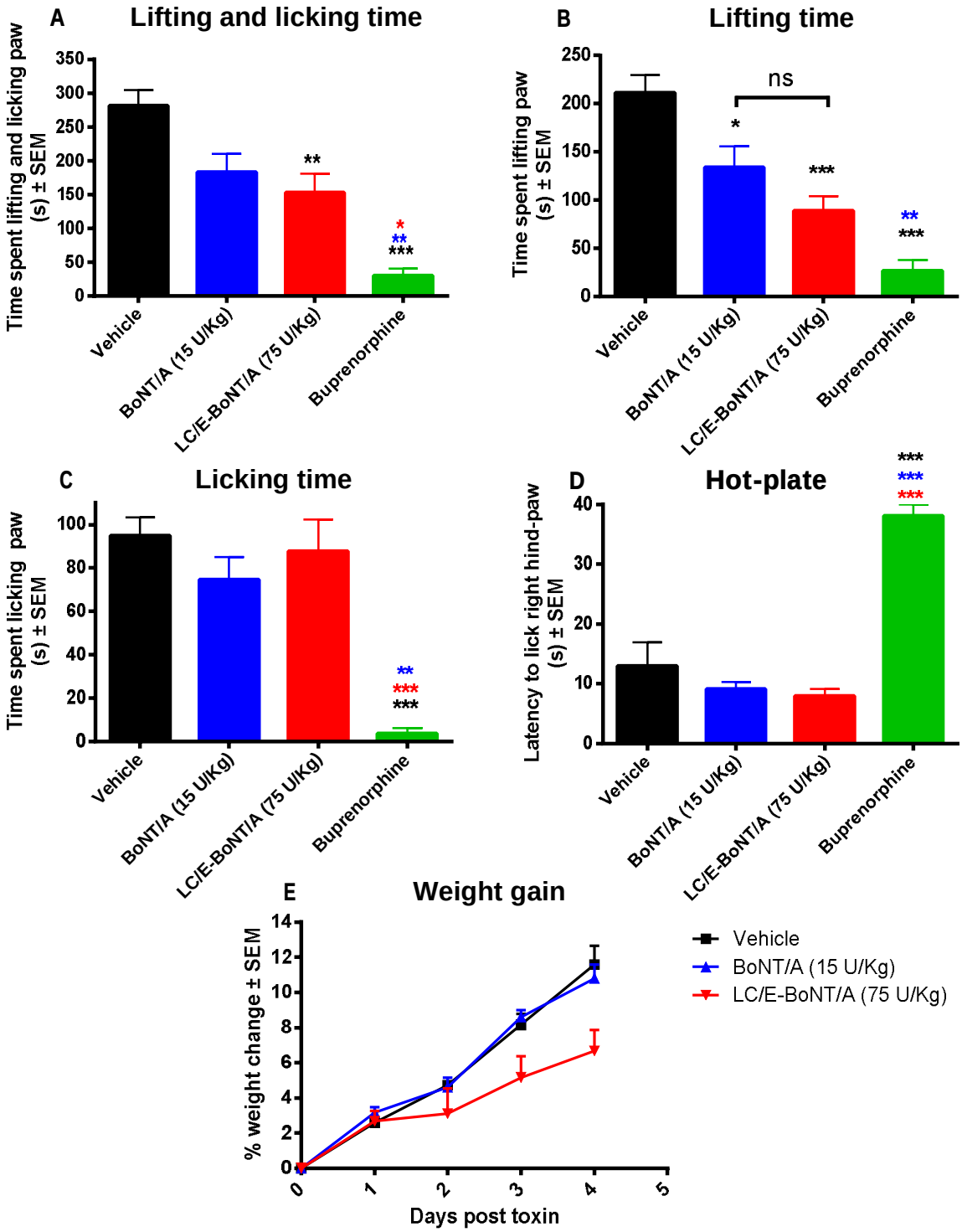

Fig. 3.9 LC/E-BoNT/A and BoNT/A reduce capsaicin evoked nocifensive pain behaviours but not on heat hyperalgesia overall in rats Total hind-paw lifting + licking time **(A),** lifting time **(B),** licking time **(C)** and heat thresholds on a hot plate set to 54.5 °C (±0.5 °C) **(D)** were plotted. Histograms represent total behaviour up to 10 minutes after capsaicin injection. Data plotted as means ± SEM and was analysed by one way ANOVA by group with a significant effect detected in licking ($F_{(3, 23)} = 12.86$, $p<0.001$), lifting ($F_{(3, 23)} = 15.24$, $p<0.001$), licking ($F_{(3, 23)} = 10.13$, $p<0.001$) and hot plate ($F_{(3, 23)} = 23.74$, $p<0.001$). Bonferroni *post hoc* tests: *, P<0.05, vs vehicle, **, P<0.01, vs vehicle, ***, P<0.001, vs vehicle, **, P<0.01, ***, P<0.001 vs. BoNT/A, *, P<0.05, vs LC/E-BoNT/A, ***, P<0.001, vs. LC/E-BoNT/A. Vehicle n=6, LC/E-BoNT/A (75 U/Kg) n= 7, BoNT/A (15 U/Kg) n=7, buprenorphine (0.2 mg/Kg) n=4. Rats weighed between 186 – 270 g at the time of capsaicin injections. Behaviour tests performed in collaboration with Dr Orla Moriarty. Vehicle: 0.5% BSA and normal saline.

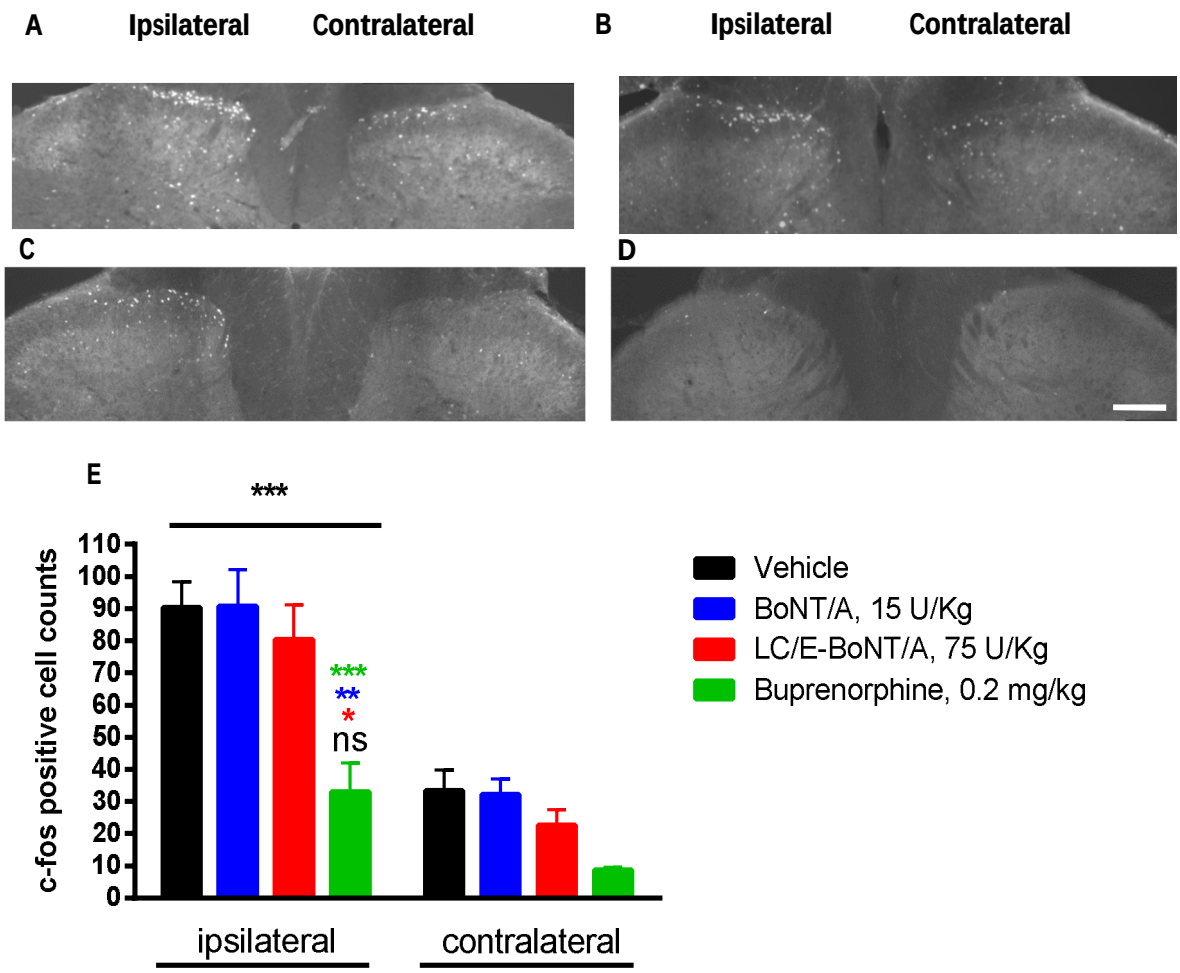

Fig. 3.10 Buprenorphine reduced capsaicin-induced c-fos expression in the L4-L5 dorsal horn of the spinal cord unlike LC/E-BoNT/A or BoNT/A, representative images and histograms (A) Vehicle, **(B)** LC/E-BoNT/A (75 U/Kg), **(C)** BoNT/A (15 U/Kg) pre-treatment (4 days before capsaicin) and **(D)** buprenorphine (0.2 mg/Kg) pre-treatment (30 minutes before capsaicin). Ipsilateral dorsal horns depicted on the left, contralateral on the right. **(E)** Data were analysed by a two-way ANOVA with side (ipsi vs. contra) and group as factors. There were significant main effects of both side ($F_{(1, 28)} = 49.67$, $p<0.001$) and group ($F_{(3, 28)} = 18.4$, $p<0.001$). Bonferroni *post hoc* tests showed that the number of c-fos positive cells increased in the superficial lumbar dorsal horn on the side ipsilateral to intra-plantar capsaicin injection compared with the contralateral side. Black symbols ipsi vs. respective contra; green symbols vs. vehicle; blue symbols vs BoNT/A; red symbols vs. LC/E-BoNT/A. Data are presented as means ± SEM, n=3-5. Each n number is an average of counts from a minimum of 4 sections/rat from L4-5 of the spinal cord. Rats used weighed 186 – 270 g at the time of capsaicin injections. Vehicle: 0.5% BSA and normal saline. Scale bar: 200 µm

Inconsistencies in effect of LC/E-BoNT/A and BoNT/A in rodent pain models and testing of a fresh batch of LC/E-BoNT/A

Observations of decreased LC/E-BoNT/A activity

Re-testing of LC/E-BoNT/A manifested a reduced anti-nociceptive profile in the rat formalin model, while BoNT/A pre-injection showed no anti-nociceptive effect

To reproduce the anti-nociceptive effect of LC/E-BoNT/A in the formalin model (Fig. 3.8) and determine its effectiveness vs BoNT/A, both toxins were tested using the formalin model, along with a vehicle control. Four days prior to formalin testing animals were pre-treated with either 75 U/Kg of LC/E-BoNT/A, 15 U/Kg of BoNT/A or vehicle (Fig. 3.11-3.12). Unexpectedly, the analgesic effect of LC/E-BoNT/A on formalin-induced behaviours was not reproduced in this study. Pre-injection of LC/E-BoNT/A did not reduce phase 2 hind-paw lifting behaviours, as shown in the pilot study (Fig. 3.11 B vs. Fig. 3.8 F). Curiously, LC/E-BoNT/A was shown to significantly reduce licking behaviour at 15 minutes after injection of formalin (Fig. 3.11 A), which was not observed in the initial pilot study (Fig. 3.8 C); LC/E-BoNT/A also seemed to show a trend in reducing hind-paw licking behaviours over the entire time-course. Examining the AUC of formalin-induced licking behaviours highlights that the overall anti-nociceptive effect of LC/E-BoNT/A on hind-paw licking was significantly greater than the vehicle pre-injection (Fig. 3.12 A). Pre-treatment of BoNT/A, however, showed no significant effect in reducing any of the formalin-induced nocifensive behaviours compared to vehicle injection (Fig. 3.11 A-C. 3.12 A-C). This result differs from previous reports by Cui et al., 2004, where BOTOX® pre-treatment reduced formalin-induced nocifensive behaviours in rats, and by Luvisetto et al., 2006, where isolated 150 kDa BoNT/A reduced formalin-induced licking behaviours in mice. Both BoNTs had a minor inhibitory effect on weight gain at 4 days post toxin (Fig. 3.11 D), less than the normal effect on rat growth curves expected of these toxin doses based on previous experience (see effect of LC/E-BoNT/A in Fig. 3.9 E). This lack of an obvious effect on weight gain and the inconsistent anti-nociceptive effect in the formalin model indicated that there may have been a potency decrease in both toxins since their last use.

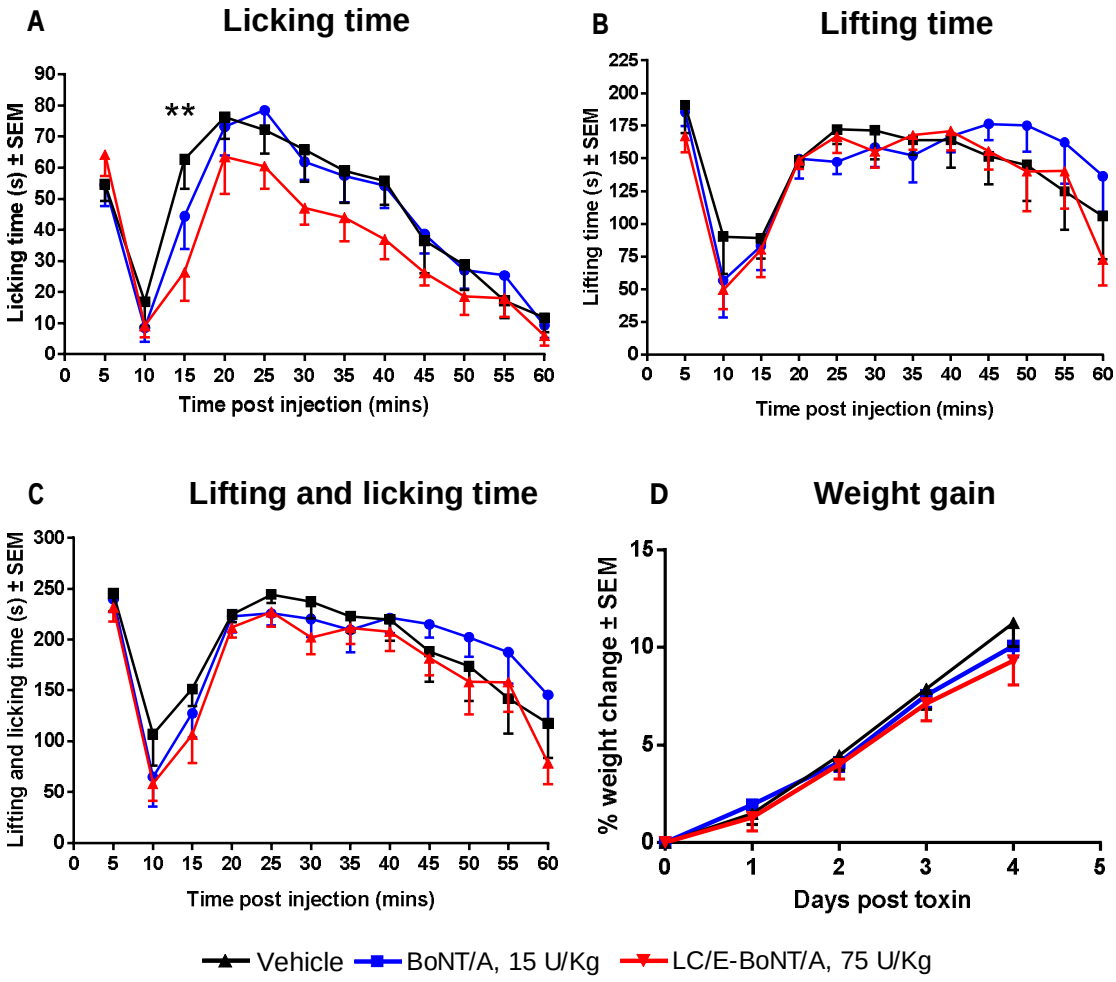

Fig. 3.11 Time-course shows anti-nociceptive effect of LC/E-BoNT/A on formalin-induced licking behaviours but not lifting, no effect of BoNT/A observed in rat formalin model Hind-paw licking time **(A),** lifting time **(B),** combined lifting and licking time **(C)** relative to formalin injection, and rat weight gain **(D)** relative to toxin injection were plotted. Data plotted as means ± SEM and was analysed by repeated measures two-way ANOVA with time and experimental group as factors. For all licking and lifting + licking there was a significant main effect of time ($F_{(11, 242)} = 29.3$, $p < 0.001$; $F_{(11, 264)} = 22.3$, $p < 0.001$) but not in lifting. No significant effect of group was detected in any parameters. Bonferroni *post hoc* tests showed a significant effect of LC/E-BoNT/A on licking time at 15 minutes post formalin, **, P<0.01, LC/E-BoNT/A vs. vehicle. BoNT/A n=9, LC/E-BoNT/A n= 8, Vehicle n=8. Rats weighing between 190 – 250 g at the time of BoNT/vehicle injections were used. Behaviour tests performed in collaboration with Dr Orla Moriarty. Vehicle: 0.5% BSA and normal saline.

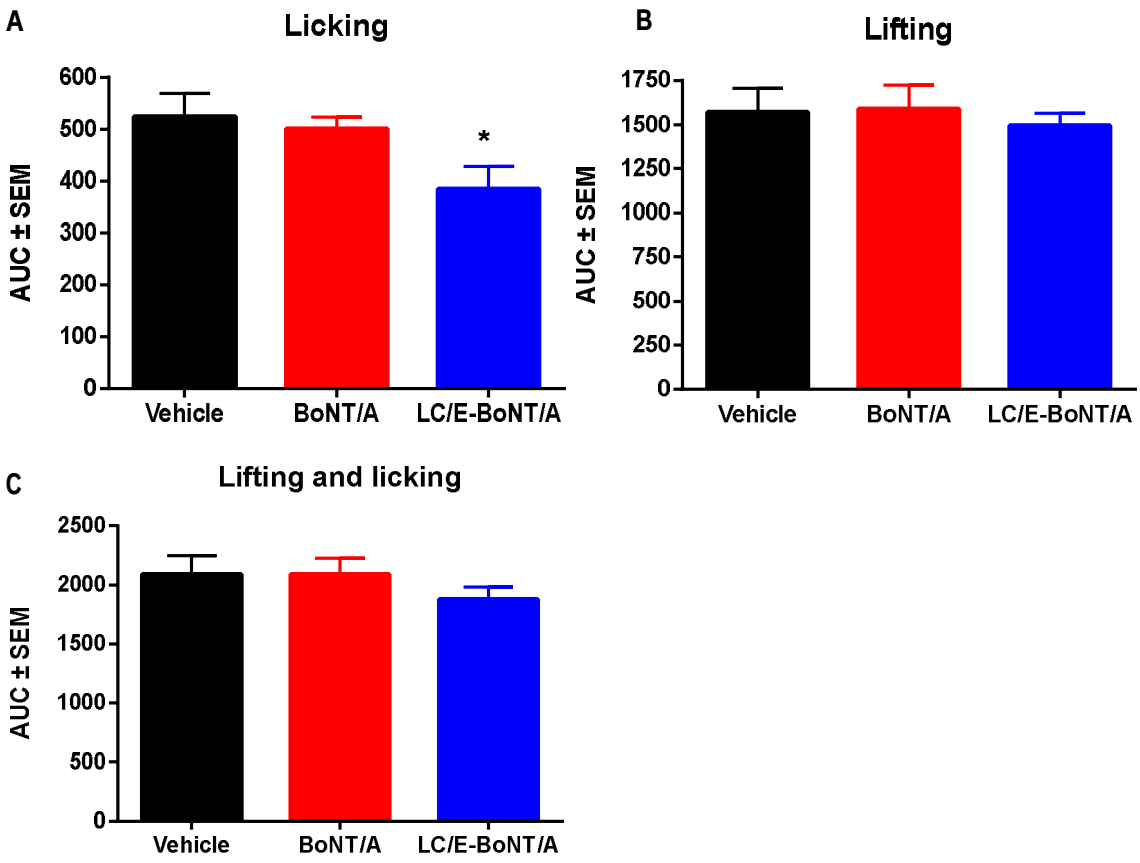

Fig. 3.12 AUC analysis confirms significant effect of LC/E-BoNT/A on overall formalin-induced licking behaviour Total hind-paw licking **(A),** lifting time **(B),** and combined lifting and licking time **(C).** Histograms represent total behaviour (60 min) after formalin injection. Data plotted as means ± SEM and was analysed by one-way ANOVA by group with a significant effect detected in licking ($F_{(2, 24)} = 3.91$, $p<0.05$). Bonferroni *post hoc* tests showed a significant effect of LC/E-BoNT/A vs vehicle, *, $P<0.05$. Vehicle n=8, LC/E-BoNT/A (75 U/Kg) n= 8, BoNT/A (15 U/Kg) n=9. Rats weighing between 190 – 250 g at the time of BoNT/vehicle injections were used. Behaviour tests performed in collaboration with Dr Orla Moriarty. Vehicle: 0.5% BSA and normal saline.

LC/E-BoNT/A and BoNT/A retained activity *in vitro* and was of acceptable purity, LC/E-BoNT/A showed reduced activity compared to results when initially produced

To determine whether long term storage at -20 °C affected the biological activity of LC/E-BoNT/A and BoNT/A, *in vitro* potency and purity tests were conducted. Both toxins were assessed using an established *in vitro* substrate cleavage assay (Wang et al., 2012) and sample purity and integrity was investigated by SDS-PAGE and protein staining. Fig. 3.13 B shows that aliquots of both toxins retained proteolytic activity, albeit diminished from when first produced (discussed in chapter 4). In Fig. 3.13 A it can be seen that under non-reducing conditions some of the LC/E-BoNT/A lacked

intact di-sulphide bonds, as shown by the presence of a faint band at the same size marker as the DTT reduced sample. This was unlikely to affect the analgesic ability of LC/E-BoNT/A as most of the non-reduced sample retained the di-sulphide bonds, while BoNT/A non-reduced sample contained only toxin with intact di-sulphide bonds. Estimated EC_{50} of the two neurotoxins (Fig. 3.13 C) showed that their LCs had similar levels of activity.

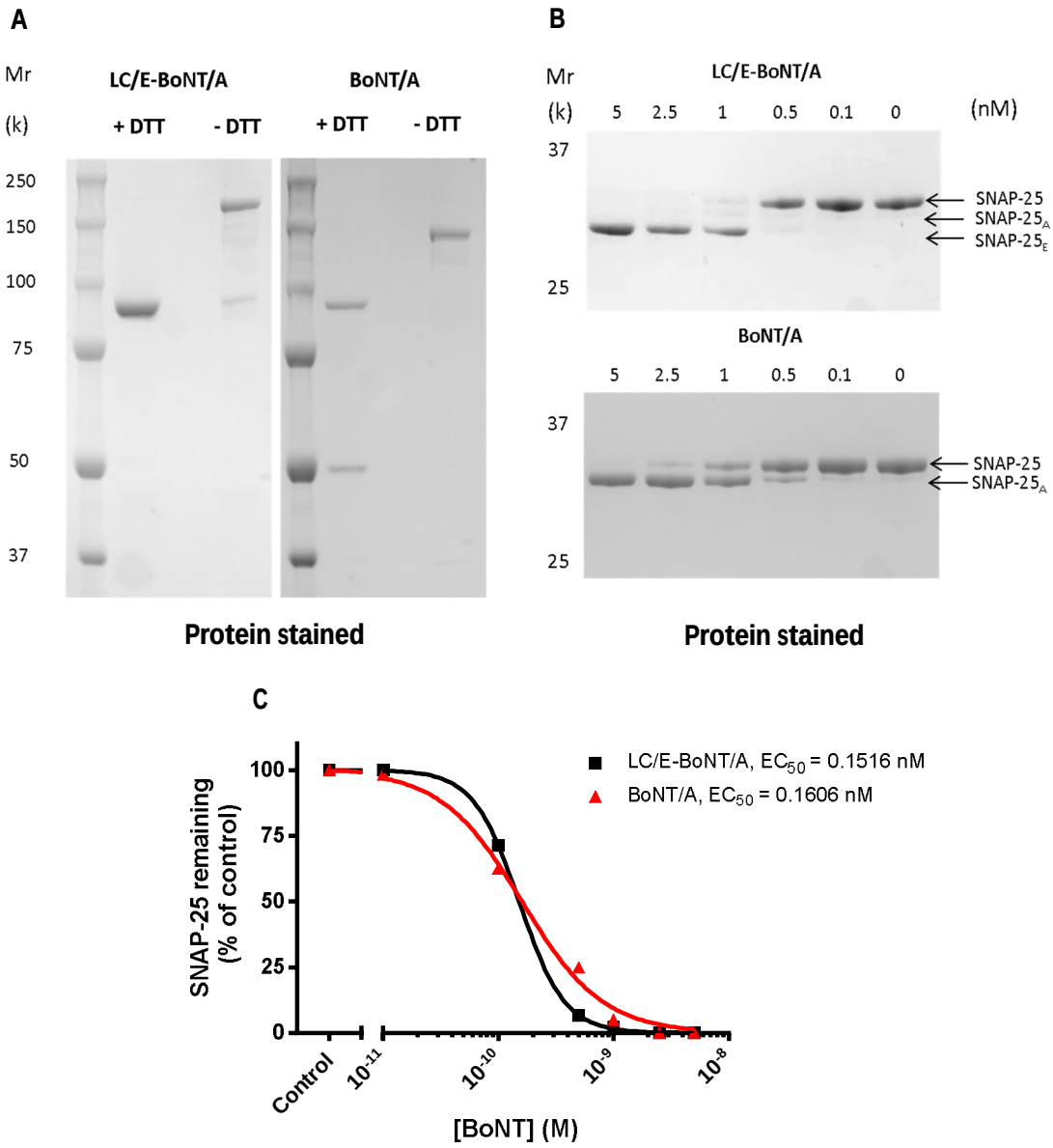

Fig. 3.13 LC/E-BoNT/A and BoNT/A samples retain integrity and proteolytic activity *in vitro* (**A**) Separation of the LC and HC are observed in the presence of DTT, which reduces the di-sulphide bond connecting the LC to the HC. A single, dense band can be seen in the lane with LC/E-BoNT/A + DTT, as the molecular mass of two LCs is equal to that of the HC (100 kDa) **(B)** Both LC/E-BoNT/A and BoNT/A cleaved recombinant SNAP-25 substrate at concentrations as low as 0.1 nM. **(C)** Estimated EC_{50} values were calculated from the cleavage assay for both toxins. **A-B:** Samples resolved by SDS-PAGE and Coomassie stained. Representative results: n=1.

MaxTD of LC/E-BoNT/A was found to have increased by 47%, indicating reduced activity

Following the results of the *in vitro* activity and purity tests for LC/E-BoNT/A and BoNT/A, a dose range study was conducted to confirm if the intra-plantar MaxTD of LC/E-BoNT/A had deviated since first being set at 75 U/Kg. Efforts were focused on LC/E-BoNT/A and not BoNT/A, to limit use of animals for these experiments. A broad range of LC/E-BoNT/A doses were injected into rats to find the upper limit where the toxin would induce locomotor dysfunction (rotarod test), muscle weakening (Kondziela grip test) and adversely affect animal health (weight gain). A "paralysis cut off" of 144 s (80% of baseline trial length of 180 s on rotarod) and 70% of pre-injection grip test performance was used to identify paralytic doses. A 3.5% decrease in weight from pre-treatment values was used as a cut-off for toxin doses considered to be unsuitable for screening in animal models. Intra-plantar injections of LC/E-BoNT/A showed a dose-response relationship in the effects on animal weight changes (Fig. 3.14 A). Based on weight loss combined with visual assessment of rat health (criteria in methods) (Fig. 3.14 D), 225-300 U/Kg were deemed unsuitable for further study. Both 225 and 300 U/Kg greatly impaired rotarod performance (Fig. 3.14 B) from day 1 post injection which began to recover at day 5 post injection. Both doses decreased grip strength (Fig. 3.14 C) to below the cut-off within two days after injection. Surprisingly, the rat treated with 125 U/Kg showed a greater decrease in grip strength performance than 175-225 U/Kg. This is likely due to the low sample sizes used per dose in this experiment and the variability between animals (n=1). Importantly, 75 U/Kg was shown to be almost indistinguishable from vehicle in its effects on weight gain, visual assessment and rotarod, but did have a minor effect on grip strength. Furthermore, there were no differences between 75-175 U/Kg on rotarod performance, and 125-175 U/Kg had no deleterious effects on animal weight gain.

Based on the initial dose range study, 90-150 U/Kg was selected to identify the new MaxTD for intra-plantar injections of LC/E-BoNT/A. The MaxTD was selected based on weight gain only since the visual assessment score, rotarod and grip test were not sensitive enough to consistently detect effects of the toxins at doses below 225 U/Kg, based on Fig. 3.14 B-C. Unexpectedly, 110-150 U/Kg

all induced weight loss in rats after injection (Fig. 3.14 E), contrary to the previous results which showed no weight loss until the dose exceeded 225 U/Kg (Fig. 3.14 A). This may be because the rats used in this dose experiment were older and less resilient to BoNT side-effects than those used in the previous study (190-230 g vs 275-350 g). To summarise the figure, 150 U/Kg caused a long-lasting decrease in body weight, reaching the cut-off at day 3 post toxin and therefore was unsuitable for further investigations. There were no major differences between 90-100 U/Kg and as neither dose induced greater than a 1% decrease in weight, these doses were too low to be the MaxTD . Slightly more weight loss was noted in rats treated with 110 U/Kg than those injected with 130 U/Kg, with both demonstrating similar patterns of weight change indicating that the doses had an approximately equal impact on animal health. The MaxTD was set at 110 U/Kg to ensure animals would not show severe adverse health effects, when the sample size was expanded for the pain studies. Together, these results show that ~47% more LC/E-BoNT/A could be injected than previously used by Wang et al., 2017a and in reported experiments until this point. This suggests that the observed inconsistency in anti-nociceptive effect between the formalin model experiments (Fig. 3.7-3.8 vs 3.11) and between the capsaicin experiment (Fig. 3.9) vs Wang et al. 2011a, may be due to decreases in potency of LC/E-BoNT/A during storage.

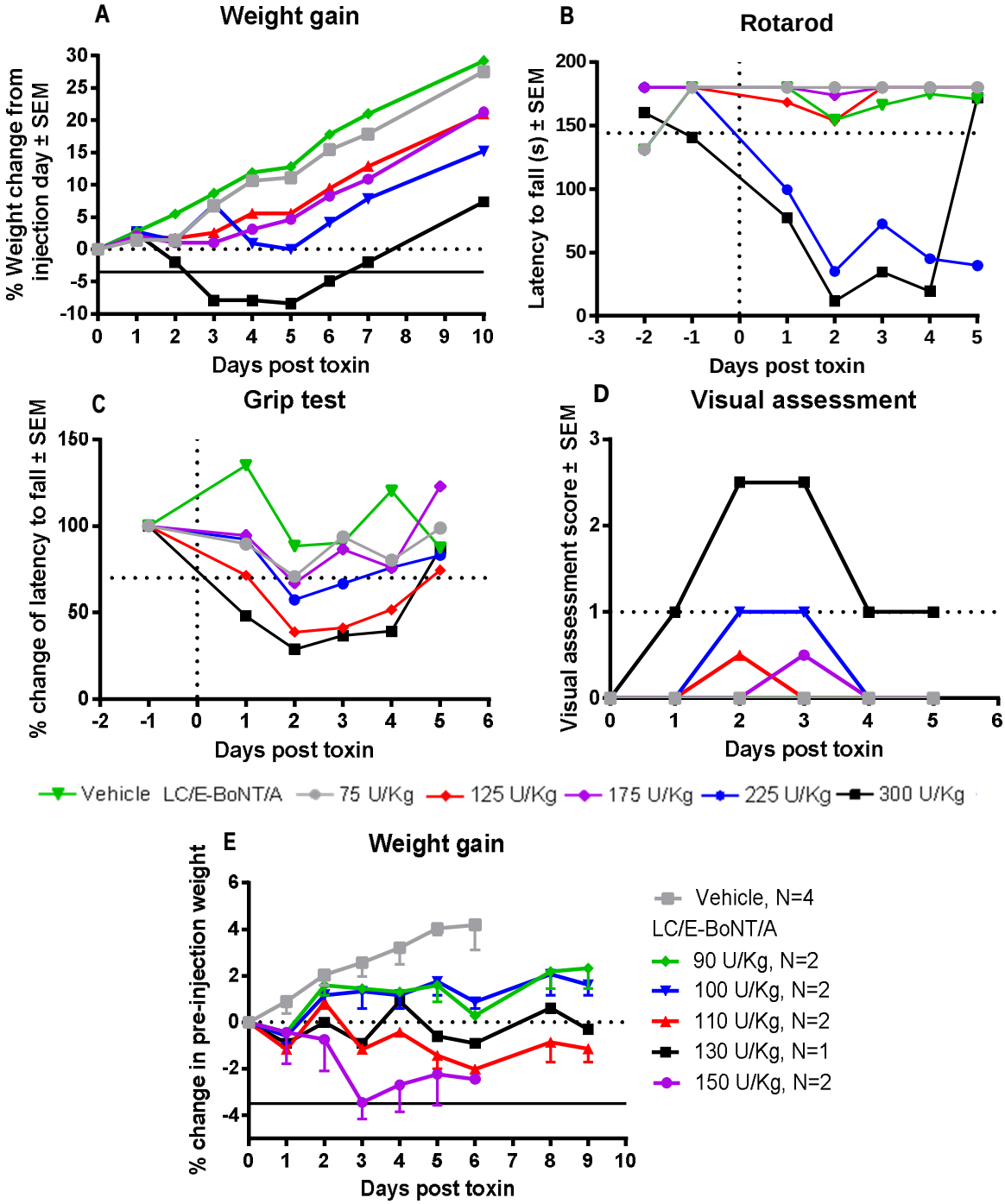

Fig. 3.14 MaxTD for intra-plantar injections of LCE/-BoNT/A was increased compared to first MaxTD of 75 U/Kg Time courses of % weight change **(A),** locomotor ability **(B),** hind limb strength **(C)** and overall animal health **(D)** relative to toxin injection (vertical dotted lines) presented. n=1 for all treatment groups. Horizontal lines in **(B)** and **(C)** indicate 80% performance cut off for rotarod (based on a 180 s trial cut-off) or 70% performance cut-off for grip strength based on average grip test performance before injection. Horizontal line in **(D)** indicates cut-off score for animal distress caused by toxin injections. **(E)** Time course of % weight change from pre-treatment weight. Data plotted as means ± SEM. The maximum tolerated dose selected for screening in the capsaicin model was based on 3.5% weight loss cut off (horizontal black line), indicating the maximum amount of weight loss that can be induced by LC/E-BoNT/A without impairing behaviour for pain studies. Horizontal dotted line at 0% (pre-injection bodyweight). Rats weighing 190 – 230 g at the time of BoNT injections were used in panels **A-D**, rats weighing 275 – 350 g at the time of toxin injection were used in **(E)**. Vehicle: 0.5% BSA and normal saline.

110 U/Kg LC/E-BoNT/A did not reproduce the antinociceptive effect of 75 U/Kg LC/E-BoNT/A in the capsaicin rat model of acute inflammatory pain

Vehicle and 110 U/Kg of LC/E-BoNT/A were injected into the hind-paw four days before intra-plantar injection of capsaicin in the ipsilateral paw. Increasing the dose of LC/E-BoNT/A from 75 U/Kg to 110 U/Kg caused a mild inhibitory effect of LC/E-BoNT/A on the rat growth curve, indicating toxin activity (Fig. 3.15 F). Despite this no significant effect on capsaicin-induced nocifensive behaviour (hind-paw flinching, lifting or licking) or heat hyperalgesia (hot-plate test) was observed (Fig. 3.15).

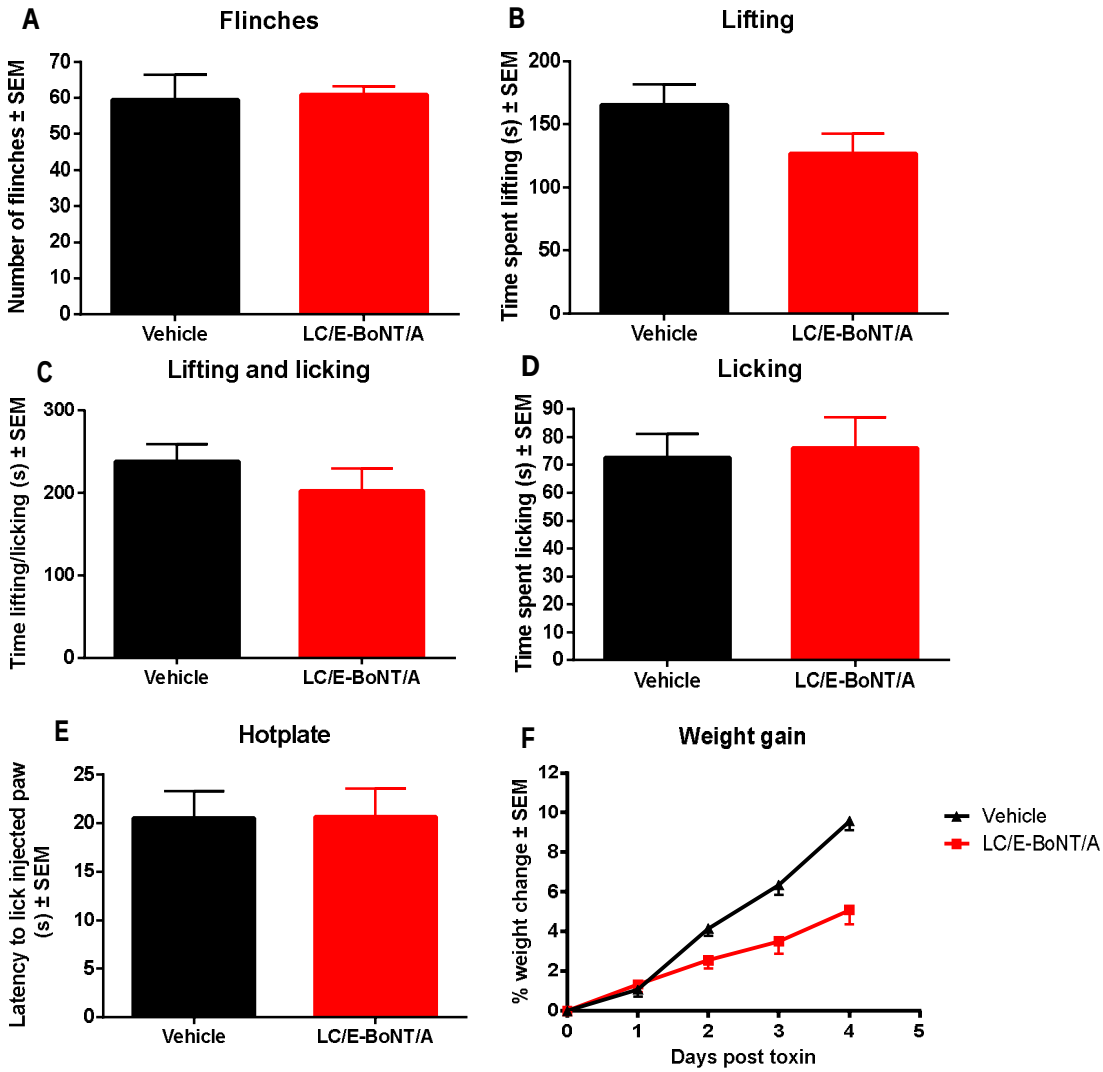

Fig. 3.15 Pre-treatment with 110 U/Kg LC/E-BoNT/A had no effect on all capsaicin-induced nocifensive behaviours in rats Total hind-paw flinches **(A)**, lifting time **(B)**, lifting + licking time **(C)** licking time **(D)** and heat thresholds **(E)** on a hot plate set to 51 °C (±0.5 °C) were plotted. Histograms represent total behaviour up to 10 minutes after capsaicin injection. Data plotted as means ± SEM and was analysed by unpaired t-tests. No significant differences between LC/E-BoNT/A or vehicle pre-treatment four days before capsaicin injection. n=10 for both groups. Rats weighing 186 – 270 g at the time of capsaicin injections were used. Vehicle: 0.5% BSA and normal saline. Behaviour tests performed in collaboration with Dr Orla Moriarty.

Establishing potency and MaxTD of a second lot of LC/E-BoNT/A

Since the anti-nociceptive effect of LC/E-BoNT/A was now absent at higher doses in the capsaicin model of pain, a new batch of LC/E-BoNT/A (batch 2) was produced and tested to reproduce the results from the capsaicin and SNI models of pain. Batch 2 was injected in a new vehicle consisting of 0.05% HSA, 10 µM $ZnCl_2$ and 0.9% NaCl, the percentage of HSA in the vehicle being based on injections of BoNT/A complex in patients (Wohlfarth et al., 1997). Since BoNTs contain zinc dependent proteases, zinc was added to the vehicle to ensure activity of the LC/E-BoNT/A was retained after injection into the rat. These pain behaviour studies were performed in collaboration with Dr Orla Moriarty.

Potency of batch 2 LC/E-BoNT/A determined by refined mouse LD_{50} which was equal to potency of previous batch of LC/E-BoNT/A

Potency of batch 2 of LC/E-BoNT/A was tested in a refined version of the mouse LD_{50} assay. Mice received intra-peritoneal injections of LC/E-BoNT/A diluted in normal saline with 0.05% HSA and 10 µM $ZnCl_2$. Once they reached a pre-determined humane endpoint (severe indrawn scaphoid abdomen with respiratory distress & pupillary dilation or weight loss of 20% from pre-injection weight), the mice were euthanized. This is a refinement to the typical BoNT/A LD_{50} assay so it does not rely on death as an endpoint (NIEHS, 2008), that was a requirement by the HPRA to gain approval for these animal studies. The final minimum lethal dose (LD_{50}) value was estimated at 6×10^7 U/mg (1 LD_{50} unit = 16.6 pg), based on the % of mice euthanised from each dose of LC/E-BoNT/A (Fig. 3.16 A). These values matched the potency of batch 1 LC/E-BoNT/A when it was first produced.

MaxTD of batch 2 LC/E-BoNT/A was set at 120 U/Kg; SNAP-25 cleavage was detected in ipsilateral plantaris muscles at doses of 75 U/Kg and signs of systemic spread of LC/E-BoNT/A found at doses of 150 U/Kg

Injections of 150 – 300 U/Kg of batch 2 of LC/E-BoNT/A into the hind-paw of rats caused profound motor paralysis as shown by the rotarod test and weight loss that was unacceptable for further animal testing (Fig. 3.16 B-C). Doses between 75-125 U/Kg caused some impairment of rotarod performance, but it was unclear if this was due to motor impairment or inconsistent behaviour in rats, based on visual assessment of rotarod performance. While injections of 125 U/Kg did not result in any more motor impairment than 75-100 U/Kg, it did induce some mild weight loss along with toxicity symptoms such as nasal/ocular discharge. While none of the individual symptoms warranted reducing the MaxTD from 125 U/Kg, the cumulative stress of all the symptoms was at the threshold of what could be considered a MaxTD. Based on this, it was decided to reduce the MaxTD to 120 U/Kg to reduce toxicity symptoms.

To confirm proteolytic activity of LC/E-BoNT/A at the site of delivery, animals that had been injected with 75 or 150 U/Kg of LC/E-BoNT/A, or vehicle, were euthanised after the dosing study behavioural tests. The plantaris muscle from the ipsilateral and contralateral paws was dissected and homogenised, these samples were used for Western blotting and subsequent staining with an anti-SNAP-25 antibody, which detected intact SNAP-25, SNAP-25_A and SNAP-25_E. This would allow for detection of SNAP-25 cleavage post toxin injection in the hind-paw to correlate with effects on behaviour post injection. Lysate from a neuroblastoma cell line (SiMa cells) that had been intoxicated with 5 nM of LC/E-BoNT/A was used as a positive control, while naive SiMa cell lysate was used as a negative control. Ipsilateral and contralateral plantaris muscles from LC/E-BoNT/A injected animals were tested, along with an ipsilateral plantaris muscle sample from a vehicle injected animal. SNAP-25_A and SNAP-25_E were present in the LC/E-BoNT/A treated SiMa cell lysate and were absent in the un-treated SiMa cell lysate. LC/E and LC/A cleaved products were detected in both ipsilateral and contralateral paws of rats injected with 150 U/Kg indicating spread of the toxin to the contralateral limb, while at 75 U/Kg SNAP-25_E and SNAP-25_A were only present in the

ipsilateral paw (Fig. 3.16 D). These results coincided with the paralytic effects of 150 U/Kg on the rotarod and adverse effects on weight gain (Fig. 3.16 B-C), indicating greater systemic toxicity at higher doses.

A

Treatment	pg/mL	Mice reaching humane endpoint (%)
LC/E-BoNT/A	500	100
LC/E-BoNT/A	166.7	100
LC/E-BoNT/A	100	100
LC/E-BoNT/A	71.4	25
Vehicle	NA	0

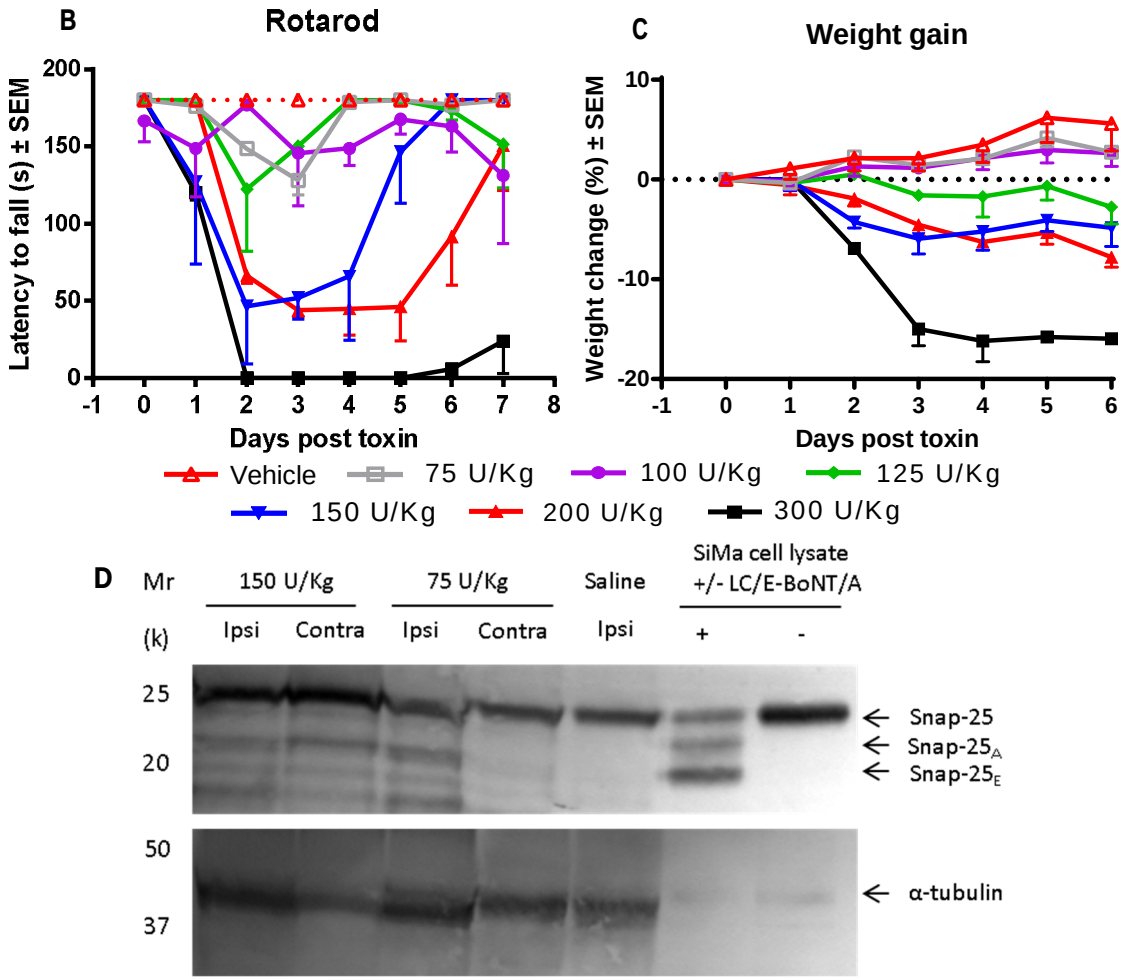

Fig. 3.16 MaxTD of batch 2 LC/E-BoNT/A was set at 120 U/Kg, proteolytic activity was confirmed in the plantaris muscles of rat hind-paws (A) Potency testing of LC/E-BoNT/A listing % of mice dying per dose of LC/E-BoNT/A, n=4 mice per dose**.** Time courses of rat locomotor ability **(B)** and % weight change **(C)** relative to toxin injection presented. n=2 rats for all treatment groups, data represents means ± SEM. Horizontal dotted line in **(C)** indicates weight loss relative to pre-treatment weight. **(D)** SNAP-25 cleavage confirmed by Western blotting of homogenised plantaris muscles harvested from culled, toxin treated rats. 45 µl of each plantaris sample was loaded with protein concentrations normalised to intact SNAP-25 content, and 5 µl of SiMa cell lysate (treated or untreated) was loaded. Mice weighing 20-22 g and rats weighing 252 – 367 g at the time of BoNT injection were used. Dr Tom Zurawski acted as lead researcher for potency testing of batch 2. Vehicle: 0.05% HSA, 10 µM $ZnCl_2$, normal saline.

Testing of batch 2 LC/E-BoNT/A in SNI and capsaicin rat pain models

After establishing the MaxTD of batch #2 LC/E-BoNT/A, two studies were designed in parallel to explore the anti-nociceptive effects of this fresh lot of toxin. As SNAP-25 cleavage was detectable in the plantaris of rats injected with 75 U/Kg of batch 2 (Fig. 3.16 D), and there was a mild effect on weight gain (Fig. 3.16 B), it was decided to test if batch 2 could reduce SNI-induced hypersensitivity at a sub- MaxTD dose (75 U/Kg). Since batch 1 has shown efficacy in the SNI model in ranges of 35 – 75 U/Kg (Wang et al., 2017a), it was expected that this dose response would be reproduced with batch 2. Meanwhile, to confirm that the inconsistent anti-nociceptive effects of batch 1 in the capsaicin and formalin models of pain were due to a loss of activity, the MaxTD (120 U/Kg) of batch 2 was tested in the capsaicin model of acute pain, against vehicle and 0.1 mg/kg buprenorphine as a positive control. The dose of buprenorphine was reduced to 0.1 mg/kg from 0.2 mg/kg, which was used in Fig. 3.9, as the higher dose induced mild sedation. These studies were performed in collaboration with Dr Orla Moriarty.

75 U/Kg of batch 2 LC/E-BoNT/A mildly inhibited SNI-induced cold hypersensitivity but had no effect on mechanical hypersensitivity

As before, rats underwent either sham or SNI surgeries and received intra-plantar injections of either LC/E-BoNT/A or vehicle. No effect of LCE/-BoNT/A was found on mechanical hypersensitivity induced by the SNI model (Fig. 3.17 A). LC/E-BoNT/A demonstrated an anti-nociceptive effect on cold hyperalgesia compared to vehicle on day 14 post surgery (Fig. 3.17 B). Interestingly, sham LC/E-BoNT/A treated rats showed increases in cold stimuli responses, with sham LC/E-BoNT/A exhibiting significantly more nocifensive behaviour than sham vehicle at day 10 post surgery. However, toxin treated animals showed marked weight loss (Fig. 3.17 C), which had not been observed in the previous dosing study (Fig. 3.16 C). It is unclear why this unexpected weight loss occurred although it may be due to variability between animals; therefore, larger sample sizes for dosing studies would be needed to address this.

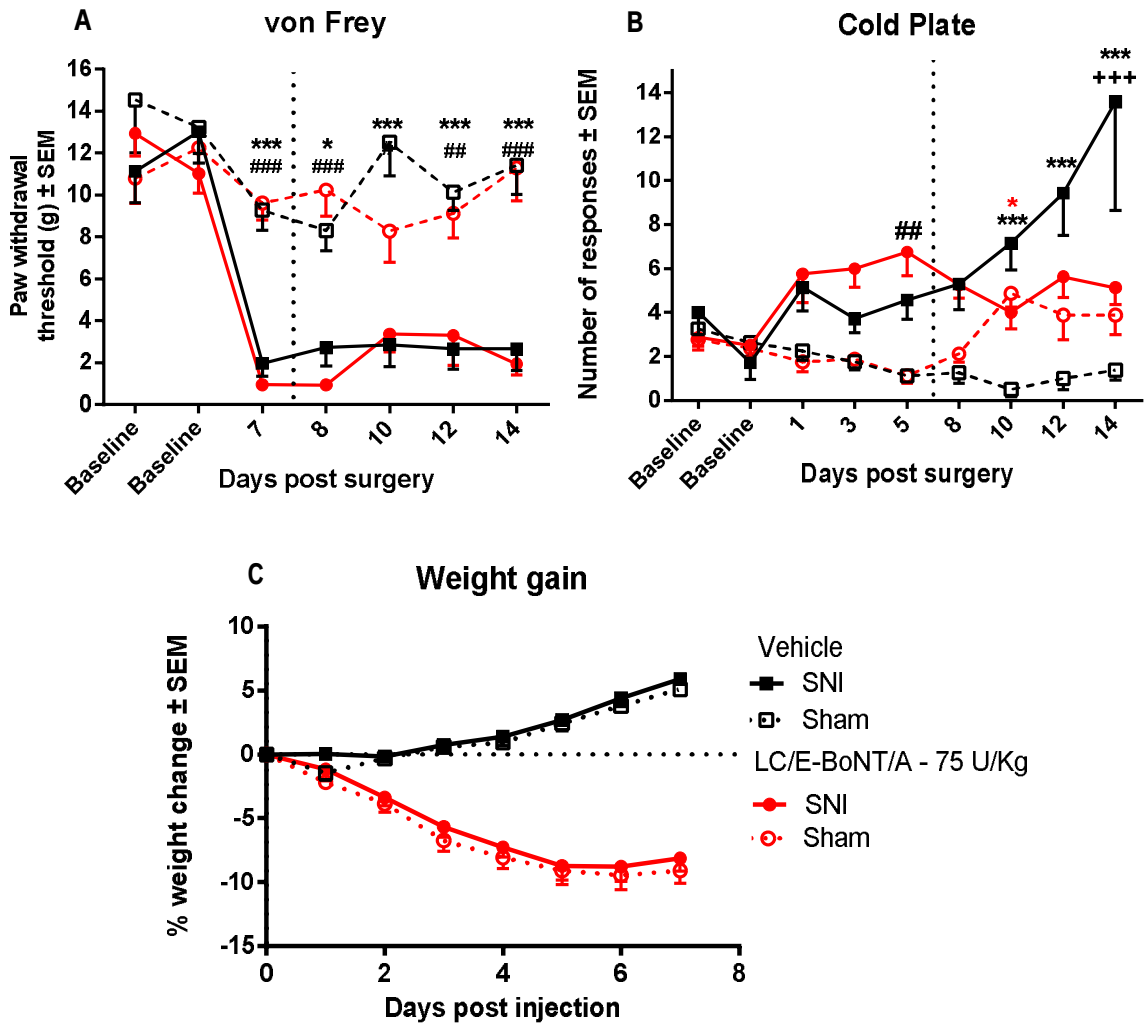

Fig. 3.17 Intra-plantar injection of LC/E-BoNT/A inhibits SNI-induced cold hypersensitivity but not mechanical hypersensitivity Time courses of mechanical **(A)** and cold **(B)** hyperalgesia were plotted, including pre-SNI baselines, post-surgery baselines and post injection of LC/E-BoNT/A or vehicle (vertical dotted line). Data represents means ± SEM, statistical analysis was performed using repeated measures two-way ANOVA and Bonferroni *post hoc* tests. For both von Frey and cold plate tests there were significant effects of time ($P<0.0001$, $F_{(6, 162)} = 27.23$, $F_{(8, 216)} = 5.215$) and of group ($P<0.0001$, $F_{(3, 162)} = 41.12$, $F_{(3, 216)} = 11.63$). After induction of the spared nerve injury model, significant mechanical hypersensitivity **(A)** developed between the sham groups and the SNI groups (#, $p<0.05$, ##, $P<0.005$, ###, $P<0.001$, Sham LC/E-BoNT/A vs SNI LC/E-BoNT/A), (*, $P<0.05$, ***, $P<0.001$, Sham vehicle vs SNI vehicle). No significant differences were detected between any groups before surgery, between the two sham groups after surgery, or between the two SNI groups after toxin injections. **(B)** 75 U/Kg of batch 2 LC/E-BoNT/A mildly inhibited progression of SNI-induced cold hyperalgesia but also caused contralateral increases in cold hypersensitivity. (+++, $P<0.001$, LC/E-BoNT/A SNI vs vehicle SNI) (*, $P<0.05$, LC/E-BoNT/A sham vs SNI sham) (***, $P<0.001$, SNI vehicle vs SNI sham) (##, $P<0.01$, Sham LC/E-BoNT/A vs SNI LC/E-BoNT/A). Rats weighing between 230-280 g at the time of SNI surgery were used. n=8 for all groups. Vehicle: 0.05% HSA, 10 µM, $ZnCl_2$, normal saline. Surgeries and behaviour tests performed in collaboration with Dr Orla Moriarty.

120 U/Kg of batch 2 LC/E-BoNT/A inhibited capsaicin-induced nocifensive behaviours and heat hypersensitivity

Rats received intra-plantar injections of 120 U/Kg LC/E-BoNT/A four days before induction of the capsaicin pain model. Following intra-plantar injection of capsaicin, nocifensive like behaviour was recorded for 10 minutes. Hargreaves testing was performed at 30 minutes post capsaicin injection and hot plate testing was performed at 50 minutes post capsaicin injection. As shown in the SNI study that ran in parallel to this, the animals injected with 120 U/Kg of batch 2 LC/E-BoNT/A showed distinct weight loss (Fig. 3.18 F), indicative of systemic toxicity. Despite this, LC/E-BoNT/A significantly reduced capsaicin-induced hind-paw lifting behaviour (Fig. 3.18 B), combined lifting and licking behaviour (Fig. 3.18 A) and response to heat stimuli on the hot plate test (Fig. 3.18 D), compared to vehicle. LC/E-BoNT/A also showed no significant difference to buprenorphine in relieving these parameters, indicating a comparable effect to buprenorphine. However, LC/E-BoNT/A showed no effect on hind-paw licking while buprenorphine was significantly more effective than both LC/E-BoNT/A and vehicle on reducing licking behaviour (Fig. 3.18 C). Lastly, capsaicin injection in the vehicle treated group was shown to significantly reduce ipsilateral heat thresholds (measured by Hargreaves test) compared to the contralateral thresholds, indicative of heat hypersensitivity. Interestingly, there was no significant difference between ipsilateral and contralateral thresholds in the LC/E-BoNT/A group, indicating LC/E-BoNT/A inhibited the development of capsaicin-induced heat hyper-sensitivity as measured by the Hargreaves test. Buprenorphine significantly increased both ipsilateral and contralateral thresholds to heat stimuli as expected (Gades et al., 2000), and these thresholds were significantly higher than the LC/E-BoNT/A and vehicle group contralateral thresholds (Fig. 3.18 E).

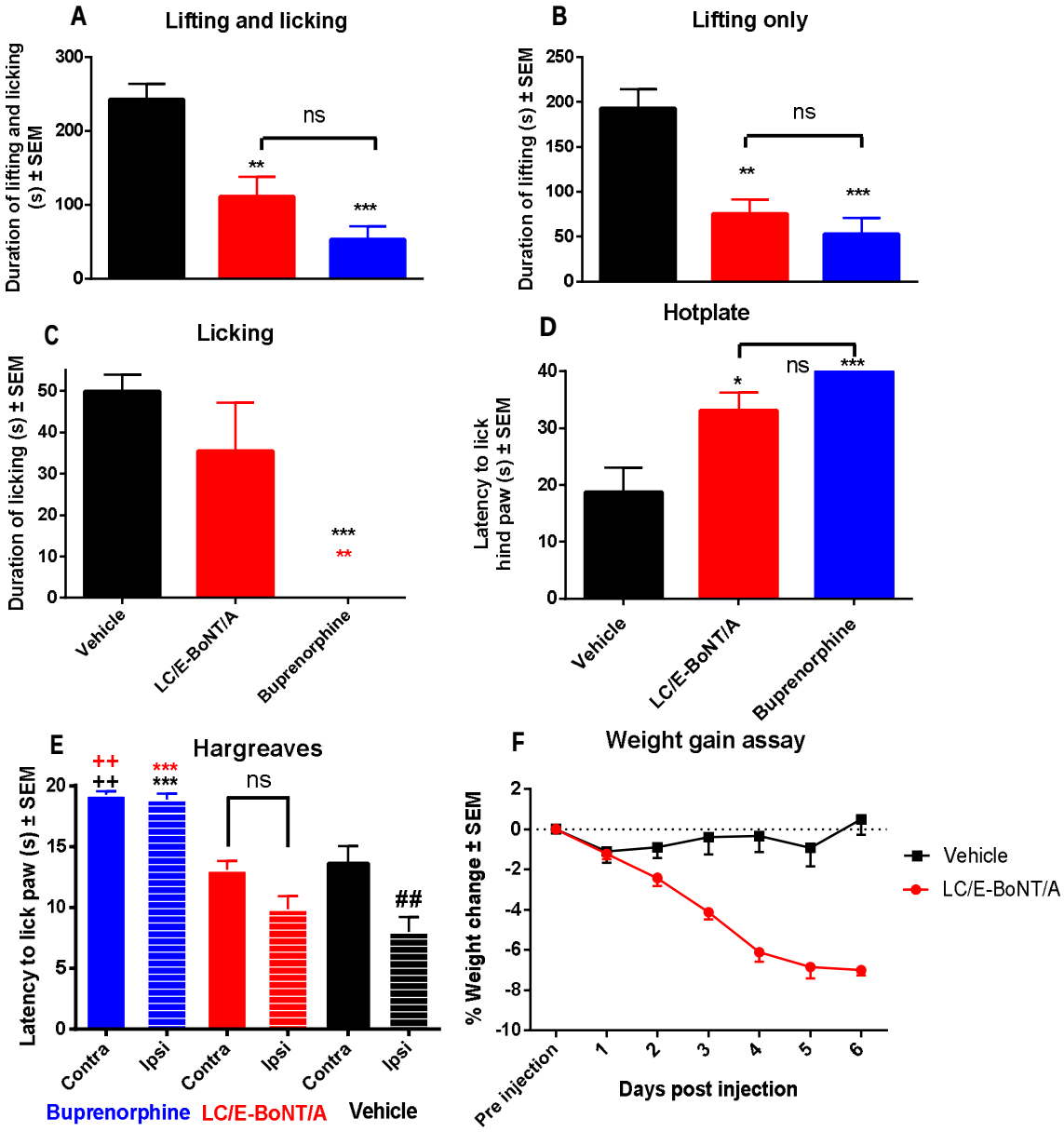

Fig. 3.18 MaxTD of batch 2 LC/E-BoNT/A relieved all capsaicin evoked nocifensive behaviours excluding hind-paw licking in rats Total hind-paw lifting + licking time **(A),** lifting time **(B)**, licking time **(C),** heat thresholds on a hot plate set to 51 °C (±0.5 °C) **(D)** and heat thresholds according to Hargreaves test **(E)** were plotted. Histograms **A-C** represent total behaviour up to 10 minutes after capsaicin injection. Histogram (**D)** displays data at 50 min post capsaicin and (**E)** shows data at 30 min post capsaicin. Data plotted as means ± SEM and were analysed by one way ANOVA by group with a significant effect detected in lifting + licking ($F_{(3, 23)} = 12.86$, $p<0.001$), lifting ($F_{(3, 23)} = 15.24$, $p<0.001$), licking ($F_{(3, 23)} = 10.13$, $p<0.001$), hot plate ($F_{(3, 23)} = 23.74$, $p<0.001$) and Hargreaves ($F_{(5, 35)} = 22.5$, $P<0.05$). Bonferroni *post hoc* tests **(A-D)**: *, P<0.05, **, P<0.01, ***, P<0.001, vs vehicle, **, P<0.01, vs. LC/E-BoNT/A. **(E)**: ***, P<0.001, vs vehicle ipsi, ***, P<0.001, vs LC/E-BoNT/A ipsi, ##, P<0.01, vs vehicle contra, ++, P<0.01, vs vehicle contra, ++, P<0.01, vs LC/E-BoNT/A contra. Rats weighing 186 – 270 g at the time of capsaicin injections were used. Vehicle n=6, LC/E-BoNT/A (120 U/Kg) n= 6, buprenorphine (0.1 mg/Kg) n=6. Vehicle: 0.05% HSA, 10 µM, $ZnCl_2$, normal saline. Behaviour tests performed in collaboration with Dr Orla Moriarty.

Summary of effects of BoNT/A and BoNT chimeras in rat models of pain

To summarise the differences of batches 1 and 2 of LC/E-BoNT/A in the different rat pain models, the results of the different toxins (BoNT/A, LC/E-BoTIM/A, LC/E-BoNT/A) have been collated into table 3.1. Batch 1 of LC/E-BoNT/A had the highest anti-nociceptive effect overall while batch 2 LC/E-BoNT/A showed a reduced anti-nociceptive effect in comparison. BoNT/A demonstrated mild or no anti-nociceptive effects overall while LC/E-BoTIM/A demonstrated a moderate effect in the SNI model, the only model it was tested in this project, and a moderate effect in the capsaicin model of pain (Wang et al., 2011a).

	LC/E-BONT/A: BATCH 1	LC/E-BONT/A: BATCH 2	LC/E-BOTIM/A	BONT/A
SNI	✓✓✓	✓	✓✓	✓
CFA	X	NA	NA	X
FORMALIN	✓, ✓✓	NA	NA	X
CAPSAICIN	X, ✓✓	✓✓	✓✓	✓
VZV	NA	NA	NA	NA

Table 3.1 Results of screening different BoNTs in rat models of inflammatory and neuropathic pain Effects of different toxins in different pain models summarised using a scale of no anti-nociceptive effect to maximum anti-nociceptive effect. Results of different experiments using the same toxin in the same model are separated by a comma. ✓ - Mild anti-nociceptive effect, ✓✓ - moderate antinociceptive effect, ✓✓✓ - maximum nociceptive effect, X – no anti-nociceptive effect, NA – Not tested in model. Testing of LC/E-BoTIM/A in capsaicin model was reported in Wang et al., 2011a.

Chapter 4 - Discussion

The Vzv rat model of post-herpetic neuralgia was found to not induce consistent hypersensitivity and thus was unsuitable for testing LC/E-BoNT/A

During attempts to establish the rat Vzv model, unexpected complications arose in the inability to reproduce consistent hyper-sensitivity. While mechanical allodynia could be induced, this only occurred in the lowest cell titre administered and no dose response was observed as reported by (Hasnie et al., 2007, Garry et al., 2005). The model was also short lived (recovering in less than two weeks) which made it unsuitable for testing of BoNTs and conflicted with other reports (Medhurst et al., 2008, Fleetwood-Walker et al., 1999). Returning to the literature to identify a reason behind the lack of reproducibility in the Vzv model, a PhD thesis describing similar issues was found (Medhurst, 2011). The author was also unable to establish the Vzv model and tried several experiments to discern any possible reason as to why, even going so far as to combine a Vzv injection with an intra-plantar capsaicin injection, to see if a secondary insult would uncover latent Vzv-induced allodynia. This proved negative and the authors confirmed that Vzv infection of the DRG was also not feasible with intra-plantar injections of Vzv infected cells, contradicting the original publications reporting this (Sadzot-Delvaux et al., 1990). Taking this comprehensive investigation into account, along with the fact that different groups publishing on this model each demonstrate different phenotypes, with Fleetwood-Walker et al. (1999) reporting heat allodynia that was not reproduced by Hasnie et al. (2007), investigations into the Vzv model were stopped. If this model was to be further explored, comparisons between the different Vzv model protocols in the literature would possibly be necessary. Four different Vzv strains (Dumas, Ellen, pOka, KMcC) have been propagated using four different cell types (MeWo, ARPE-15, MRC-5, CV-1) and administered to three different rat strains (Sprague Dawley, Wistar, Random-hooded) (Hasnie et al., 2007, Guedon et al., 2015, Medhurst et al., 2008, Fleetwood-Walker et al., 1999, Zhang et al., 2011a, Garry et al., 2005, Guedon et al., 2014). Considering the wide variety in protocols and the different presentations of the models seen in this work, by Medhurst (2011) and other published

reports (Fleetwood-Walker et al., 1999, Hasnie et al., 2007), it's probable that the issues lie in the lack of standardised protocols for this model. The specific combination of rat, viral strain and cell type used in this work have all individually been used in successfully induced Vzv models in the literature, but the specific combination of these three has not been published on yet. Considering that different strains of rats (and even the same strain from different suppliers) can show significantly different pain behaviours within the same pain model or after treatment with the same analgesic (Benoliel et al., 2002, Kristensen et al., 2017, Banik et al., 2002), it is possible that the Sprauge Dawley rats used in this project were not as sensitive to symptoms of PHN induced by the Ellen strain of Vzv when administered via MRC-5 cells.

Batch 1 LC/E-BoNT/A exhibited a promising anti-nociceptive effect in capsaicin and formalin rat models of pain, but did not show an effect on capsaicin-induced c-fos expression in the L4-L5 dorsal horn

This project was the first to investigate the effects of LC/E-BoNT/A in the formalin model of acute pain, the first rodent pre-clinical model used to test the analgesic efficacy of BOTOX® (Cui et al., 2004). Interestingly, a significant effect on phase I flinching behaviour in the LC/E-BoNT/A treated group was observed, although this was not seen in any other phase 1 behavioural parameters. As intra-plantar injections of BoNT/A or BOTOX® have previously been reported to have no effect on phase I formalin behaviour (Pavone and Luvisetto, 2010, Cui et al., 2004), it can be speculated that this analgesic effect of LC/E-BoNT/A is a result of the LC/E tethered to BoNT/A. Cleavage of SNAP-25 by LC/A or LC/E produces truncated SNAP-25_A or SNAP-25_E, respectively, impairing correct SNARE complex formation, which prevents vesicular fusion to the plasma membrane, thus, inhibiting the release of neurotransmitters. BoNT/A inhibition of exocytosis has been reported to be reversed by increasing synaptic concentrations of Ca^{2+}. Mice suffering from botulism recover after treatment with 4-aminopyradine (4-AP), a compound that increases free calcium inside nerve terminals (Lundh et al., 1977). Interestingly, SNAP-25_A has been shown to retain the ability to form SDS-resistant SNARE complexes, while SNAP-25_E cleavage products cannot; this discrepancy is likely due to the differences in cleavage length and suggests that LC/E-mediated cleavage may result in

more effective inhibition (Hayashi et al., 1994). This has been demonstrated in reports that BoNT/A inhibition of Ca^{2+} evoked norepinephrine release *in vitro* can be overridden by increasing Ca^{2+} concentrations in cell incubation media. Increasing the Ca^{2+} concentration did not undo BoNT/E-induced blockades of NE release, demonstrating the Ca^{2+} resistant blockade of exocytosis resulting from SNAP-25_E (Gerona et al., 2000, Banerjee et al., 1996). BoNT/A blockade of CGRP release was found to be reversed by capsaicin evoked increases in intracellular Ca^{2+} *in vitro*, and like the Ca^{2+} evoked release of NE, was also prevented by LC/E. Despite this, inhibition of CGRP release from either the peripheral (in the hind-paw) or central terminals (in the spinal cord) of nociceptors is unlikely to explain the LC/E-BoNT/A mediated reduction in phase 1 formalin flinching. This is because while phase 1 formalin pain is believed to be driven by activation of peripheral nociceptors by the initial injury (Cui et al., 2004), CGRP plays a facilitatory role in developing sensitisation e.g. via vasodilation at the injury site or by acting synergistically with substance P to drive wind-up in the spine (Latremoliere and Woolf, 2009, Oku et al., 1987, Le Greves et al., 1985). This is further supported by the evidence that CGRP KO mice show no change in phase 1 formalin behaviour compared to WT mice (Shinohara et al., 2017). Unfortunately, due to variations in the anti-nociceptive effect of LC/E-BoNT/A between different experiments in this work it was not possible to obtain samples to investigate CGRP release in the LC/E-BoNT/A vs. vehicle treated rats in the capsaicin or formalin model experiments. Phase 1 of the formalin model is believed to be a behavioural response to fast depolarisation of nociceptors by a noxious stimuli (milliseconds) (McNamara et al., 2007), not from the prolonged effects of CGRP release (Oku et al., 1987). Inhibition of glutamate release at the central terminal of the nociceptor, which mediates the rapid transmission of a nocifensive signal at the dorsal horn (Millan, 1999), could explain this reduction in phase 1 nocifensive behaviours. Retrograde transport of LC/E-BoNT/A to the central nociceptor terminals in the dorsal horn could mediate this, where the production of SNAP-25_E could hypothetically provide a more stable blockade of glutamate release, resistant to the sustained excitatory signals coming from the formalin injury. Interestingly, direct injection of BoNT/A into the spinal cord, at a dose 40-times lower than the normal intra-plantar dose can also inhibit phase 1

behaviours (Lee et al., 2011b, Matak et al., 2017). This would indicate that the amount of active LC/A transported to the central nociceptive terminals from an intra-plantar injection is insufficient to block glutamate release in response to formalin. Furthermore, it took 10 days for intrathecal injections of BoNT/A to inhibit phase 1 formalin behaviours, while only 1 day for an anti-nociceptive effect to be observed in phase 2. This could mean that it requires 10 days for sufficient SNAP-25_A to accumulate, so the increase in intracellular Ca^{2+} from sustained nocifensive signalling doesn't reverse the blockade of glutamate. Considering that a larger amount of LC/E-BoNT/A can be injected into the hind-paw compared to BoNT/A (75 vs 15 U/Kg), this could mean that a greater amount of active protein is successfully transported to the central terminal of the nociceptor to cleave SNAP-25. Secondly, as LC/E-BoNT/A contains the LC/E, this would induce a Ca^{2+} resistant blockade of glutamate release, despite sustained activity from formalin activation of nociceptors. Unfortunately, due to the lack of reproducibility of the anti-nociceptive effects of LC/E-BoNT/A, further studies into the mechanism behind these observations were not possible.

Reports have provided strong evidence for retrograde transport of BoNT/A (Antonucci et al., 2008) and some researchers believe that this may be linked to its antinociceptive effect (Bach-Rojecky and Lackovic, 2009, Antonucci et al., 2008, Matak and Lackovic, 2014). However, the hypothesis that active BoNT/A can undergo retrograde transport and transcytosis to the CNS is still a point of contention in the literature with a comprehensive critique of this hypothesis provided by (Aoki and Francis, 2011), and experiments by (Cai et al., 2017) having shown that distal effects of BoNT/A may be due to systemic spread of high doses of neurotoxin and not necessarily retrograde transport. However, it is unclear how LC/E-BoNT/A could induce an effect on phase 1 formalin behaviour if its mechanism of action was solely limited to the hind-paw. LC/E-BoNT/A is not the only BoNT to have demonstrated an anti-nociceptive effect on phase 1 formalin behaviour. Intra-plantar administration of BoNT/B has been shown to reduce phase I formalin behaviours in mice (Luvisetto et al., 2006), although this has not been reproduced by other groups (Marino et al., 2014). BoNT/B cleaves different SNAREs (VAMP 1 and 2) to BoNT/A and BoNT/E, but its inhibition of neurotransmitter release has been shown to be resistant to Ca^{2+} triggers, like BoNT/E (Banerjee et

al., 1996, Gerona et al., 2000). This could mean that BoNT/B inhibition of phase 1 formalin behaviours is similar to the proposed mechanism for LC/E-BoNT/A, and that intra-plantar injection of BoNT/B is transported to the central terminal of nociceptors resulting in a blockade of glutamate release resistant to increased intracellular Ca^{2+} from incoming action potentials induced by formalin.

As expected, LC/E-BoNT/A treated rats showed significant reductions in phase 2 lifting and flinching responses compared to the vehicle group; however, there was no effect on paw licking behaviour or combined lifting/licking behaviours, in contrast to previous findings with BOTOX® (Cui et al., 2004). Considering previous reports that BoNT/A complex effectively relieved formalin phase 2 behaviours (Cui et al., 2004), it is unexpected that the LC/E-BoNT/A analgesia is present in only two of the four behaviour paradigms in phase 2. Further investigations, administering intrathecal injections of LC/E-BoNT/A to rats before intra-plantar injection of formalin could provide more clarity on this anomaly, as intrathecal injections of BoNT/A have shown superior efficacy over intra-plantar injections (Bach-Rojecky et al., 2010, Luvisetto et al., 2006, Lee et al., 2011b). If intrathecal injections of LC/E-BoNT/A were to provide superior pain relief on all four of the behaviours present in phase 1 and 2, it would indicate a limitation of the analgesia that can be induced by peripheral injections of LC/E-BoNT/A over central injections. To investigate whether the effects of LC/E-BoNT/A on phase 1 are a result of cleavage of SNAP-25 in the hind-paw or retrograde transport of the toxin to the dorsal horn, a timeline of different intra-plantar injections of LC/E-BoNT/A could be compared to identify how long after treatment is required for an effect on phase 1 to occur. If it takes longer for analgesia to be induced on phase 1 than phase 2, this could indicate the phase 1 analgesia is dependent on the length of time for a required amount of the toxin to be transported to central terminals in the dorsal horn to block release of glutamate from the central nociceptive terminals. If the onset of phase 1 analgesia were to correlate with detection of $SNAP\text{-}25_E$ in dorsal horn samples from treated animals, this would provide important data on the mechanism of phase 1 pain relief by LC/E-BoNT/A.

To delve deeper into the differences between LC/E-BoNT/A and BoNT/A, a direct comparison was designed using the capsaicin model of pain. This model was selected as capsaicin induces the release of CGRP from nociceptors *in vitro* (Sauer et al., 1999) and induces hyperalgesia *in vivo* (Massaad et al., 2004), most likely through neurogenic inflammation of the hind-paw. As capsaicin-induced CGRP release is blocked by cleavage of SNAP-25 by LC/E but not LC/A *in vitro* (Meng et al., 2009), it was expected that LC/E-BoNT/A would outperform BoNT/A in pain relief of the capsaicin model. Both BoNT/A and LC/E-BoNT/A reduced hind-paw lifting behaviour compared to vehicle but neither toxin reduced paw licking or heat hyperalgesia against this control. Furthermore, LC/E-BoNT/A significantly reduced overall lifting/licking behaviour, in contrast to BoNT/A which did not. While LC/E-BoNT/A outperformed BoNT/A on acute pain behaviours (compared to vehicle) as expected, it did not affect hypersensitivity to heat or acute paw licking. This was surprising, as LC/E-BoTIM/A (which has one less active protease than LC/E-BoNT/A) reduced capsaicin-induced heat hyperalgesia and hind-paw licking (Wang et al., 2011a). Furthermore, buprenorphine-induced (analgesic positive control) pain relief correlated with a significant reduction in c-fos immunohistochemical staining in the superficial dorsal horn (L4-L5 region); neither LC/E-BoNT/A nor BoNT/A reduced c-fos staining despite showing significant anti-nociceptive effects. However, this result is not unique to neurotoxins tested within this project. While BOTOX®-induced analgesia has been shown to reduce c-fos expression in the formalin model (Matak et al., 2017), Bitox (a non-paralytic variant of BoNT/A) was shown to have no effect on formalin or capsaicin-induced c-fos staining, and yet reduced capsaicin-induced mechanical hyperalgesia. Also, like the mixed anti-nociceptive effects of BoNTs in this project, Bitox showed efficacy on only certain pain measures (capsaicin-induced mechanical hyperalgesia) but no effect on formalin-induced flinching or capsaicin-induced heat hyperalgesia (Mangione et al., 2016). The fact that two modified preparations of BoNT/A (LC/E-BoNT/A and Bitox) have shown unexpected differences in anti-nociceptive effect compared to work published on BOTOX®, highlights the lack of understanding of the full mechanism of BoNT/A-mediated analgesia.

One possible explanation for the variations between the capsaicin experiment and those conducted by Wang et al., 2011 is that the batches of BoNT/A and LC/E-BoNT/A used in this study had a later time of onset than previous aliquots of BoNT/A and LC/E-BoTIM/A used by Wang et al. (2011a). In this experiment, both neurotoxins were injected four days before capsaicin, to replicate the experimental conditions by Wang et al. However, the samples of LC/E-BoNT/A and BoNT/A used in Fig. 3.9-3.10 may require more time to cleave sufficient amounts of SNAP-25 to have a similar anti-nociceptive effect as those reported in Wang et al. Future experiments to identify the optimum time to inject LC/E-BoNT/A or LC/E-BoTIM/A before injection of capsaicin would help identify if these differences were a result of sample variation between studies.

Potency changes of LC/E-BoNT/A batch 1 suggest that long-term storage affects toxin activity

After the pilot study testing batch 1 LC/E-BoNT/A vs. vehicle in the rat formalin model (Fig. 3.7-3.8), the experiment was repeated to reproduce the anti-nociceptive effect of batch 1 LC/E-BoNT/A and compare this with the anti-nociceptive effect of BoNT/A (Fig. 3.11-3.12). Surprisingly, re-testing the same batch of LC/E-BoNT/A only showed an effect in reducing phase 2 hind-paw licking behaviours and not on phase 2 paw lifting or on phase 1 flinching behaviours, as were previously observed. Furthermore, BoNT/A had no significant effect on acute pain behaviours. This unexpected result raised the question as to why BoNT/A showed no effect on the formalin model, when BOTOX® was reported to reduce formalin-induced pain (Cui et al., 2004). Since the tested batches of BoNT/A and LC/E-BoNT/A (batch 1) were produced in 2013-2014 it was deemed prudent to determine if there had been any loss of activity due to long term storage at -20 °C. Reports on the effect of long term freezing on BOTOX® potency are contradictory. FDA product labelling recommends that BOTOX® be disposed of 4 hours after reconstitution (Allergan, 2002), while one group have shown that freezing of reconstituted BOTOX® for up to 180 days has no effect on BOTOX® treatment satisfaction in humans (Parsa et al., 2007). These effects were not noted in a mouse LD_{50} however, where freezer storage at -70 °C for two weeks of reconstituted BOTOX® resulted in a 69.8%

decrease in bioactivity (231% increase in LD_{50} value) and a 43.9% potency decrease (78.4% LD_{50} increase) as soon as 12 hours after freezing (Gartlan and Hoffman, 1993).

To investigate the potential activity loss, both samples of LC/E-BoNT/A and BoNT/A were checked for purity and integrity by protein staining and activity of their proteases tested using the *in vitro* cleavage assay (Wang et al., 2008). When originally produced in 2014 BoNT/A was shown to produce SNAP-25 cleavage at a concentration of 0.39 nM, and re-testing of these samples showed detectable cleavage as low as 0.5 nM, therefore not indicating an obvious change in LC activity *in vitro*. However, the *in vitro* cleavage assay only tests the activity of the LC in the presence of a recombinantly expressed SNAP-25 fragment, not the ability of the neurotoxin to bind and enter neurons and translocate its LC into the cytosol, which could alter the potency of BoNT/A, if compromised. Testing of batch 1 LC/E-BoNT/A showed faintly detectable cleavage at a concentration of 0.01 nM and obvious cleavage at 0.1 nM when tested in 2013, yet retesting showed slight SNAP-25 cleavage only as low as 0.5 nM, indicating a noticeable shift in potency of the LCs *in vitro*. Thus, further investigations on potential effects of long-term storage at -20 °C of the neurotoxins used in this project are needed. As LC/E-BoNT/A was the only toxin to show a noticeable loss of potency *in vitro*, and the main objective of this project was testing of this toxin, efforts to confirm the inconsistent anti-nociceptive effect of LC/E-BoNT/A over BoNT/A were prioritised.

While the BoNT/A sample showed no signs of precipitation or degradation, with the di-sulphide bonds remaining intact, the unreduced samples of LC/E-BoNT/A showed faint bands in line with the size of the reduced toxin, indicating that di-sulphide bridge of a small fraction of the neurotoxin was not correctly formed. However, these bands were also present when batch 1 LC/E-BoNT/A was initially produced and were therefore unlikely to cause the reduction in anti-nociceptive effect. The reduced potency *in vitro* of batch 1 LC/E-BoNT/A was mirrored *in vivo* by the increased MaxTD of 110 U/Kg, 47% more than the original 75 U/Kg dose used for the pain studies until this point. Considering such a large increase in the MaxTD it was expected that this dose was now too low to

have an anti-nociceptive effect since BOTOX® has a very narrow margin between a therapeutically effective and ineffective dose. While BOTOX® has been shown to demonstrate a dose response in anti-nociceptive effect between 3.5 – 30 U/Kg (Cui et al., 2004), a decrease as low as 0.5 U/Kg was shown to be the difference between a therapeutically effective (3.5 U/Kg) and ineffective dose (3 U/Kg) in rat models of carrageenan-induced inflammatory pain (Bach-Rojecky and Lackovic, 2005). After identifying such a large increase in the MaxTD of batch 1 LC/E-BoNT/A, it was anticipated that testing of 110 U/Kg of LC/E-BoNT/A in the capsaicin model of pain would demonstrate a clear anti-nociceptive effect on all behavioural paradigms. However, 110 U/Kg of batch 1 of LC/E-BoNT/A had no effect on reducing capsaicin-induced pain-like behaviours. This was surprising as expected effects of 110 U/Kg on slowing weight gain were observed in the rats used in the capsaicin experiment, which indicated that batch 1 LC/E-BoNT/A was active *in vivo.* Furthermore, higher doses of batch 1 used in the study which identified 110 U/Kg as the new MaxTD, had induced paralysis indicating toxin activity. Based on the gradual loss of anti-nociceptive activity along with the increase in doses required to induce paralysis or weight loss in rats, it seemed LC/E-BoNT/A activity had diminished overtime, and the anti-nociceptive potency degraded more rapidly than the paralytic effects of the toxin. Since increasing the total amount of batch 1 LC/E-BoNT/A protein did not recover the analgesic effects, this implied that the analgesic potency of the entire sample was impaired. As the anti-nociceptive effect was absent while paralytic symptoms were still observed, the two mechanisms may be independent of each other, with the analgesic effect dependent on successful entry into nociceptors, while paralysis is dependent on entry into motor neurons. Therefore, the putative binding and entry of batch 1 LC/E-BoNT/A into nociceptors may have been impaired during long term storage, while binding to motor neurons was retained. As successful binding of BoNT/A to neurons is dependent on the presence of SV2, with SV2C being the most sensitive to BoNT/A (Dong et al., 2006), it may be that hind-paw motor neurons express higher levels of SV2, or of SV2C specifically, than the nociceptors in the hind-paw. If the efficacy of batch 1 LC/E-BoNT/A's binding domain were reduced, then it may be more likely to enter motor neurons than nociceptors. To investigate this, total protein levels of SV2 and its different isoforms in

cultured motor neurons and sensory neurons could be compared by Western blotting. By also intoxicating motor neuron and sensory neuron cultures with batch 1 of LC/E-BoNT/A and measuring the amount of SNAP-25 cleavage at different time-points, any potential differences in the toxin's ability to bind, enter and cleave SNAP-25 in each type of neuron culture can be identified. These experiments could shed light on this speculative hypothesis.

Batches 1 and 2 of LC/E-BoNT/A demonstrate different anti-nociceptive and toxicity profiles in rat models of SNI and capsaicin-induced pain

As batch 1 of LC/E-BoNT/A was no longer viable for testing, a fresh batch of LC/E-BoNT/A (batch 2) was produced and fully characterised to be used in animal studies. Based on behavioural tests the MaxTD of batch 2 was found to be 120 U/Kg, which was tested in the capsaicin model of pain against vehicle and buprenorphine. Since batch 1 had previously shown no effect on the hot-plate test (a measure of heat hyperalgesia) after injection capsaicin, the Hargreaves test was selected to measure heat allodynia in this experiment using batch 2. As the Hargreaves test measures response time to a gradually increasing temperature, a decrease in response time indicates a reduced heat threshold which is indicative of heat allodynia (Deuis and Vetter, 2016). The hot-plate measures latency to respond to an already noxious stimulus and so reductions in response time are taken as a hyperalgesic response (Richardson et al., 1997). Using both tests would investigate if LC/E-BoNT/A showed anti-nociceptive effects on only certain types of heat hypersensitisation, i.e. could LC/E-BoNT/A recover a decreased noxious heat threshold on the Hargreaves (allodynia), but not improve latency to respond to a constant noxious heat stimulus on the hotplate (hyperalgesia). Interestingly, batch 2 LC/E-BoNT/A was shown to have a significant effect on heat hyperalgesia compared to vehicle, as measured by the hotplate test, unlike batch 1. Furthermore, batch 2 inhibited capsaicin-induced heat allodynia measured by the Hargreaves test. Capsaicin significantly reduced paw withdrawal latencies in the ipsilateral vs. contralateral hind-paws in the vehicle treated group, which is typical of the model (Gilchrist et al., 1996). While there was no significant difference on heat allodynia between the vehicle treated group and LC/E-BoNT/A treated group, there was also no significant difference between the contralateral and ipsilateral paw thresholds

for the LC/E-BoNT/A group after capsaicin injection. This indicated that pre-treatment of batch 2 LC/E-BoNT/A prevented capsaicin-induced heat allodynia in comparison to contralateral hind-paw thresholds (unlike vehicle pre-treatment). This did not provide enough pain relief to be significantly improved over vehicle pre-treatment however. Interestingly, there was no significant difference between batch 2 LC/E-BoNT/A and buprenorphine-induced analgesia on the hot plate test, but there was a significant difference between the two groups on the Hargreaves test. Buprenorphine is known to increase thresholds to noxious heat (Abram et al., 1997), while BoNT/A is not (Cui et al., 2004). Despite this, batch 2 LC/E-BoNT/A increased the heat thresholds to a similar level as buprenorphine on the hot-plate test, but not on the Hargreaves test. This could be indicative of a greater effect of LC/E on heat hyperalgesia compared to the LC/A, likely via inhibition of peripheral CGRP release reducing neurogenic inflammation associated with capsaicin injections (O'Neill et al., 2012, Wang et al., 2011a). To further investigate this a fresh batch of BoNT/A would need to be produced for a direct comparison with LC/E-BoNT/A in the capsaicin model. Overall, batch 2 of LC/E-BoNT/A had an improved effect on heat hyperalgesia compared to the previous experiment with batch 1, and inhibited capsaicin-induced heat allodynia.

The anti-nociceptive effect of batch 1 on capsaicin-induced hind-paw lifting and combined lifting/licking behaviour was reproduced with batch 2. Unlike batch 1, lifting and licking behaviour in batch 2 treated rats was not significantly different to buprenorphine treated rats, though this is likely due to the lower dose of buprenorphine used in this study, rather than a superior effect of batch 2 over batch 1. Like batch 1, there was no significant effect of batch 2 on reducing hind-paw licking behaviour, while this was inhibited by buprenorphine. As LC/E-BoTIM/A had been previously reported to reduce capsaicin-induced paw licking (Wang et al., 2011a), it was unexpected that this fresh batch of LC/E-BoNT/A would not have an effect on paw licking behaviour, despite reducing the other forms of pain measured. Furthermore, all rats treated with batch 2 LC/E-BoNT/A in this experiment showed greater weight loss than was expected from the dosing studies. As a result, it is possible that the changes in nocifensive behaviour in response to capsaicin were influenced by an adverse reaction to LC/E-BoNT/A and are not purely analgesia-induced. This indicates that future

experiments to calculate the MaxTD will need larger sample sizes ($n \geq 4$) to improve accuracy and ensure rat behavioural responses are not altered by adverse reactions to neurotoxin injections in pain studies. The possibility of variation being derived from differences in the lead-researchers in charge of behaviour experiments and the facilities where tests were undertaken also remains. The experiments presented in Wang et al., 2011a were performed in the pain research animal facility in National University of Ireland Galway, while experiments described in this thesis were performed in DCU primarily by John Nealon, but some studies were also performed in collaboration with other researchers including Drs Orla Moriarty and Laura Casals. While all measures to reduce inter-researcher variability were implemented where possible, due to the nature of behavioural testing in animals some differences in animal handling or testing could have been unaccounted for.

In parallel to the experiments with batch #2 in the capsaicin model, a lower dose of batch #2 LC/E-BoNT/A (75 U/Kg) was tested in the SNI model, to see if sub-MaxTD doses of batch #2 would also relieve SNI-induced pain, like the reports using batch 1 (Wang et al., 2017a). Interestingly, batch 2 LC/E-BoNT/A had no effect on mechanical hypersensitivity but did prevent cold hyperalgesia increasing on day 7 after injection. Curiously, sham operated animals that received injections of LC/E-BoNT/A showed an increase in contralateral cold hyperalgesia, reaching significance on day 3 post injection compared to the vehicle treated sham group. Furthermore, both sham and SNI groups that were treated with 75 U/Kg of batch 2 LC/E-BoNT/A showed significant weight loss. Therefore, it is likely this increase in cold allodynia was a symptom of the adverse reaction of the rats to batch 2 LC/E-BoNT/A. Batch 2 of LC/E-BoNT/A caused signs of toxicity at both 120 U/Kg and 75 U/Kg, which were not observed in the dosing studies. As both the sham and SNI groups showed the same decrease in weight from 75 U/Kg of batch 2, the weight loss was not propagated by the severity of the SNI model. Not only did these injections of batch 2 show more adverse reactions in the animals than in the dosing study, but the dose response in weight loss observed in the dosing study was absent, as the 75 U/Kg dose had the same effect as 120 U/Kg. As the animals used for these different injections were all within the same weight range, this indicates differences between the aliquots of batch 2 that were defrosted for the dosing and pain experiments. Out of the two

behaviour studies conducted with batch 2 of LC/E-BoNT/A, 120 U/Kg significantly reduced capsaicin-induced pain and 75 U/Kg had a token effect on SNI-induced cold hyperalgesia, but both doses induced weight loss in rats. Since weight loss was consistent in both studies this could be interpreted that the anti-nociceptive effects were not a symptom of the toxicity, and more analgesia was induced with the higher dose of LC/E-BoNT/A. However, this highlights a difference between batch 1 and batch 2 of LC/E-BoNT/A. While batch 1 of LC/E-BoNT/A showed an analgesic effect with mild effects on animal weight, batch 2 induced more severe symptoms of weight loss, and required higher doses to induce an antinociceptive effect. Therefore, batch 2 of LC/E-BoNT/A may be entering motor neurons but less successfully binding to nociceptors until administered at a higher dose (120 U/Kg). After testing two different batches of LC/E-BoNT/A, with several different doses, in a number of different pain models, it is clear that further investigations into the batch differences need to be undertaken to understand the variation that is occurring in these studies, which will require careful comparison of the production of the different batches of LC/E-BoNT/A.

Rat hind-limbs proved highly susceptible to paralysis after intra-articular injections of BoNTs, limiting the amount of toxin that could be administered

Before induction of the model, appropriate doses of batch 1 LC/E-BoNT/A and BoNT/A for injection into the knee had to be determined. These results indicated that the knee joint was far more susceptible to paralytic effects than the paw, with final doses of each only at 1/3 of what could be injected into the paw (LC/E-BoNT/A - 25 vs. 75 U/Kg, BoNT/A - 5 vs. 15 U/Kg). However, these dose limitations for the knee joint are not reported or discussed in the literature. Reports from the clinic indicate that intra-articular injections of BOTOX® of 100 - 200 U produce no paralytic effects (Boon et al., 2010), which are in range with doses used for dermal injections in neuropathic pain conditions (typically between 50-200 U); however, dermal injections vary based on condition and are typically across multiple injection sites (Oh and Chung, 2015). Due to use of multiple intra-dermal injections for BOTOX® treatment of neuropathic pain across a broad range of injection sites, it is difficult to discern if the observed dose limitations in the rat knee vs. the rat hind-paw correlate with practises in the clinic.

Published data on BOTOX® injections in the rat knee are also limited. Only Yoo et al. (2014) have reported intra-articular injections of BOTOX® (20 U per rat, estimated at 50 – 80 U/Kg based on reported rat weights) into the rat knee joint but included no behaviour data or discussion of adverse paralytic effects. The closest comparison that can be made within the literature to susceptibility of the rat knee joint to BoNT-induced paralysis, are the injections of BOTOX® into the knee joint of mice (0.3-0.5 U) by Mahowald et al. (2009), which were similar to that of the intra-plantar doses used for mice by other labs (0.2-0.4 U) (Matak et al., 2017). Mahowald et al. commented in the discussion of the knee joint experiments that "the high doses of botulinum toxin used in the early studies were associated with temporary limb weakness, but not with systemic weakness or other observed toxicity". This observation is very similar to the results in Fig. 3.5, where obvious limping of the injected hind-limb was noted while weight gain (indicative of systemic toxicity) wasn't greatly affected, except by higher doses of BoNT/A (70 – 100 U/Kg). It is not clear if the high dose (causing limb weakness) they are referring to is 0.3 - 0.5 U or a higher dose not stated in the paper; therefore, the doses used in their experiments testing for therapeutic relief in their arthritic model may have had some motor effect.

To identify any reported differences in intra-articular injections of BoNT/A the literature review also extended to published reports on injections of BOTOX® into the rat ankle joint. This was to investigate if the anatomical structure of a joint capsule played a role in the dose limitations observed, and if this was consistent with other joints. Two papers on injections of BOTOX® into the rat CFA inflamed ankle were found (Fan et al., 2017, Wang et al., 2017c); both studies tested injections of 10 U of BOTOX® into the rat ankle (estimated to be 25 U/Kg based on the reported rat weights), while Fan et al. also tested injections of 1 U and 3 U (~ 2.5 U/Kg and 7.5 U/Kg). These lower doses are in range of intra-plantar doses of BOTOX® used in rats in other pain models (Park et al., 2006, Cui et al., 2004); unfortunately Fan et al. only tested for adverse effects from the toxin injections by measures such as weight loss, hunched behaviour, and loss of appetite, without assessing limb weakness. From the reported dosing study for the knee MaxTD, it was found that weight loss did not always correlate with obvious limb dragging behaviours and used other

measures such as DAS and weight bearing to assess paralysis. Wang et al. (2017c) stated that no weakness was observed in the animals but did not explain how this was tested, however the authors acknowledged that side effects of the BOTOX® injections had not been fully evaluated and digital gait analysis would need to be used to identify an accurate dose to test in further studies. Based on the lack of appropriate evaluation of limb weakness it is not possible to confirm that the doses used did not induce paralysis and if there are similar dose limitations of the ankle joint as with the knee joint.

Testing of LC/E-BoNT/A and BoNT/A in the CFA knee inflammation model showed no effects of either toxin on functional limb recovery, joint sensitivity or swelling. Considering the knee doses (LC/E-BoNT/A - 25 U/Kg, BoNT/A – 5 U/Kg) were much lower than the intra-plantar doses (LC/E-BoNT/A - 75 U/Kg, BoNT/A – 15 U/Kg) that showed analgesic effects in the SNI and capsaicin models, it is likely that the doses administered were simply too low to have an anti-nociceptive or anti-inflammatory effect on the model. Interestingly, injections of 2.5 U/Kg of BOTOX® (a lower dose than those used by Cui et al. 2004 and Bach-Rojecky and Lackovic et al., 2005) into the rat ankle have been shown to have a partial analgesic effect on reduced hind-paw thresholds in a model of CFA injection into the ankle (Fan et al., 2017). This may be due to the smaller amount of CFA injected into the ankle compared to the knee (50 µl vs. 150 µl), and so there is potentially less inflammation and pain to reduce in this model which could be accomplished with a lower dose of neurotoxin. One method to overcome the dose limitation of the knee would be to administer intra-plantar injections of the neurotoxins to rats that have received CFA injections to the ankle. This would take advantage of the higher dose limit of the rat hind-paw. Secondary hyperalgesia is induced in the hind-paw by injections of CFA into the ankle and would likely be reduced as shown by (Mangione et al., 2016) who tested intra-plantar injections of Bitox in this model. The group showed a reduction in hind-paw hypersensitivity induced by the CFA injection into the ankle after an injection of Bitox into the sensitised hind-paw. Furthermore, intra-plantar injection of the LC/E-BoNT/A or BoNT/A could also reduce primary hyperalgesia and swelling at the CFA injected joint in this model. Reports have shown that Dysport® can reduce hyperalgesia in both rat hind-paws (bilateral anti-

nociceptive effect) in streptozotocin-induced diabetic polyneuropathy after an injection into only one hind-paw (unilateral injection) (Favre-Guilmard et al., 2017). Unilateral injection of Dysport® was also shown to have bilateral anti-nociceptive effects on rats injected in both hind-paws with Carrageenan (Favre-Guilmard et al., 2017). Considering these interesting analgesic effects are distal from the injection site, it is possible that an intra-plantar injection of LC/E-BoNT/A and BoNT/A could relieve hyperalgesia at the CFA inflamed ankle.

LC/E-BoNT/A completely reversed SNI sensitivity at select time points, and attenuated mechanical hypersensitivity to a greater extent than BoNT/A or LC/E-BoTIM/A

Injection of batch 1 LC/E-BoNT/A injection following SNI surgery was found to significantly improve mechanical pain withdrawal thresholds compared to LC/E-BoTIM/A, at days 3 and 7 post injection, and was significantly more efficacious than BoNT/A during days 3-10 post injection. It was also found to completely recover SNI-induced mechanical allodynia at days 3 and 7 post injection. There was no significant difference between LC/E-BoTIM/A and BoNT/A in relieving mechanical allodynia, however LC/E-BoTIM/A did improve von Frey thresholds compared to vehicle, while BoNT/A showed a non-significant increase in thresholds. This indicates that LC/E-BoTIM/A is a more viable therapeutic for the relief of neuropathic pain than BoNT/A, and LC/E-BoNT/A is the best of all three toxins tested. Since both LC/E-BoNT/A and LC/E-BoTIM/A contain an active LC/E, the greater number of amino acids cleaved from SNAP-25 by these molecules is assumed to underlie their greater efficacy in relieving mechanical allodynia. However, it is unclear as to what specific mechanism LC/E cleavage can act through to reduce SNI-induced pain at the hind-paw injection site. LC/E-BoNT/A and LC/E-BoTIM/A were expected to have a superior effect on pain relief to BoNT/A, based on their ability to block capsaicin-induced CGRP release *in vitro* (Wang et al., 2017a, Wang et al., 2011a). However, the SNI model shows decreased innervation of CGRP expressing neurons in the sensitised lateral side of the hind-paw (where the neurotoxins were injected) after injury (Duraku et al., 2012), indicating that inhibition of peripheral CGRP release by LC/E cleaved SNAP-25 is not the mechanism of analgesia for the chimeric neurotoxins in the SNI model. BoNT/A inhibits the fusion of TRPV1 and TRPA1 to the plasmalemma *in vitro* which can prevent upregulation

of these receptors in response to inflammatory mediators in painful conditions (Meng et al., 2016). LC/E-BoNT/A also inhibits the fusion of these channels (Nugent et al., 2018) and this was proposed to play another role in the anti-nociceptive mechanism of the toxin; however, neither of these receptors play obvious roles in mechanical allodynia induced by the SNI model. Deletion of TRPV1 expressing neurons by injections of resiniferatoxin (a TRPV1 agonist) showed no effect on von Frey thresholds while reducing pin prick hyperalgesia, indicating TRPV1 does not mediate static tactile allodynia in the SNI model (Yamamoto et al., 2013). TRPA1 knockdown mice have also shown mechanical hypersensitivity as measured by the von Frey test demonstrating that TRPA1 also does not mediate tactile allodynia in the SNI model (Eid et al., 2008). Furthermore, mRNA expression of both TRPV1 and TRPA1 is reduced in the DRG after SNI and does not return to normal until 3 months after injury (Staaf et al., 2009). Therefore, peripheral activity of these molecules in the hind-paw is unlikely to play a role in BoNT mediated recovery of von Frey thresholds in the SNI model. Since the superior effects of SNAP-25_E over SNAP-25_A on CGRP release are mediated by intracellular Ca^{2+}(Meng et al., 2009, Meng et al., 2007), there may be other pain inducing neurotransmitters and peptides whose Ca^{2+} dependent release is blocked by LC/E-BoNT/A and LC/E-BoTIM/A, which could underlie their effectiveness in in the SNI model. One can hypothesise that these two chimeras also prevent fusion of pain-inducing receptors other than TRPV1 and TRPA1, that BoNT/A may be unable to block due to sustained calcium uptake in peripheral or central sensitisation. P2X3 and P2X2/3 receptors are of particular interest as P2X receptor antagonists have been shown to reduce SNI-induced mechanical allodynia measured by von Frey tests (Chen et al., 2005). Exploring the effects of SNAP-25_E on the docking of these receptors *in vitro* by immunohistochemical staining of P2X receptor docking pre and post intoxication with LC/E-BoNT/A could provide more information on the mechanisms of action behind these toxins' analgesic effect in the SNI model.

As neuropathic pain models are driven strongly by ectopic activity from the site of nerve injury and the DRG, these serve to initiate and maintain mechanisms of central sensitisation (Costigan et al., 2009, Amir et al., 2005). If LC/E-BoNT/A is transported to either the DRG or central terminals in the dorsal horn via the spared sural nerve, then it could act as a potent inhibitor of the ectopic impulse

generation driving neuropathic pain. This spontaneous firing is expected to be driven by Na_V channels (Wang et al., 2011b), and Na_V1.3 specifically is known to be upregulated in the DRG of SNI rats (Berta et al., 2008). Inhibition of Na_V 1.3 upregulation in the DRG could be a target for LC/E-BoNT/A mediated relief of SNI pain; however, blocking Na_V 1.3 activity is not effective at relieving symptoms of SNI-induced neuropathic pain, and so the exact role the Na_v channels play in generating spontaneous impulses in neuropathic pain is unclear (Lindia et al., 2005). While LC/E-BoNT/A inhibition of CGRP release in the hind-paw is not likely to have an effect in inhibiting the development of SNI-induced pain, preventing CGRP release at the central terminals would aid in reducing the effects of SP release at the dorsal horn (Oku et al., 1987) and inhibiting action potential wind-up driven by these two neuropeptides(De Felipe et al., 1998). As increases of intracellular Ca^{2+} are characteristic of central sensitisation in the dorsal horn (Latremoliere and Woolf, 2009), LC/E-BoNT/A inhibition of the release of CGRP would be resistant to Ca^{2+} concentrations, unlike BoNT/A, and explain its more effective relief of SNI mechanical allodynia.

Lastly, it is also possible that the different doses of toxins injected could underlie the differences in anti-nociceptive effect. Since both LC/E-BoNT/A and LC/E-BoTIM/A were administered at higher doses than BoNT/A (75 vs 15 U/Kg), more total protein was being delivered to the hind-paw to cleave SNAP-25 and thus reduce SNI-induced pain. Converting the doses into raw values shows that approximately 38 pg of BoNT/A was injected per rat, compared to 320 pg of LC/E-BoNT/A and 938 pg of LC/E-BoTIM/A. This highlights that ~10 times more LC/E-BoNT/A than BoNT/A could be injected into the hind-paw without inducing paralysis, and ~25 times more LC/E-BoTIM/A than BoNT/A could be injected. This is surprising as LD_{50} values for these toxins indicated that LC/E-BoNT/A was only half as potent than BoNT/A, while LC/E-BoTIM/A was 5 times less potent than BoNT/A. These results show that it is possible that the paralytic potency of the toxin does not directly correlate with the anti-nociceptive mechanisms of BoNTs. Also, if the amount of SNARE cleaving protein being delivered was the main factor behind the analgesic mechanisms, it would be expected that LC/E-BoTIM/A would have had a greater effect in the SNI model than LC/E-BoNT/A, as 3 times more LC/E-BoTIM/A than LC/E-BoNT/A could be injected. Another question is why the

doses in LD_{50} units of each toxin varied at the plantar injection site? If LD_{50} units normalise the toxin concentrations based on activity, all toxins should have had the same MaxTD when injected into the hind-paw. The variation in MaxTD doses between the three toxins seems to indicate that the neurotoxins have different potencies in the hind-paw, which was not captured in the LD_{50} as this assay relied on intra-peritoneal injections, which is a very different environment for toxin uptake than the hind-paw. Further studies investigating the potency differences of these toxins and how this may contribute to their anti-nociceptive and paralytic effects are required.

Another question that arises from the results of the SNI study is why does LC/E-BoNT/A provide superior analgesia to LC/E-BoTIM/A in neuropathic pain. LC/E-BoNT/A retains an active LC/A while LC/E-BoTIM/A has an inactive LC/A mutant. Since LC/E and LC/A both target SNAP-25 and both neurotoxins produce $SNAP\text{-}25_E$, what additional benefit does LC/A provide to LC/E-BoNT/A over LC/E-BoTIM/A? As shown by the Western blots of plantaris muscle from LC/E-BoNT/A injected rats used in the dosing studies (Fig. 3.16 D), $SNAP\text{-}25_A$ and $SNAP\text{-}25_E$ were present *in vivo* at 8-9 days post injection of toxin, while LC/E-BoTIM/A only produces $SNAP\text{-}25_E$ *in vivo* (Wang et al., 2011a). One possibility is that the presence of two different cleaved SNAP-25 products may have a synergistic effect on analgesia in the SNI model. While cleavage of SNAP-25 by LC/E induces a robust blockade of vesicular fusion, cleavage of SNAP-25 by BoNT/A results in production of SDS-resistant complexes, whose inhibition of vesicular fusion can be reversed by sustained increases in intracellular Ca^{2+} unlike LC/E (Hayashi et al., 1994, Meng et al., 2009, Lu, 2015). Sustained increases of intracellular Ca^{2+} is characteristic of both peripheral and central sensitisation (Hagenacker et al., 2008, Latremoliere and Woolf, 2009). It is tempting to postulate that LC/E cleaved SNAP-25 may inhibit the docking of peripheral or central (if BoNTs undergo retrograde transport) opioid receptors, while LC/A inhibition of vesicular fusion will be reversed by increased intracellular Ca^{2+} and allow for fusion of opioid receptors to the plasma membrane. Evidence suggests that delta opioid receptors (DORs) in the rat DRG and dorsal horn are associated with LDCVs containing neuropeptides such as CGRP (Bao et al., 2003, Zhang et al., 1998), highlighting a SNARE mediated pathway of membrane fusion for DORs. Upregulation of μ-opioid receptors (MORs) have been

found in the DRG, dorsal horn and paw skin and upregulation of DORs have been found in DRGs and sciatic nerves in a number of nerve injury models (Stein et al., 2009, Bushlin et al., 2010) indicating that nerve injury may induce mechanisms to improve sensitivity to endogenous opioids, in order to inhibit pain. Hypothetically, a therapeutic that solely produces SNAP-25_E will inhibit release of pain inducing neurotransmitters and neuropeptides more effectively than BoNT/A, but also potentially prevent opioid receptor docking, an endogenous mechanism of pain inhibition. As LC/E-BoNT/A produces a mixed population of SNAP-25_E and SNAP-25_A at the presynaptic terminal, there could be a population of partially functional SNARE complexes present to allow docking of opioid receptors for endogenous pain inhibition, while the LC/E prevents formation of enough of these complexes to reduce release of pain inducing neurotransmitters. Experiments designed to investigate the ability of BoNT/A and LC/E-BoNT/A to inhibit MOR or DOR fusion to the plasma membrane would shed light on the potential of this tentative hypothesis.

Conclusions:

While the analgesic effect of LC/E-BoNT/A varied between different batches and potentially lost potency over long term storage, promising results in both acute inflammatory and chronic neuropathic pain models indicate its value as an improvement over BoNT/A for pain relief. Future experiments to evaluate this novel chimera will rely on identifying the role the LC/A plays in the superior anti-nociceptive effect of LC/E-BoNT/A over LC/E-BoTIM/A. Further work into the role that the dose differences between LC/E-BoNT/A, LC/E-BoTIM/A and BoNT/A play in their analgesic mechanisms would also be of value, and if alternative injection routes would prove suitable to utilise LC/E-BoNT/A in relieving models of chronic joint inflammatory pain. This will allow for a greater understanding of not only the anti-nociceptive mechanisms of these neurotoxins, but of the mechanisms behind different pre-clinical pain models.

Bibliography:

ABBOTT, F. V. & BONDER, M. 1997. Options for management of acute pain in the rat. *Vet Rec,* 140**,** 553-7.

ABRAM, S. E., MAMPILLY, G. A. & MILOSAVLJEVIC, D. 1997. Assessment of the potency and intrinsic activity of systemic versus intrathecal opioids in rats. *Anesthesiology,* 87**,** 127-34; discussion 27A-29A.

ALINE BOER, P., UENO, M., SANT'ANA, J. S., SAAD, M. J. & GONTIJO, J. A. 2005. Expression and localization of NK(1)R, substance P and CGRP are altered in dorsal root ganglia neurons of spontaneously hypertensive rats (SHR). *Brain Res Mol Brain Res,* 138**,** 35-44.

ALLERGAN, I. 2002. Botox cosmetic (botulinum toxin type A) purified neurotoxin complex [package insert] Allergan Pharmaceuticals (Ireland) Ltd. A subsidiary of: Allergan, Inc. 2525 Dupont Dr. Irvine, California 92612.

ALLERGAN, I. 2018. Botox cosmetic (botulinum toxin type A) purified neurotoxin complex [package insert] Allergan Pharmaceuticals (Ireland) Ltd. A subsidiary of: Allergan, Inc. 2525 Dupont Dr. Irvine, California 92612.

AMAYA, F., IZUMI, Y., MATSUDA, M. & SASAKI, M. 2013. Tissue injury and related mediators of pain exacerbation. *Curr Neuropharmacol,* 11**,** 592-7.

AMIR, R., KOCSIS, J. D. & DEVOR, M. 2005. Multiple interacting sites of ectopic spike electrogenesis in primary sensory neurons. *J Neurosci,* 25**,** 2576-85.

ANSEL, J. C., BROWN, J. R., PAYAN, D. G. & BROWN, M. A. 1993. Substance P selectively activates TNF-alpha gene expression in murine mast cells. *J Immunol,* 150**,** 4478-85.

ANTONUCCI, F., ROSSI, C., GIANFRANCESCHI, L., ROSSETTO, O. & CALEO, M. 2008. Long-distance retrograde effects of botulinum neurotoxin A. *J Neurosci,* 28**,** 3689-96.

AOKI, K. R. & FRANCIS, J. 2011. Updates on the antinociceptive mechanism hypothesis of botulinum toxin A. *Parkinsonism Relat Disord,* 17 Suppl 1**,** S28-33.

APALLA, Z., SOTIRIOU, E., LALLAS, A., LAZARIDOU, E. & IOANNIDES, D. 2013. Botulinum toxin A in postherpetic neuralgia: a parallel, randomized, double-blind, single-dose, placebo-controlled trial. *Clin J Pain,* 29**,** 857-64.

AURORA, S. K., DODICK, D. W., DIENER, H. C., DEGRYSE, R. E., TURKEL, C. C., LIPTON, R. B. & SILBERSTEIN, S. D. 2014. OnabotulinumtoxinA for chronic migraine: efficacy, safety, and tolerability in patients who received all five treatment cycles in the PREEMPT clinical program. *Acta Neurol Scand,* 129**,** 61-70.

BABA, H., JI, R. R., KOHNO, T., MOORE, K. A., ATAKA, T., WAKAI, A., OKAMOTO, M. & WOOLF, C. J. 2003. Removal of GABAergic inhibition facilitates polysynaptic A fiber-mediated excitatory transmission to the superficial spinal dorsal horn. *Mol Cell Neurosci,* 24**,** 818-30.

BACH-ROJECKY, L. & LACKOVIC, Z. 2005. Antinociceptive effect of botulinum toxin type a in rat model of carrageenan and capsaicin induced pain. *Croat Med J,* 46**,** 201-8.

BACH-ROJECKY, L. & LACKOVIC, Z. 2009. Central origin of the antinociceptive action of botulinum toxin type A. *Pharmacol Biochem Behav,* 94**,** 234-8.

BACH-ROJECKY, L., RELJA, M. & LACKOVIC, Z. 2005. Botulinum toxin type A in experimental neuropathic pain. *J Neural Transm (Vienna),* 112**,** 215-9.

BACH-ROJECKY, L., SALKOVIC-PETRISIC, M. & LACKOVIC, Z. 2010. Botulinum toxin type A reduces pain supersensitivity in experimental diabetic neuropathy: bilateral effect after unilateral injection. *Eur J Pharmacol,* 633**,** 10-4.

BAKHLE, Y. S. & BOTTING, R. M. 1996. Cyclooxygenase-2 and its regulation in inflammation. *Mediators Inflamm,* 5**,** 305-23.

BANERJEE, A., KOWALCHYK, J. A., DASGUPTA, B. R. & MARTIN, T. F. 1996. SNAP-25 is required for a late postdocking step in Ca2+-dependent exocytosis. *J Biol Chem,* 271**,** 20227-30.

BANIK, R. K., KASAI, M. & MIZUMURA, K. 2002. Reexamination of the difference in susceptibility to adjuvant-induced arthritis among LEW/Crj, Slc/Wistar/ST and Slc/SD rats. *Exp Anim,* 51**,** 197-201.

BAO, L., JIN, S. X., ZHANG, C., WANG, L. H., XU, Z. Z., ZHANG, F. X., WANG, L. C., NING, F. S., CAI, H. J., GUAN, J. S., XIAO, H. S., XU, Z. Q., HE, C., HOKFELT, T., ZHOU, Z. & ZHANG, X. 2003. Activation of delta opioid receptors induces receptor insertion and neuropeptide secretion. *Neuron,* 37**,** 121-33.

BARON, R. 2006. Mechanisms of disease: neuropathic pain--a clinical perspective. *Nat Clin Pract Neurol,* 2**,** 95-106.

BARRETT, A. C., SMITH, E. S. & PICKER, M. J. 2003. Capsaicin-induced hyperalgesia and mu-opioid-induced antihyperalgesia in male and female Fischer 344 rats. *J Pharmacol Exp Ther,* 307**,** 237-45.

BARTON, N. J., STRICKLAND, I. T., BOND, S. M., BRASH, H. M., BATE, S. T., WILSON, A. W., CHESSELL, I. P., REEVE, A. J. & MCQUEEN, D. S. 2007. Pressure application measurement (PAM): a novel behavioural technique for measuring hypersensitivity in a rat model of joint pain. *J Neurosci Methods,* 163**,** 67-75.

BASBAUM, A. I., BAUTISTA, D. M., SCHERRER, G. & JULIUS, D. 2009. Cellular and molecular mechanisms of pain. *Cell,* 139**,** 267-84.

BENECKE, R., JOST, W. H., KANOVSKY, P., RUZICKA, E., COMES, G. & GRAFE, S. 2005. A new botulinum toxin type A free of complexing proteins for treatment of cervical dystonia. *Neurology,* 64**,** 1949-51.

BENOLIEL, R., ELIAV, E. & TAL, M. 2002. Strain-dependent modification of neuropathic pain behaviour in the rat hindpaw by a priming painful trigeminal nerve injury. *Pain,* 97**,** 203-12.

BERTA, T., POIROT, O., PERTIN, M., JI, R. R., KELLENBERGER, S. & DECOSTERD, I. 2008. Transcriptional and functional profiles of voltage-gated Na(+) channels in injured and non-injured DRG neurons in the SNI model of neuropathic pain. *Mol Cell Neurosci,* 37**,** 196-208.

BINDER, W. J., BRIN, M. F., BLITZER, A., SCHOENROCK, L. D. & POGODA, J. M. 2000. Botulinum toxin type A (BOTOX) for treatment of migraine headaches: an open-label study. *Otolaryngol Head Neck Surg,* 123**,** 669-76.

BINSHTOK, A. M., WANG, H., ZIMMERMANN, K., AMAYA, F., VARDEH, D., SHI, L., BRENNER, G. J., JI, R. R., BEAN, B. P., WOOLF, C. J. & SAMAD, T. A. 2008. Nociceptors are interleukin-1beta sensors. *J Neurosci,* 28**,** 14062-73.

BINZ, T. & RUMMEL, A. 2009. Cell entry strategy of clostridial neurotoxins. *J Neurochem,* 109**,** 1584-95.

BIOLEGEND.COM. *Synaptic vesicle exocytosis* [Online]. Available: https://www.biolegend.com/NewsLegend/021616synaptic/index.htm [Accessed 07/10/2018 2018].

BLACK, J. D. & DOLLY, J. O. 1986. Interaction of 125I-labeled botulinum neurotoxins with nerve terminals. I. Ultrastructural autoradiographic localization and quantitation of distinct membrane acceptors for types A and B on motor nerves. *J Cell Biol,* 103**,** 521-34.

BOON, A. J., SMITH, J., DAHM, D. L., SORENSON, E. J., LARSON, D. R., FITZ-GIBBON, P. D., DYKSTRA, D. D. & SINGH, J. A. 2010. Efficacy of intra-articular botulinum toxin type A in painful knee osteoarthritis: a pilot study. *PM R,* 2**,** 268-76.

BOSTOCK, H., CAMPERO, M., SERRA, J. & OCHOA, J. L. 2005. Temperature-dependent double spikes in C-nociceptors of neuropathic pain patients. *Brain,* 128**,** 2154-63.

BRAIN, S. D., WILLIAMS, T. J., TIPPINS, J. R., MORRIS, H. R. & MACINTYRE, I. 1985. Calcitonin gene-related peptide is a potent vasodilator. *Nature,* 313**,** 54-6.

BREIVIK, H., COLLETT, B., VENTAFRIDDA, V., COHEN, R. & GALLACHER, D. 2006. Survey of chronic pain in Europe: prevalence, impact on daily life, and treatment. *Eur J Pain,* 10**,** 287-333.

BROIDE, R. S., RUBINO, J., NICHOLSON, G. S., ARDILA, M. C., BROWN, M. S., AOKI, K. R. & FRANCIS, J. 2013. The rat Digit Abduction Score (DAS) assay: a physiological model for assessing botulinum neurotoxin-induced skeletal muscle paralysis. *Toxicon,* 71**,** 18-24.

BUDAI, D. & LARSON, A. A. 1996. Role of substance P in the modulation of C-fiber-evoked responses of spinal dorsal horn neurons. *Brain Res,* 710**,** 197-203.

BULDYREV, I., TANNER, N. M., HSIEH, H. Y., DODD, E. G., NGUYEN, L. T. & BALKOWIEC, A. 2006. Calcitonin gene-related peptide enhances release of native brain-derived neurotrophic factor from trigeminal ganglion neurons. *J Neurochem,* 99**,** 1338-50.
BUSHLIN, I., ROZENFELD, R. & DEVI, L. A. 2010. Cannabinoid-opioid interactions during neuropathic pain and analgesia. *Curr Opin Pharmacol,* 10**,** 80-6.
CAI, B. B., FRANCIS, J., BRIN, M. F. & BROIDE, R. S. 2017. Botulinum neurotoxin type A-cleaved SNAP25 is confined to primary motor neurons and localized on the plasma membrane following intramuscular toxin injection. *Neuroscience,* 352**,** 155-169.
CAMPBELL, J. N. & MEYER, R. A. 2006. Mechanisms of neuropathic pain. *Neuron,* 52**,** 77-92.
CARLTON, S. M. & COGGESHALL, R. E. 1999. Inflammation-induced changes in peripheral glutamate receptor populations. *Brain Res,* 820**,** 63-70.
CARVALHO, A. L., DUARTE, C. B. & CARVALHO, A. P. 2000. Regulation of AMPA receptors by phosphorylation. *Neurochem Res,* 25**,** 1245-55.
CDC 1998. *Botulism in the United States, 1899-1996; handbook for epidemiologists, clinicians, and laboratory workers,* U.S. Dept. of Health and Human Services, Public Health Service, Centers for Disease Control and Prevention, National Center for Infectious Diseases, Division of Bacterial and Mycotic Diseases.
CERRITO, F., LAZZARO, M. P., GAUDIO, E., ARMINIO, P. & ALOISI, G. 1993. 5HT2-receptors and serotonin release: their role in human platelet aggregation. *Life Sci,* 53**,** 209-15.
CERVERO, F. & LAIRD, J. M. 1996. From acute to chronic pain: mechanisms and hypotheses. *Prog Brain Res,* 110**,** 3-15.
CHATTERJEA, D. & MARTINOV, T. 2015. Mast cells: versatile gatekeepers of pain. *Mol Immunol,* 63**,** 38-44.
CHEN, B. S. & ROCHE, K. W. 2007. Regulation of NMDA receptors by phosphorylation. *Neuropharmacology,* 53**,** 362-8.
CHEN, S. 2012. Clinical uses of botulinum neurotoxins: current indications, limitations and future developments. *Toxins (Basel),* 4**,** 913-39.
CHEN, S. & BARBIERI, J. T. 2006. Unique substrate recognition by botulinum neurotoxins serotypes A and E. *J Biol Chem,* 281**,** 10906-11.
CHEN, Y., LI, G. W., WANG, C., GU, Y. & HUANG, L. Y. 2005. Mechanisms underlying enhanced P2X receptor-mediated responses in the neuropathic pain state. *Pain,* 119**,** 38-48.
CHEN, Y. W., CHIU, Y. W., CHEN, C. Y. & CHUANG, S. K. 2015. Botulinum toxin therapy for temporomandibular joint disorders: a systematic review of randomized controlled trials. *Int J Oral Maxillofac Surg,* 44**,** 1018-26.
COE, M. A., LOFWALL, M. R. & WALSH, S. L. 2019. Buprenorphine Pharmacology Review: Update on Transmucosal and Long-acting Formulations. *J Addict Med,* 13**,** 93-103.
COHEN, J. I. & NGUYEN, H. 1997. Varicella-zoster virus glycoprotein I is essential for growth of virus in Vero cells. *J Virol,* 71**,** 6913-20.
COLASANTE, C., ROSSETTO, O., MORBIATO, L., PIRAZZINI, M., MOLGO, J. & MONTECUCCO, C. 2013. Botulinum neurotoxin type A is internalized and translocated from small synaptic vesicles at the neuromuscular junction. *Mol Neurobiol,* 48**,** 120-7.
CONSTANTIN, C. E., MAIR, N., SAILER, C. A., ANDRATSCH, M., XU, Z. Z., BLUMER, M. J., SCHERBAKOV, N., DAVIS, J. B., BLUETHMANN, H., JI, R. R. & KRESS, M. 2008. Endogenous tumor necrosis factor alpha (TNFalpha) requires TNF receptor type 2 to generate heat hyperalgesia in a mouse cancer model. *J Neurosci,* 28**,** 5072-81.
COSTIGAN, M., SCHOLZ, J. & WOOLF, C. J. 2009. Neuropathic pain: a maladaptive response of the nervous system to damage. *Annu Rev Neurosci,* 32**,** 1-32.
COX, B. M., CHRISTIE, M. J., DEVI, L., TOLL, L. & TRAYNOR, J. R. 2015. Challenges for opioid receptor nomenclature: IUPHAR Review 9. *Br J Pharmacol,* 172**,** 317-23.
CUI, M., KHANIJOU, S., RUBINO, J. & AOKI, K. R. 2004. Subcutaneous administration of botulinum toxin A reduces formalin-induced pain. *Pain,* 107**,** 125-33.
DA SILVA, L. F., DESANTANA, J. M. & SLUKA, K. A. 2010. Activation of NMDA receptors in the brainstem, rostral ventromedial medulla, and nucleus reticularis gigantocellularis

mediates mechanical hyperalgesia produced by repeated intramuscular injections of acidic saline in rats. *J Pain,* 11**,** 378-87.
DAHAN, A., AARTS, L. & SMITH, T. W. 2010. Incidence, Reversal, and Prevention of Opioid-induced Respiratory Depression. *Anesthesiology,* 112**,** 226-38.
DALLEL, R., RABOISSON, P., CLAVELOU, P., SAADE, M. & WODA, A. 1995. Evidence for a peripheral origin of the tonic nociceptive response to subcutaneous formalin. *Pain,* 61**,** 11-6.
DALZIEL, R. G., BINGHAM, S., SUTTON, D., GRANT, D., CHAMPION, J. M., DENNIS, S. A., QUINN, J. P., BOUNTRA, C. & MARK, M. A. 2004. Allodynia in rats infected with varicella zoster virus--a small animal model for post-herpetic neuralgia. *Brain Res Brain Res Rev,* 46**,** 234-42.
DE FELIPE, C., HERRERO, J. F., O'BRIEN, J. A., PALMER, J. A., DOYLE, C. A., SMITH, A. J., LAIRD, J. M., BELMONTE, C., CERVERO, F. & HUNT, S. P. 1998. Altered nociception, analgesia and aggression in mice lacking the receptor for substance P. *Nature,* 392**,** 394-7.
DECOSTERD, I. & WOOLF, C. J. 2000. Spared nerve injury: an animal model of persistent peripheral neuropathic pain. *Pain,* 87**,** 149-58.
DEUIS, J. R. & VETTER, I. 2016. The thermal probe test: A novel behavioral assay to quantify thermal paw withdrawal thresholds in mice. *Temperature (Austin),* 3**,** 199-207.
DEVESA, I., FERRANDIZ-HUERTAS, C., MATHIVANAN, S., WOLF, C., LUJAN, R., CHANGEUX, J. P. & FERRER-MONTIEL, A. 2014. alphaCGRP is essential for algesic exocytotic mobilization of TRPV1 channels in peptidergic nociceptors. *Proc Natl Acad Sci U S A,* 111**,** 18345-50.
DHAKED, R. K., SINGH, M. K., SINGH, P. & GUPTA, P. 2010. Botulinum toxin: bioweapon & magic drug. *Indian J Med Res,* 132**,** 489-503.
DIXON, W. J. 1980. Efficient analysis of experimental observations. *Annu Rev Pharmacol Toxicol,* 20**,** 441-62.
DJOUHRI, L. & LAWSON, S. N. 2004. Abeta-fiber nociceptive primary afferent neurons: a review of incidence and properties in relation to other afferent A-fiber neurons in mammals. *Brain Res Brain Res Rev,* 46**,** 131-45.
DJOUHRI, L., NEWTON, R., LEVINSON, S. R., BERRY, C. M., CARRUTHERS, B. & LAWSON, S. N. 2003. Sensory and electrophysiological properties of guinea-pig sensory neurones expressing Nav 1.7 (PN1) Na+ channel alpha subunit protein. *J Physiol,* 546**,** 565-76.
DODICK, D. W., MAUSKOP, A., ELKIND, A. H., DEGRYSE, R., BRIN, M. F., SILBERSTEIN, S. D. & GROUP, B. C. S. 2005. Botulinum toxin type a for the prophylaxis of chronic daily headache: subgroup analysis of patients not receiving other prophylactic medications: a randomized double-blind, placebo-controlled study. *Headache,* 45**,** 315-24.
DOLLY, J. O., WANG, J., ZURAWSKI, T. H. & MENG, J. 2011. Novel therapeutics based on recombinant botulinum neurotoxins to normalize the release of transmitters and pain mediators. *FEBS J,* 278**,** 4454-66.
DONALDSON, L. F. 2009. Neurogenic Mechanisms in Arthritis. *In:* JANCSÓ, G. B. (ed.) *NeuroImmune Biology.* Elsevier, 8, 211-241.
DONG, M., YEH, F., TEPP, W. H., DEAN, C., JOHNSON, E. A., JANZ, R. & CHAPMAN, E. R. 2006. SV2 is the protein receptor for botulinum neurotoxin A. *Science,* 312**,** 592-6.
DRENTH, J. P. & WAXMAN, S. G. 2007. Mutations in sodium-channel gene SCN9A cause a spectrum of human genetic pain disorders. *J Clin Invest,* 117**,** 3603-9.
DREW, L. J., RUGIERO, F. & WOOD, J. N. 2007. Chapter 15 - Touch. *In:* HAMILL, O. P. (ed.) *Current Topics in Membranes.* Academic Press, 59, 425-465.
DUERSCHMIED, D., SUIDAN, G. L., DEMERS, M., HERR, N., CARBO, C., BRILL, A., CIFUNI, S. M., MAULER, M., CICKO, S., BADER, M., IDZKO, M., BODE, C. & WAGNER, D. D. 2013. Platelet serotonin promotes the recruitment of neutrophils to sites of acute inflammation in mice. *Blood,* 121**,** 1008-15.
DURAKU, L. S., HOSSAINI, M., HOENDERVANGERS, S., FALKE, L. L., KAMBIZ, S., MUDERA, V. C., HOLSTEGE, J. C., WALBEEHM, E. T. & RUIGROK, T. J. 2012. Spatiotemporal dynamics of re-innervation and hyperinnervation patterns by uninjured CGRP fibers in the rat foot sole epidermis after nerve injury. *Mol Pain,* 8**,** 61.

DURHAM, P. L., CADY, R. & CADY, R. 2004. Regulation of calcitonin gene-related peptide secretion from trigeminal nerve cells by botulinum toxin type A: implications for migraine therapy. *Headache,* 44**,** 35-42; discussion 42-3.

DWORKIN, R. H., O'CONNOR, A. B., BACKONJA, M., FARRAR, J. T., FINNERUP, N. B., JENSEN, T. S., KALSO, E. A., LOESER, J. D., MIASKOWSKI, C., NURMIKKO, T. J., PORTENOY, R. K., RICE, A. S., STACEY, B. R., TREEDE, R. D., TURK, D. C. & WALLACE, M. S. 2007. Pharmacologic management of neuropathic pain: evidence-based recommendations. *Pain,* 132**,** 237-51.

EID, S. R., CROWN, E. D., MOORE, E. L., LIANG, H. A., CHOONG, K. C., DIMA, S., HENZE, D. A., KANE, S. A. & URBAN, M. O. 2008. HC-030031, a TRPA1 selective antagonist, attenuates inflammatory- and neuropathy-induced mechanical hypersensitivity. *Mol Pain,* 4**,** 48.

EISELE, K. H., FINK, K., VEY, M. & TAYLOR, H. V. 2011. Studies on the dissociation of botulinum neurotoxin type A complexes. *Toxicon,* 57**,** 555-65.

EISENBERG, E., MCNICOL, E. D. & CARR, D. B. 2005. Efficacy and safety of opioid agonists in the treatment of neuropathic pain of nonmalignant origin: systematic review and meta-analysis of randomized controlled trials. *JAMA,* 293**,** 3043-52.

ELEOPRA, R., TUGNOLI, V., ROSSETTO, O., DE GRANDIS, D. & MONTECUCCO, C. 1998. Different time courses of recovery after poisoning with botulinum neurotoxin serotypes A and E in humans. *Neurosci Lett,* 256**,** 135-8.

FAN, C., CHU, X., WANG, L., SHI, H. & LI, T. 2017. Botulinum toxin type A reduces TRPV1 expression in the dorsal root ganglion in rats with adjuvant-arthritis pain. *Toxicon,* 133**,** 116-122.

FANG, D., KONG, L. Y., CAI, J., LI, S., LIU, X. D., HAN, J. S. & XING, G. G. 2015. Interleukin-6-mediated functional upregulation of TRPV1 receptors in dorsal root ganglion neurons through the activation of JAK/PI3K signaling pathway: roles in the development of bone cancer pain in a rat model. *Pain,* 156**,** 1124-44.

FAVRE-GUILMARD, C., CHABRIER, P. E. & KALINICHEV, M. 2017. Bilateral analgesic effects of abobotulinumtoxinA (Dysport((R))) following unilateral administration in the rat. *Eur J Pain,* 21**,** 927-937.

FISCHER, A. & MONTAL, M. 2007. Crucial role of the disulfide bridge between botulinum neurotoxin light and heavy chains in protease translocation across membranes. *J Biol Chem,* 282**,** 29604-11.

FISCHER, M., CARLI, G., RABOISSON, P. & REEH, P. 2014. The interphase of the formalin test. *Pain,* 155**,** 511-21.

FLEETWOOD-WALKER, S. M., QUINN, J. P., WALLACE, C., BLACKBURN-MUNRO, G., KELLY, B. G., FISKERSTRAND, C. E., NASH, A. A. & DALZIEL, R. G. 1999. Behavioural changes in the rat following infection with varicella-zoster virus. *J Gen Virol,* 80 (Pt 9)**,** 2433-6.

FLOR, H., NIKOLAJSEN, L. & STAEHELIN JENSEN, T. 2006. Phantom limb pain: a case of maladaptive CNS plasticity? *Nat Rev Neurosci,* 7**,** 873-81.

FORAN, P. G., MOHAMMED, N., LISK, G. O., NAGWANEY, S., LAWRENCE, G. W., JOHNSON, E., SMITH, L., AOKI, K. R. & DOLLY, J. O. 2003. Evaluation of the therapeutic usefulness of botulinum neurotoxin B, C1, E, and F compared with the long lasting type A. Basis for distinct durations of inhibition of exocytosis in central neurons. *J Biol Chem,* 278**,** 1363-71.

FREVERT, J. 2010. Content of botulinum neurotoxin in Botox(R)/Vistabel(R), Dysport(R)/Azzalure(R), and Xeomin(R)/Bocouture(R). *Drugs R D,* 10**,** 67-73.

FURLAN, A. D., SANDOVAL, J. A., MAILIS-GAGNON, A. & TUNKS, E. 2006. Opioids for chronic noncancer pain: a meta-analysis of effectiveness and side effects. *CMAJ,* 174**,** 1589-94.

GÁBOR JANCSÓ, M. K., VIKTOR HORVÁTH, PÉTER SÁNTHA, JÓZSEF NAGY 2009. Sensory Nerves as Modulators of Cutaneous Inflammatory Reactions in Health and Disease. *In:* JANCSÓ, G. (ed.) *Neuroimmune Biology.* Elsevier, 8, 1-36.

GADES, N. M., DANNEMAN, P. J., WIXSON, S. K. & TOLLEY, E. A. 2000. The magnitude and duration of the analgesic effect of morphine, butorphanol, and buprenorphine in rats and mice. *Contemp Top Lab Anim Sci,* 39**,** 8-13.

GARRY, E. M., DELANEY, A., ANDERSON, H. A., SIRINATHSINGHJI, E. C., CLAPP, R. H., MARTIN, W. J., KINCHINGTON, P. R., KRAH, D. L., ABBADIE, C. & FLEETWOOD-WALKER, S. M. 2005. Varicella zoster virus induces neuropathic changes in rat dorsal root ganglia and behavioral reflex sensitisation that is attenuated by gabapentin or sodium channel blocking drugs. *Pain,* 118**,** 97-111.

GARTLAN, M. G. & HOFFMAN, H. T. 1993. Crystalline preparation of botulinum toxin type A (Botox): degradation in potency with storage. *Otolaryngol Head Neck Surg,* 108**,** 135-40.

GERONA, R. R., LARSEN, E. C., KOWALCHYK, J. A. & MARTIN, T. F. 2000. The C terminus of SNAP25 is essential for Ca(2+)-dependent binding of synaptotagmin to SNARE complexes. *J Biol Chem,* 275**,** 6328-36.

GILCHRIST, H. D., ALLARD, B. L. & SIMONE, D. A. 1996. Enhanced withdrawal responses to heat and mechanical stimuli following intraplantar injection of capsaicin in rats. *Pain,* 67**,** 179-88.

GOLD, M. S. & GEBHART, G. F. 2010. Nociceptor sensitization in pain pathogenesis. *Nat Med,* 16**,** 1248-57.

GOLDBERG, D. S. & MCGEE, S. J. 2011. Pain as a global public health priority. *BMC Public Health,* 11**,** 770.

GOLLI, N. E., DALLAGI, Y., RAHALI, D., REJEB, I. & FAZAA, S. E. 2016. Neurobehavioral assessment following e-cigarette refill liquid exposure in adult rats. *Toxicol Mech Methods,* 26**,** 435-42.

GRONBLAD, M., KONTTINEN, Y. T., KORKALA, O., LIESI, P., HUKKANEN, M. & POLAK, J. M. 1988. Neuropeptides in synovium of patients with rheumatoid arthritis and osteoarthritis. *J Rheumatol,* 15**,** 1807-10.

GU, S. & JIN, R. 2013. Assembly and function of the botulinum neurotoxin progenitor complex. *Curr Top Microbiol Immunol,* 364**,** 21-44.

GUEDON, J. M., YEE, M. B., ZHANG, M., HARVEY, S. A., GOINS, W. F. & KINCHINGTON, P. R. 2015. Neuronal changes induced by Varicella Zoster Virus in a rat model of postherpetic neuralgia. *Virology,* 482**,** 167-80.

GUEDON, J. M., ZHANG, M., GLORIOSO, J. C., GOINS, W. F. & KINCHINGTON, P. R. 2014. Relief of pain induced by varicella-zoster virus in a rat model of post-herpetic neuralgia using a herpes simplex virus vector expressing enkephalin. *Gene Ther,* 21**,** 694-702.

GUSTAVSSON, N., WU, B. & HAN, W. 2012. Calcium sensing in exocytosis. *Adv Exp Med Biol,* 740**,** 731-57.

HABERMANN, E. 1974. 125I-labeled neurotoxin from *Clostridium botulinum* A: preparation, binding to synaptosomes and ascent to the spinal cord. *Naunyn Schmiedebergs Arch Pharmacol,* 281**,** 47-56.

HAGENACKER, T., LEDWIG, D. & BUSSELBERG, D. 2008. Feedback mechanisms in the regulation of intracellular calcium ([Ca2+]i) in the peripheral nociceptive system: role of TRPV-1 and pain related receptors. *Cell Calcium,* 43**,** 215-27.

HAGENAH, R., BENECKE, R. & WIEGAND, H. 1977. Effects of type A botulinum toxin on the cholinergic transmission at spinal Renshaw cells and on the inhibitory action at Ia inhibitory interneurones. *Naunyn Schmiedebergs Arch Pharmacol,* 299**,** 267-72.

HARCUS, A. H., WARD, A. E. & SMITH, D. W. 1980. Buprenorphine in postoperative pain: results in 7500 patients. *Anaesthesia,* 35**,** 382-6.

HASNIE, F. S., BREUER, J., PARKER, S., WALLACE, V., BLACKBEARD, J., LEVER, I., KINCHINGTON, P. R., DICKENSON, A. H., PHEBY, T. & RICE, A. S. 2007. Further characterization of a rat model of varicella zoster virus-associated pain: Relationship between mechanical hypersensitivity and anxiety-related behavior, and the influence of analgesic drugs. *Neuroscience,* 144**,** 1495-508.

HAYASHI, T., MCMAHON, H., YAMASAKI, S., BINZ, T., HATA, Y., SUDHOF, T. C. & NIEMANN, H. 1994. Synaptic vesicle membrane fusion complex: action of clostridial neurotoxins on assembly. *EMBO J,* 13**,** 5051-61.

HENDRIKSEN, C. F. M., MORTON, D. B. & LTD, L. A. 1999. *Humane endpoints in animal experiments for biomedical research: proceedings of the international conference, 22-25 November 1998, Zeist, the Netherlands*, Royal Society of Medicine Press.
HIRSCH, S., CORRADINI, L., JUST, S., ARNDT, K. & DOODS, H. 2013. The CGRP receptor antagonist BIBN4096BS peripherally alleviates inflammatory pain in rats. *Pain,* 154**,** 700-7.
HU, Y., GUAN, X., FAN, L., LI, M., LIAO, Y., NIE, Z. & JIN, L. 2013. Therapeutic efficacy and safety of botulinum toxin type A in trigeminal neuralgia: a systematic review. *J Headache Pain,* 14**,** 72.
HUMEAU, Y., DOUSSAU, F., GRANT, N. J. & POULAIN, B. 2000. How botulinum and tetanus neurotoxins block neurotransmitter release. *Biochimie,* 82**,** 427-46.
HUNSKAAR, S. & HOLE, K. 1987. The formalin test in mice: dissociation between inflammatory and non-inflammatory pain. *Pain,* 30**,** 103-14.
HUNT, S. P., PINI, A. & EVAN, G. 1987. Induction of c-fos-like protein in spinal cord neurons following sensory stimulation. *Nature,* 328**,** 632-4.
JABBARI, B. & MACHADO, D. 2011. Treatment of refractory pain with botulinum toxins--an evidence-based review. *Pain Med,* 12**,** 1594-606.
JAGGI, A. S., JAIN, V. & SINGH, N. 2011. Animal models of neuropathic pain. *Fundam Clin Pharmacol,* 25**,** 1-28.
JAHN, R. & FASSHAUER, D. 2012. Molecular machines governing exocytosis of synaptic vesicles. *Nature,* 490**,** 201-7.
JANSEN, L. M., VAN DER HORST-BRUINSMA, I. E., VAN SCHAARDENBURG, D., BEZEMER, P. D. & DIJKMANS, B. A. 2001. Predictors of radiographic joint damage in patients with early rheumatoid arthritis. *Ann Rheum Dis,* 60**,** 924-7.
JI, R. R., SAMAD, T. A., JIN, S. X., SCHMOLL, R. & WOOLF, C. J. 2002. p38 MAPK activation by NGF in primary sensory neurons after inflammation increases TRPV1 levels and maintains heat hyperalgesia. *Neuron,* 36**,** 57-68.
JIN, X. & GEREAU, R. W. T. 2006. Acute p38-mediated modulation of tetrodotoxin-resistant sodium channels in mouse sensory neurons by tumor necrosis factor-alpha. *J Neurosci,* 26**,** 246-55.
JOHNSON, A. R. & ERDOS, E. G. 1973. Release of histamine from mast cells by vasoactive peptides. *Proc Soc Exp Biol Med,* 142**,** 1252-6.
JULIUS, D. 2013. TRP channels and pain. *Annu Rev Cell Dev Biol,* 29**,** 355-84.
KAWABATA, A. 2011. Prostaglandin E2 and pain--an update. *Biol Pharm Bull,* 34**,** 1170-3.
KAWASAKI, Y., ZHANG, L., CHENG, J. K. & JI, R. R. 2008. Cytokine mechanisms of central sensitization: distinct and overlapping role of interleukin-1beta, interleukin-6, and tumor necrosis factor-alpha in regulating synaptic and neuronal activity in the superficial spinal cord. *J Neurosci,* 28**,** 5189-94.
KE, J., LONG, X., LIU, Y., ZHANG, Y. F., LI, J., FANG, W. & MENG, Q. G. 2007. Role of NF-kappaB in TNF-alpha-induced COX-2 expression in synovial fibroblasts from human TMJ. *J Dent Res,* 86**,** 363-7.
KIDD, B. L., MAPP, P. I., BLAKE, D. R., GIBSON, S. J. & POLAK, J. M. 1990. Neurogenic influences in arthritis. *Ann Rheum Dis,* 49**,** 649-52.
KIDD, B. L. & URBAN, L. A. 2001. Mechanisms of inflammatory pain. *Br J Anaesth,* 87**,** 3-11.
KING, W. 2013. Acute Pain, Subacute Pain, and Chronic Pain. *In:* GEBHART, G. F. & SCHMIDT, R. F. (eds.) *Encyclopedia of Pain.* Berlin, Heidelberg: Springer Berlin Heidelberg, 60-63.
KOHNO, T., WANG, H., AMAYA, F., BRENNER, G. J., CHENG, J. K., JI, R. R. & WOOLF, C. J. 2008. Bradykinin enhances AMPA and NMDA receptor activity in spinal cord dorsal horn neurons by activating multiple kinases to produce pain hypersensitivity. *J Neurosci,* 28**,** 4533-40.
KRESS, H. G. 2009. Clinical update on the pharmacology, efficacy and safety of transdermal buprenorphine. *Eur J Pain,* 13**,** 219-30.

KRISTENSEN, P. J., HEEGAARD, A. M., HESTEHAVE, S., JEGGO, R. D., BJERRUM, O. J. & MUNRO, G. 2017. Vendor-derived differences in injury-induced pain phenotype and pharmacology of Sprague-Dawley rats: Does it matter? *Eur J Pain,* 21**,** 692-704.

KUMAR, A., KAUR, H. & SINGH, A. 2018. Neuropathic Pain models caused by damage to central or peripheral nervous system. *Pharmacol Rep,* 70**,** 206-216.

LATREMOLIERE, A. & WOOLF, C. J. 2009. Central sensitization: a generator of pain hypersensitivity by central neural plasticity. *J Pain,* 10**,** 895-926.

LAU, C. G. & ZUKIN, R. S. 2007. NMDA receptor trafficking in synaptic plasticity and neuropsychiatric disorders. *Nat Rev Neurosci,* 8**,** 413-26.

LAVAND'HOMME, P. 2011. The progression from acute to chronic pain. *Curr Opin Anaesthesiol,* 24**,** 545-50.

LAVIN, Y. & MERAD, M. 2013. Macrophages: gatekeepers of tissue integrity. *Cancer Immunol Res,* 1**,** 201-9.

LAWRENCE, G. W., OVSEPIAN, S. V., WANG, J., AOKI, K. R. & DOLLY, J. O. 2012. Extravesicular intraneuronal migration of internalized botulinum neurotoxins without detectable inhibition of distal neurotransmission. *Biochem J,* 441**,** 443-52.

LE GREVES, P., NYBERG, F., TERENIUS, L. & HOKFELT, T. 1985. Calcitonin gene-related peptide is a potent inhibitor of substance P degradation. *Eur J Pharmacol,* 115**,** 309-11.

LEE, H. S., LEE, C. H., TSAI, H. C. & SALTER, D. M. 2009. Inhibition of cyclooxygenase 2 expression by diallyl sulfide on joint inflammation induced by urate crystal and IL-1beta. *Osteoarthritis Cartilage,* 17**,** 91-9.

LEE, M., SILVERMAN, S. M., HANSEN, H., PATEL, V. B. & MANCHIKANTI, L. 2011a. A comprehensive review of opioid-induced hyperalgesia. *Pain Physician,* 14**,** 145-61.

LEE, W. H., SHIN, T. J., KIM, H. J., LEE, J. K., SUH, H. W., LEE, S. C. & SEO, K. 2011b. Intrathecal administration of botulinum neurotoxin type A attenuates formalin-induced nociceptive responses in mice. *Anesth Analg,* 112**,** 228-35.

LEKAN, H. A., CARLTON, S. M. & COGGESHALL, R. E. 1996. Sprouting of A beta fibers into lamina II of the rat dorsal horn in peripheral neuropathy. *Neurosci Lett,* 208**,** 147-50.

LEMBECK, F. & HOLZER, P. 1979. Substance P as neurogenic mediator of antidromic vasodilation and neurogenic plasma extravasation. *Naunyn Schmiedebergs Arch Pharmacol,* 310**,** 175-83.

LESKE, H., HAASE, R., RESTLE, F., SCHICHOR, C., ALBRECHT, V., VIZOSO PINTO, M. G., TONN, J. C., BAIKER, A. & THON, N. 2012. Varicella zoster virus infection of malignant glioma cell cultures: a new candidate for oncolytic virotherapy? *Anticancer Res,* 32**,** 1137-44.

LI, J., CHEN, J. & KIRSNER, R. 2007. Pathophysiology of acute wound healing. *Clin Dermatol,* 25**,** 9-18.

LIN, Q., PENG, Y. B. & WILLIS, W. D. 1996. Inhibition of primate spinothalamic tract neurons by spinal glycine and GABA is reduced during central sensitization. *J Neurophysiol,* 76**,** 1005-14.

LINDIA, J. A., KOHLER, M. G., MARTIN, W. J. & ABBADIE, C. 2005. Relationship between sodium channel NaV1.3 expression and neuropathic pain behavior in rats. *Pain,* 117**,** 145-53.

LIU, B., LINLEY, J. E., DU, X., ZHANG, X., OOI, L., ZHANG, H. & GAMPER, N. 2010. The acute nociceptive signals induced by bradykinin in rat sensory neurons are mediated by inhibition of M-type K+ channels and activation of Ca2+-activated Cl- channels. *J Clin Invest,* 120**,** 1240-52.

LIU, X. J., GINGRICH, J. R., VARGAS-CABALLERO, M., DONG, Y. N., SENGAR, A., BEGGS, S., WANG, S. H., DING, H. K., FRANKLAND, P. W. & SALTER, M. W. 2008. Treatment of inflammatory and neuropathic pain by uncoupling Src from the NMDA receptor complex. *Nat Med,* 14**,** 1325-32.

LOESER, J. D., ARENDT-NIELSEN, L., BARON, R., BASBAUM, A., BOND, M., BREIVIK, H., CLAUW, D., LAAT, A. D., DWORKIN, R., GIAMBERARDINO, M. A., GOADSBY, P., HAANPAA, M., OKIFUJI, A., PAICE, J. & WODA, A. 2011. Part III: Pain Terms, A Current List with Definitions and Notes on Usage. *Classification of Chronic Pain.* Second edition ed. Seattle: IASP Press.

LOYD, D. R., HENRY, M. A. & HARGREAVES, K. M. 2013. Serotonergic neuromodulation of peripheral nociceptors. *Semin Cell Dev Biol,* 24**,** 51-7.
LOYD, D. R., WEISS, G., HENRY, M. A. & HARGREAVES, K. M. 2011. Serotonin increases the functional activity of capsaicin-sensitive rat trigeminal nociceptors via peripheral serotonin receptors. *Pain,* 152**,** 2267-76.
LU, B. 2015. The destructive effect of botulinum neurotoxins on the SNARE protein: SNAP-25 and synaptic membrane fusion. *PeerJ,* 3**,** e1065.
LUNDH, H., LEANDER, S. & THESLEFF, S. 1977. Antagonism of the paralysis produced by botulinum toxin in the rat. The effects of tetraethylammonium, guanidine and 4-aminopyridine. *J Neurol Sci,* 32**,** 29-43.
LUVISETTO, S., MARINELLI, S., COBIANCHI, S. & PAVONE, F. 2007. Anti-allodynic efficacy of botulinum neurotoxin A in a model of neuropathic pain. *Neuroscience,* 145**,** 1-4.
LUVISETTO, S., MARINELLI, S., LUCCHETTI, F., MARCHI, F., COBIANCHI, S., ROSSETTO, O., MONTECUCCO, C. & PAVONE, F. 2006. Botulinum neurotoxins and formalin-induced pain: central vs. peripheral effects in mice. *Brain Res,* 1082**,** 124-31.
MA, Q. P., HILL, R. & SIRINATHSINGHJI, D. 2001. Colocalization of CGRP with 5-HT1B/1D receptors and substance P in trigeminal ganglion neurons in rats. *Eur J Neurosci,* 13**,** 2099-104.
MAHOWALD, M. L., KRUG, H. E., SINGH, J. A. & DYKSTRA, D. 2009. Intra-articular Botulinum Toxin Type A: a new approach to treat arthritis joint pain. *Toxicon,* 54**,** 658-67.
MAHOWALD, M. L., SINGH, J. A. & DYKSTRA, D. 2006. Long term effects of intra-articular botulinum toxin A for refractory joint pain. *Neurotox Res,* 9**,** 179-88.
MALSCH, P., ANDRATSCH, M., VOGL, C., LINK, A. S., ALZHEIMER, C., BRIERLEY, S. M., HUGHES, P. A. & KRESS, M. 2014. Deletion of interleukin-6 signal transducer gp130 in small sensory neurons attenuates mechanonociception and down-regulates TRPA1 expression. *J Neurosci,* 34**,** 9845-56.
MANGIONE, A. S., OBARA, I., MAIARU, M., GERANTON, S. M., TASSORELLI, C., FERRARI, E., LEESE, C., DAVLETOV, B. & HUNT, S. P. 2016. Nonparalytic botulinum molecules for the control of pain. *Pain,* 157**,** 1045-55.
MANNAIONI, P. F., DI BELLO, M. G., RASPANTI, S., GAMBASSI, F., MUGNAI, L. & MASINI, E. 1993. Histamine release by human platelets. *Agents and Actions,* 38**,** C203-C205.
MAPP, P. I., KIDD, B. L., GIBSON, S. J., TERRY, J. M., REVELL, P. A., IBRAHIM, N. B., BLAKE, D. R. & POLAK, J. M. 1990. Substance P-, calcitonin gene-related peptide- and C-flanking peptide of neuropeptide Y-immunoreactive fibres are present in normal synovium but depleted in patients with rheumatoid arthritis. *Neuroscience,* 37**,** 143-53.
MARINELLI, S., VACCA, V., RICORDY, R., UGGENTI, C., TATA, A. M., LUVISETTO, S. & PAVONE, F. 2012. The analgesic effect on neuropathic pain of retrogradely transported botulinum neurotoxin A involves Schwann cells and astrocytes. *PLoS One,* 7**,** e47977.
MARINO, M. J., TERASHIMA, T., STEINAUER, J. J., EDDINGER, K. A., YAKSH, T. L. & XU, Q. 2014. Botulinum toxin B in the sensory afferent: transmitter release, spinal activation, and pain behavior. *Pain,* 155**,** 674-84.
MASSAAD, C. A., SAFIEH-GARABEDIAN, B., POOLE, S., ATWEH, S. F., JABBUR, S. J. & SAADE, N. E. 2004. Involvement of substance P, CGRP and histamine in the hyperalgesia and cytokine upregulation induced by intraplantar injection of capsaicin in rats. *J Neuroimmunol,* 153**,** 171-82.
MATAK, I. & LACKOVIC, Z. 2014. Botulinum toxin A, brain and pain. *Prog Neurobiol,* 119-120**,** 39-59.
MATAK, I., TEKUS, V., BOLCSKEI, K., LACKOVIC, Z. & HELYES, Z. 2017. Involvement of substance P in the antinociceptive effect of botulinum toxin type A: Evidence from knockout mice. *Neuroscience,* 358**,** 137-145.
MAYER, M. L., WESTBROOK, G. L. & GUTHRIE, P. B. 1984. Voltage-dependent block by Mg^{2+} of NMDA responses in spinal cord neurones. *Nature,* 309**,** 261-3.
MCCLEANE, G. 2008. Topical analgesic agents. *Clin Geriatr Med,* 24**,** 299-312, vii.

MCMAHON, H. T., FORAN, P., DOLLY, J. O., VERHAGE, M., WIEGANT, V. M. & NICHOLLS, D. G. 1992. Tetanus toxin and botulinum toxins type A and B inhibit glutamate, gamma-aminobutyric acid, aspartate, and met-enkephalin release from synaptosomes. Clues to the locus of action. *J Biol Chem,* 267**,** 21338-43.

MCNAMARA, C. R., MANDEL-BREHM, J., BAUTISTA, D. M., SIEMENS, J., DERANIAN, K. L., ZHAO, M., HAYWARD, N. J., CHONG, J. A., JULIUS, D., MORAN, M. M. & FANGER, C. M. 2007. TRPA1 mediates formalin-induced pain. *Proc Natl Acad Sci U S A,* 104**,** 13525-30.

MEDHURST, S. J. 2011. *Investigating the association between P2X7 receptors, microglia and the actions of morphine.* PhD. , University of Edinburgh.

MEDHURST, S. J., COLLINS, S. D., BILLINTON, A., BINGHAM, S., DALZIEL, R. G., BRASS, A., ROBERTS, J. C., MEDHURST, A. D. & CHESSELL, I. P. 2008. Novel histamine H3 receptor antagonists GSK189254 and GSK334429 are efficacious in surgically-induced and virally-induced rat models of neuropathic pain. *Pain,* 138**,** 61-9.

MEIER, T., WASNER, G., FAUST, M., KUNTZER, T., OCHSNER, F., HUEPPE, M., BOGOUSSLAVSKY, J. & BARON, R. 2003. Efficacy of lidocaine patch 5% in the treatment of focal peripheral neuropathic pain syndromes: a randomized, double-blind, placebo-controlled study. *Pain,* 106**,** 151-8.

MENDELL, L. M. & WALL, P. D. 1965. Responses of Single Dorsal Cord Cells to Peripheral Cutaneous Unmyelinated Fibres. *Nature,* 206**,** 97-9.

MENG, J., OVSEPIAN, S. V., WANG, J., PICKERING, M., SASSE, A., AOKI, K. R., LAWRENCE, G. W. & DOLLY, J. O. 2009. Activation of TRPV1 mediates calcitonin gene-related peptide release, which excites trigeminal sensory neurons and is attenuated by a retargeted botulinum toxin with anti-nociceptive potential. *J Neurosci,* 29**,** 4981-92.

MENG, J., WANG, J., LAWRENCE, G. & DOLLY, J. O. 2007. Synaptobrevin I mediates exocytosis of CGRP from sensory neurons and inhibition by botulinum toxins reflects their anti-nociceptive potential. *J Cell Sci,* 120**,** 2864-74.

MENG, J., WANG, J., STEINHOFF, M. & DOLLY, J. O. 2016. TNFalpha induces co-trafficking of TRPV1/TRPA1 in VAMP1-containing vesicles to the plasmalemma via Munc18-1/syntaxin1/SNAP-25 mediated fusion. *Sci Rep,* 6**,** 21226.

MERSKEY, H., ADDISON, R. G., BERIC, A., BLUMBERG, H., BOGDUK, N., BOIVIE, J., BOND, M. R., BONICA, J. J., BOYD, D. B., DEATHE, A. B., DEVOR, M., GRABOIS, M., GYBELS, J. M., HANSSON, P. T., JENSEN, T. S., LOESER, J. D., RAJ, P. P., SCADDING, J. W., SJAASTAD, O. M., SPANGFORT, E., TAIT, B., TASKER, R. R., TURK, D. C., VERVEST, A., WADDELL, J. G., WALL, P. D. & WATSON, C. P. N. 1994. *Classification of chronic pain,* Seattle, IASP press.

MILLAN, M. J. 1999. The induction of pain: an integrative review. *Prog Neurobiol,* 57**,** 1-164.

MILNER, R. & DOHERT, C. 2015. Pathophysiology of Pain in the Peripheral Nervous System. *In:* R. SHANE TUBBS, E. R., MOHAMMADALI M. SHOJA, MARIOS LOUKAS, NICHOLAS BARBARO, ROBERT J. SPINNER (ed.). Academic Press, 2, 3-22.

MORRA, M. E., ELGEBALY, A., ELMARAEZY, A., KHALIL, A. M., ALTIBI, A. M., VU, T. L., MOSTAFA, M. R., HUY, N. T. & HIRAYAMA, K. 2016. Therapeutic efficacy and safety of Botulinum Toxin A Therapy in Trigeminal Neuralgia: a systematic review and meta-analysis of randomized controlled trials. *J Headache Pain,* 17**,** 63.

MUIR, W. W., 3RD & WOOLF, C. J. 2001. Mechanisms of pain and their therapeutic implications. *J Am Vet Med Assoc,* 219**,** 1346-56.

MURASE, K. & RANDIC, M. 1984. Actions of substance P on rat spinal dorsal horn neurones. *J Physiol,* 346**,** 203-17.

MURASE, K., RYU, P. D. & RANDIC, M. 1986. Substance P augments a persistent slow inward calcium-sensitive current in voltage-clamped spinal dorsal horn neurons of the rat. *Brain Res,* 365**,** 369-76.

NEUMANN, S., DOUBELL, T. P., LESLIE, T. & WOOLF, C. J. 1996. Inflammatory pain hypersensitivity mediated by phenotypic switch in myelinated primary sensory neurons. *Nature,* 384**,** 360-4.

NIEHS 2008. Report on the ICCVAM-NICEATM/ECVAM Scientific Workshop on Alternative Methods to Refine, Reduce or Replace the Mouse LD50 Assay for Botulinum Toxin Testing NIH NIEHS.

NUGENT, M., YUSEF, Y. R., MENG, J., WANG, J. & DOLLY, J. O. 2018. A SNAP-25 cleaving chimera of botulinum neurotoxin /A and /E prevents TNFalpha-induced elevation of the activities of native TRP channels on early postnatal rat dorsal root ganglion neurons. *Neuropharmacology,* 138**,** 257-266.

O'NEILL, J., BROCK, C., OLESEN, A. E., ANDRESEN, T., NILSSON, M. & DICKENSON, A. H. 2012. Unravelling the mystery of capsaicin: a tool to understand and treat pain. *Pharmacol Rev,* 64**,** 939-71.

OH, H. M. & CHUNG, M. E. 2015. Botulinum Toxin for Neuropathic Pain: A Review of the Literature. *Toxins (Basel),* 7**,** 3127-54.

OKU, R., SATOH, M., FUJII, N., OTAKA, A., YAJIMA, H. & TAKAGI, H. 1987. Calcitonin gene-related peptide promotes mechanical nociception by potentiating release of substance P from the spinal dorsal horn in rats. *Brain Res,* 403**,** 350-4.

PARADA, C. A., TAMBELI, C. H., CUNHA, F. Q. & FERREIRA, S. H. 2001. The major role of peripheral release of histamine and 5-hydroxytryptamine in formalin-induced nociception. *Neuroscience,* 102**,** 937-44.

PARK, H. J., LEE, Y., LEE, J., PARK, C. & MOON, D. E. 2006. The effects of botulinum toxin A on mechanical and cold allodynia in a rat model of neuropathic pain. *Can J Anaesth,* 53**,** 470-7.

PARK, J. & PARK, H. J. 2017. Botulinum Toxin for the Treatment of Neuropathic Pain. *Toxins (Basel),* 9.

PARSA, A. A., LYE, K. D. & PARSA, F. D. 2007. Reconstituted botulinum type A neurotoxin: clinical efficacy after long-term freezing before use. *Aesthetic Plast Surg,* 31**,** 188-91; discussion 192-3.

PAVONE, F. & LUVISETTO, S. 2010. Botulinum neurotoxin for pain management: insights from animal models. *Toxins (Basel),* 2**,** 2890-913.

PAVONE, F. & UEDA, H. 2014. Is BoNT/B useful for pain treatment? *Pain,* 155**,** 649-50.

PHARMACEUTICALS, M. 2011. XEOMIN (incobotulinumtoxinA) [package insert], Merz pharmaceuticals LLC, U.S.A, A subsidiary of: Merz Pharma GmbH & Co KGaA.

PINHO-RIBEIRO, F. A., VERRI, W. A., JR. & CHIU, I. M. 2017. Nociceptor Sensory Neuron-Immune Interactions in Pain and Inflammation. *Trends Immunol,* 38**,** 5-19.

PIRAZZINI, M., AZARNIA TEHRAN, D., LEKA, O., ZANETTI, G., ROSSETTO, O. & MONTECUCCO, C. 2016. On the translocation of botulinum and tetanus neurotoxins across the membrane of acidic intracellular compartments. *Biochim Biophys Acta,* 1858**,** 467-74.

PIRAZZINI, M., ROSSETTO, O., ELEOPRA, R. & MONTECUCCO, C. 2017. Botulinum Neurotoxins: Biology, Pharmacology, and Toxicology. *Pharmacol Rev,* 69**,** 200-235.

POZEK, J. P., BEAUSANG, D., BARATTA, J. L. & VISCUSI, E. R. 2016. The Acute to Chronic Pain Transition: Can Chronic Pain Be Prevented? *Med Clin North Am,* 100**,** 17-30.

PURVES, D. 2004. *Neuroscience,* Sunderland, Massachusetts U.S.A., Sinauer Associates, Inc.

RAFTERY, M. N., RYAN, P., NORMAND, C., MURPHY, A. W., DE LA HARPE, D. & MCGUIRE, B. E. 2012. The economic cost of chronic noncancer pain in Ireland: results from the PRIME study, part 2. *J Pain,* 13**,** 139-45.

RAGHAVENDRA, V., TANGA, F. Y. & DELEO, J. A. 2004. Complete Freunds adjuvant-induced peripheral inflammation evokes glial activation and proinflammatory cytokine expression in the CNS. *Eur J Neurosci,* 20**,** 467-73.

RAOOF, R., WILLEMEN, H. & EIJKELKAMP, N. 2018. Divergent roles of immune cells and their mediators in pain. *Rheumatology (Oxford),* 57**,** 429-440.

RAYMOND, J. R., MUKHIN, Y. V., GELASCO, A., TURNER, J., COLLINSWORTH, G., GETTYS, T. W., GREWAL, J. S. & GARNOVSKAYA, M. N. 2001. Multiplicity of mechanisms of serotonin receptor signal transduction. *Pharmacol Ther,* 92**,** 179-212.

RIBEIRO-DA-SILVA, A. 1995. Ultrastructural features of the colocalization of calcitonin gene related peptide with substance P or somatostatin in the dorsal horn of the spinal cord. *Can J Physiol Pharmacol,* 73**,** 940-4.
RICHARDSON, J. D., AANONSEN, L. & HARGREAVES, K. M. 1997. SR 141716A, a cannabinoid receptor antagonist, produces hyperalgesia in untreated mice. *Eur J Pharmacol,* 319**,** R3-4.
RICHARDSON, J. D. & VASKO, M. R. 2002. Cellular mechanisms of neurogenic inflammation. *J Pharmacol Exp Ther,* 302**,** 839-45.
RIZO, J. 2018. Mechanism of neurotransmitter release coming into focus. *Protein Sci,* 27**,** 1364-1391.
RNCEUS.COM. *Nociceptive pain* [Online]. Available: http://www.rnceus.com/ages/nociceptive.htm [Accessed 24/06/2018 2018].
ROHACS, T., THYAGARAJAN, B. & LUKACS, V. 2008. Phospholipase C mediated modulation of TRPV1 channels. *Mol Neurobiol,* 37**,** 153-63.
ROMERO-SANDOVAL, E. A., HORVATH, R. J. & DELEO, J. A. 2008. Neuroimmune interactions and pain: focus on glial-modulating targets. *Curr Opin Investig Drugs,* 9**,** 726-34.
ROSSETTO, O., PIRAZZINI, M. & MONTECUCCO, C. 2014. Botulinum neurotoxins: genetic, structural and mechanistic insights. *Nat Rev Microbiol,* 12**,** 535-49.
SADZOT-DELVAUX, C., MERVILLE-LOUIS, M. P., DELREE, P., MARC, P., PIETTE, J., MOONEN, G. & RENTIER, B. 1990. An in vivo model of varicella-zoster virus latent infection of dorsal root ganglia. *J Neurosci Res,* 26**,** 83-9.
SAMAD, T. A., MOORE, K. A., SAPIRSTEIN, A., BILLET, S., ALLCHORNE, A., POOLE, S., BONVENTRE, J. V. & WOOLF, C. J. 2001. Interleukin-1beta-mediated induction of Cox-2 in the CNS contributes to inflammatory pain hypersensitivity. *Nature,* 410**,** 471-5.
SANDRINI, G., DE ICCO, R., TASSORELLI, C., SMANIA, N. & TAMBURIN, S. 2017. Botulinum neurotoxin type A for the treatment of pain: not just in migraine and trigeminal neuralgia. *J Headache Pain,* 18**,** 38.
SARAVANAN, P., RAJASEGER, G., ERIC, Y. P.-H. & MOOCHHALA, S. 2015. Botulinum Toxin: Present Knowledge and Threats. *In:* GOPALAKRISHNAKONE, P., BALALI-MOOD, M., LLEWELLYN, L. & SINGH, B. R. (eds.) *Biological Toxins and Bioterrorism.* Dordrecht: Springer Netherlands, 29-42.
SAUER, S. K., BOVE, G. M., AVERBECK, B. & REEH, P. W. 1999. Rat peripheral nerve components release calcitonin gene-related peptide and prostaglandin E2 in response to noxious stimuli: evidence that nervi nervorum are nociceptors. *Neuroscience,* 92**,** 319-25.
SCHAFERS, M., LEE, D. H., BRORS, D., YAKSH, T. L. & SORKIN, L. S. 2003. Increased sensitivity of injured and adjacent uninjured rat primary sensory neurons to exogenous tumor necrosis factor-alpha after spinal nerve ligation. *J Neurosci,* 23**,** 3028-38.
SCHAIBLE, H. G. 2007. Peripheral and central mechanisms of pain generation. *Handb Exp Pharmacol.* Springer-Verlag Berlin Heidelberg, 177, 3-28.
SCHNITZER, T. J. 2006. Update on guidelines for the treatment of chronic musculoskeletal pain. *Clin Rheumatol,* 25 Suppl 1**,** S22-9.
SHINOHARA, K., WATABE, A. M., NAGASE, M., OKUTSU, Y., TAKAHASHI, Y., KURIHARA, H. & KATO, F. 2017. Essential role of endogenous calcitonin gene-related peptide in pain-associated plasticity in the central amygdala. *Eur J Neurosci,* 46**,** 2149-2160.
SHORTLAND, P., KINMAN, E. & MOLANDER, C. 1997. Sprouting of A-fibre primary afferents into lamina II in two rat models of neuropathic pain. *Eur J Pain,* 1**,** 215-27.
SILBERSTEIN, S., MATHEW, N., SAPER, J. & JENKINS, S. 2000. Botulinum toxin type A as a migraine preventive treatment. For the BOTOX Migraine Clinical Research Group. *Headache,* 40**,** 445-50.
SILBERSTEIN, S. D., DODICK, D. W., AURORA, S. K., DIENER, H. C., DEGRYSE, R. E., LIPTON, R. B. & TURKEL, C. C. 2015. Per cent of patients with chronic migraine who responded per onabotulinumtoxinA treatment cycle: PREEMPT. *J Neurol Neurosurg Psychiatry,* 86**,** 996-1001.

SINGH, J. A., MAHOWALD, M. L., KUSHNARYOV, A., GOELZ, E. & DYKSTRA, D. 2009. Repeat injections of intra-articular botulinum toxin a for the treatment of chronic arthritis joint pain. *J Clin Rheumatol,* 15**,** 35-8.

SIVILOTTI, L. G., THOMPSON, S. W. & WOOLF, C. J. 1993. Rate of rise of the cumulative depolarization evoked by repetitive stimulation of small-caliber afferents is a predictor of action potential windup in rat spinal neurons in vitro. *J Neurophysiol,* 69**,** 1621-31.

SLUKA, K. A., KALRA, A. & MOORE, S. A. 2001. Unilateral intramuscular injections of acidic saline produce a bilateral, long-lasting hyperalgesia. *Muscle Nerve,* 24**,** 37-46.

SOLSTICE NEUROSCIENCES, I. 2009. Myobloc® (rimabotulinumtoxinB) Injection [package insert], Solstice Neurosciences, Inc., South San Francisco, CA 94080

STAAF, S., OERTHER, S., LUCAS, G., MATTSSON, J. P. & ERNFORS, P. 2009. Differential regulation of TRP channels in a rat model of neuropathic pain. *Pain,* 144**,** 187-99.

STATON, P. C., WILSON, A. W., BOUNTRA, C., CHESSELL, I. P. & DAY, N. C. 2007. Changes in dorsal root ganglion CGRP expression in a chronic inflammatory model of the rat knee joint: differential modulation by rofecoxib and paracetamol. *Eur J Pain,* 11**,** 283-9.

STEIN, C., CLARK, J. D., OH, U., VASKO, M. R., WILCOX, G. L., OVERLAND, A. C., VANDERAH, T. W. & SPENCER, R. H. 2009. Peripheral mechanisms of pain and analgesia. *Brain Res Rev,* 60**,** 90-113.

SUGIUAR, T., BIELEFELDT, K. & GEBHART, G. F. 2004. TRPV1 function in mouse colon sensory neurons is enhanced by metabotropic 5-hydroxytryptamine receptor activation. *J Neurosci,* 24**,** 9521-30.

SUGIURA, S., LAHAV, R., HAN, J., KOU, S. Y., BANNER, L. R., DE PABLO, F. & PATTERSON, P. H. 2000. Leukaemia inhibitory factor is required for normal inflammatory responses to injury in the peripheral and central nervous systems in vivo and is chemotactic for macrophages in vitro. *Eur J Neurosci,* 12**,** 457-66.

SUN, R. Q., TU, Y. J., LAWAND, N. B., YAN, J. Y., LIN, Q. & WILLIS, W. D. 2004. Calcitonin gene-related peptide receptor activation produces PKA- and PKC-dependent mechanical hyperalgesia and central sensitization. *J Neurophysiol,* 92**,** 2859-66.

SUPOWIT, S. C., ZHAO, H., KATKI, K. A., GUPTA, P. & DIPETTE, D. J. 2011. Bradykinin and prostaglandin E(1) regulate calcitonin gene-related peptide expression in cultured rat sensory neurons. *Regul Pept,* 167**,** 105-11.

SVARD, H. 2016. *HOW TO USE CATWALK XT AND INCAPACITANCE TESTER IN NON-CLINICAL PAIN RESEARCH* [Online]. Available: https://www.noldus.com/blog/how-use-catwalk-xt-and-incapacitance-tester-non-clinical-pain-research [Accessed 03/12/2018.

SVENSSON, C. I., MARSALA, M., WESTERLUND, A., CALCUTT, N. A., CAMPANA, W. M., FRESHWATER, J. D., CATALANO, R., FENG, Y., PROTTER, A. A., SCOTT, B. & YAKSH, T. L. 2003. Activation of p38 mitogen-activated protein kinase in spinal microglia is a critical link in inflammation-induced spinal pain processing. *J Neurochem,* 86**,** 1534-44.

TARSY, D. & FIRST, E. R. 1999. Painful cervical dystonia: clinical features and response to treatment with botulinum toxin. *Mov Disord,* 14**,** 1043-5.

THOMPSON, S. W., KING, A. E. & WOOLF, C. J. 1990. Activity-Dependent Changes in Rat Ventral Horn Neurons in vitro; Summation of Prolonged Afferent Evoked Postsynaptic Depolarizations Produce a d-2-Amino-5-Phosphonovaleric Acid Sensitive Windup. *Eur J Neurosci,* 2**,** 638-49.

TIFFANY, C. W. & BURCH, R. M. 1989. Bradykinin stimulates tumor necrosis factor and interleukin-1 release from macrophages. *FEBS Lett,* 247**,** 189-92.

TODD, A. J. 2010. Neuronal circuitry for pain processing in the dorsal horn. *Nat Rev Neurosci,* 11**,** 823-36.

TOKUNAGA, A., SAIKA, M. & SENBA, E. 1998. 5-HT2A receptor subtype is involved in the thermal hyperalgesic mechanism of serotonin in the periphery. *Pain,* 76**,** 349-55.

TOLEDO-ARAL, J. J., MOSS, B. L., HE, Z. J., KOSZOWSKI, A. G., WHISENAND, T., LEVINSON, S. R., WOLF, J. J., SILOS-SANTIAGO, I., HALEGOUA, S. & MANDEL, G. 1997. Identification of PN1,

a predominant voltage-dependent sodium channel expressed principally in peripheral neurons. *Proc Natl Acad Sci U S A,* 94**,** 1527-32.

TOMINAGA, M., CATERINA, M. J., MALMBERG, A. B., ROSEN, T. A., GILBERT, H., SKINNER, K., RAUMANN, B. E., BASBAUM, A. I. & JULIUS, D. 1998. The cloned capsaicin receptor integrates multiple pain-producing stimuli. *Neuron,* 21**,** 531-43.

TOMINAGA, M., WADA, M. & MASU, M. 2001. Potentiation of capsaicin receptor activity by metabotropic ATP receptors as a possible mechanism for ATP-evoked pain and hyperalgesia. *Proc Natl Acad Sci U S A,* 98**,** 6951-6.

TONTODONATI, M., URSINI, T., POLILLI, E., VADINI, F., DI MASI, F., VOLPONE, D. & PARRUTI, G. 2012. Post-herpetic neuralgia. *Int J Gen Med,* 5**,** 861-71.

TREEDE, R. D., RIEF, W., BARKE, A., AZIZ, Q., BENNETT, M. I., BENOLIEL, R., COHEN, M., EVERS, S., FINNERUP, N. B., FIRST, M. B., GIAMBERARDINO, M. A., KAASA, S., KOSEK, E., LAVAND'HOMME, P., NICHOLAS, M., PERROT, S., SCHOLZ, J., SCHUG, S., SMITH, B. H., SVENSSON, P., VLAEYEN, J. W. & WANG, S. J. 2015. A classification of chronic pain for ICD-11. *Pain,* 156**,** 1003-7.

VARRASSI, G., MULLER-SCHWEFE, G., PERGOLIZZI, J., ORONSKA, A., MORLION, B., MAVROCORDATOS, P., MARGARIT, C., MANGAS, C., JAKSCH, W., HUYGEN, F., COLLETT, B., BERTI, M., ALDINGTON, D. & AHLBECK, K. 2010. Pharmacological treatment of chronic pain - the need for CHANGE. *Curr Med Res Opin,* 26**,** 1231-45.

VASKO, M. R., CAMPBELL, W. B. & WAITE, K. J. 1994. Prostaglandin E2 enhances bradykinin-stimulated release of neuropeptides from rat sensory neurons in culture. *J Neurosci,* 14**,** 4987-97.

VASO, A., ADAHAN, H. M., GJIKA, A., ZAHAJ, S., ZHURDA, T., VYSHKA, G. & DEVOR, M. 2014. Peripheral nervous system origin of phantom limb pain. *Pain,* 155**,** 1384-91.

VELNAR, T., BAILEY, T. & SMRKOLJ, V. 2009. The wound healing process: an overview of the cellular and molecular mechanisms. *J Int Med Res,* 37**,** 1528-42.

WALL, P. D., SCADDING, J. W. & TOMKIEWICZ, M. M. 1979. The production and prevention of experimental anesthesia dolorosa. *Pain,* 6**,** 175-82.

WANG, H., EHNERT, C., BRENNER, G. J. & WOOLF, C. J. 2006. Bradykinin and peripheral sensitization. *Biol Chem,* 387**,** 11-4.

WANG, J., CASALS-DIAZ, L., ZURAWSKI, T., MENG, J., MORIARTY, O., NEALON, J., EDUPUGANTI, O. P. & DOLLY, O. 2017a. A novel therapeutic with two SNAP-25 inactivating proteases shows long-lasting anti-hyperalgesic activity in a rat model of neuropathic pain. *Neuropharmacology,* 118**,** 223-232.

WANG, J., MENG, J., LAWRENCE, G. W., ZURAWSKI, T. H., SASSE, A., BODEKER, M. O., GILMORE, M. A., FERNANDEZ-SALAS, E., FRANCIS, J., STEWARD, L. E., AOKI, K. R. & DOLLY, J. O. 2008. Novel chimeras of botulinum neurotoxins A and E unveil contributions from the binding, translocation, and protease domains to their functional characteristics. *J Biol Chem,* 283**,** 16993-7002.

WANG, J., MENG, J., NUGENT, M., TANG, M. & DOLLY, J. O. 2017b. Neuronal entry and high neurotoxicity of botulinum neurotoxin A require its N-terminal binding sub-domain. *Sci Rep,* 7**,** 44474.

WANG, J., ZURAWSKI, T. H., MENG, J., LAWRENCE, G., OLANGO, W. M., FINN, D. P., WHEELER, L. & DOLLY, J. O. 2011a. A dileucine in the protease of botulinum toxin A underlies its long-lived neuroparalysis: transfer of longevity to a novel potential therapeutic. *J Biol Chem,* 286**,** 6375-85.

WANG, J., ZURAWSKI, T. H., MENG, J., LAWRENCE, G. W., AOKI, K. R., WHEELER, L. & DOLLY, J. O. 2012. Novel chimeras of botulinum and tetanus neurotoxins yield insights into their distinct sites of neuroparalysis. *FASEB J,* 26**,** 5035-48.

WANG, L., WANG, K., CHU, X., LI, T., SHEN, N., FAN, C., NIU, Z., ZHANG, X. & HU, L. 2017c. Intra-articular injection of Botulinum toxin A reduces neurogenic inflammation in CFA-induced arthritic rat model. *Toxicon,* 126**,** 70-78.

WANG, W., GU, J., LI, Y. Q. & TAO, Y. X. 2011b. Are voltage-gated sodium channels on the dorsal root ganglion involved in the development of neuropathic pain? *Mol Pain,* 7**,** 16.
WATKINS, L. R. & MAIER, S. F. 2002. Beyond neurons: evidence that immune and glial cells contribute to pathological pain states. *Physiol Rev,* 82**,** 981-1011.
WELCH, M. J., PURKISS, J. R. & FOSTER, K. A. 2000. Sensitivity of embryonic rat dorsal root ganglia neurons to *Clostridium botulinum* neurotoxins. *Toxicon,* 38**,** 245-58.
WHO 1996. *Cancer pain relief : with a guide to opioid availability,* Geneva, World Health Organization.
WILSON, A. W., MEDHURST, S. J., DIXON, C. I., BONTOFT, N. C., WINYARD, L. A., BRACKENBOROUGH, K. T., DE ALBA, J., CLARKE, C. J., GUNTHORPE, M. J., HICKS, G. A., BOUNTRA, C., MCQUEEN, D. S. & CHESSELL, I. P. 2006. An animal model of chronic inflammatory pain: pharmacological and temporal differentiation from acute models. *Eur J Pain,* 10**,** 537-49.
WOHLFARTH, K., GOSCHEL, H., FREVERT, J., DENGLER, R. & BIGALKE, H. 1997. Botulinum A toxins: units versus units. *Naunyn Schmiedebergs Arch Pharmacol,* 355**,** 335-40.
WONG, G. Y. & GAVVA, N. R. 2009. Therapeutic potential of vanilloid receptor TRPV1 agonists and antagonists as analgesics: Recent advances and setbacks. *Brain Res Rev,* 60**,** 267-77.
WOOLF, C. J. & MANNION, R. J. 1999. Neuropathic pain: aetiology, symptoms, mechanisms, and management. *Lancet,* 353**,** 1959-64.
WOOLF, C. J., SHORTLAND, P. & COGGESHALL, R. E. 1992. Peripheral nerve injury triggers central sprouting of myelinated afferents. *Nature,* 355**,** 75-8.
WOOLF, C. J. & THOMPSON, S. W. 1991. The induction and maintenance of central sensitization is dependent on N-methyl-D-aspartic acid receptor activation; implications for the treatment of post-injury pain hypersensitivity states. *Pain,* 44**,** 293-9.
WU, G., RINGKAMP, M., MURINSON, B. B., POGATZKI, E. M., HARTKE, T. V., WEERAHANDI, H. M., CAMPBELL, J. N., GRIFFIN, J. W. & MEYER, R. A. 2002. Degeneration of myelinated efferent fibers induces spontaneous activity in uninjured C-fiber afferents. *J Neurosci,* 22**,** 7746-53.
XIAO, L., MACKEY, S., HUI, H., XONG, D., ZHANG, Q. & ZHANG, D. 2010. Subcutaneous injection of botulinum toxin a is beneficial in postherpetic neuralgia. *Pain Med,* 11**,** 1827-33.
YAMAMOTO, S., OHSAWA, M. & ONO, H. 2013. Contribution of TRPV1 receptor-expressing fibers to spinal ventral root after-discharges and mechanical hyperalgesia in a spared nerve injury (SNI) rat model. *J Pharmacol Sci,* 121**,** 9-16.
YOO, K. Y., LEE, H. S., CHO, Y. K., LIM, Y. S., KIM, Y. S., KOO, J. H., YOON, S. J., LEE, J. H., JANG, K. H. & SONG, S. H. 2014. Anti-inflammatory effects of botulinum toxin type a in a complete Freund's adjuvant-induced arthritic knee joint of hind leg on rat model. *Neurotox Res,* 26**,** 32-9.
YUAN, R. Y., SHEU, J. J., YU, J. M., CHEN, W. T., TSENG, I. J., CHANG, H. H. & HU, C. J. 2009. Botulinum toxin for diabetic neuropathic pain: a randomized double-blind crossover trial. *Neurology,* 72**,** 1473-8.
ZHANG, G. H., LV, M. M., WANG, S., CHEN, L., QIAN, N. S., TANG, Y., ZHANG, X. D., REN, P. C., GAO, C. J., SUN, X. D. & XU, L. X. 2011a. Spinal astrocytic activation is involved in a virally-induced rat model of neuropathic pain. *PLoS One,* 6**,** e23059.
ZHANG, J. M. & AN, J. 2007. Cytokines, inflammation, and pain. *Int Anesthesiol Clin,* 45**,** 27-37.
ZHANG, T., ADATIA, A., ZARIN, W., MOITRI, M., VIJENTHIRA, A., CHU, R., THABANE, L. & KEAN, W. 2011b. The efficacy of botulinum toxin type A in managing chronic musculoskeletal pain: a systematic review and meta analysis. *Inflammopharmacology,* 19**,** 21-34.
ZHANG, X., BAO, L., ARVIDSSON, U., ELDE, R. & HOKFELT, T. 1998. Localization and regulation of the delta-opioid receptor in dorsal root ganglia and spinal cord of the rat and monkey: evidence for association with the membrane of large dense-core vesicles. *Neuroscience,* 82**,** 1225-42.
ZHANG, X., HUANG, J. & MCNAUGHTON, P. A. 2005. NGF rapidly increases membrane expression of TRPV1 heat-gated ion channels. *EMBO J,* 24**,** 4211-23.

Appendix

	BONT/A	LC/E-BOTIM/A	LAB SAMPLE LC/E-BONT/A	BATCH 1 LC/E-BONT/A	BATCH 2 LC/E-BONT/A (TP.001)
EXPRESSION	Shaker culture, auto-induction	Shaker culture, auto-induction	Shaker culture, auto-induction	Bioreactor, auto-induction	Bioreactor, IPTG induction
HARVESTING CELLS FROM CULTURE	Centrifugation of *E. coli* expressing BoNT	Centrifugation of *E. coli* expressing BoNT	Centrifugation of *E. coli* expressing BoNT	Tangential flow filtration of *E. coli* expressing BoNT	Tangential flow filtration of *E. coli* expressing BoNT
CELL LYSIS AND HARVESTING OF BONTS	Cell pellet from culture incubated in lysozyme, protease inhibitor cocktail and benzonase [1]	Cell pellet from culture incubated in lysozyme, protease inhibitor cocktail and benzonase [1]	Cell pellet from culture incubated in lysozyme, protease inhibitor cocktail and benzonase [1]	Cell lysis by high pressure homogenisation	Cell lysis by high pressure homogenisation
	Centrifugation to remove insoluble particles	Centrifugation to remove insoluble particles	Centrifugation to remove insoluble particles	Tangential flow filtration to remove insoluble particles	Centrifugation to remove insoluble particles
				Filtering to reduce host cells	Filtering to reduce host cells
TOXIN PURIFICATION	IMAC purification	IMAC purification	IMAC purification	IMAC purification	IMAC purification
	Gel filtration	Gel filtration	Gel filtration	Gel filtration	Gel filtration
	Anion-exchange chromatography	Cation-exchange chromatography	Cation-exchange chromatography	Cation-exchange chromatography	Cation-exchange chromatography
	Gel filtration	Gel filtration	Gel filtration	Gel filtration	
	Thrombin incubation [2]	Thrombin incubation [3]	Thrombin incubation [3]	Thrombin incubation [3]	Thrombin incubation [4]
	Halt reaction with 1 mM final concentration of PMSF	Halt reaction with 1 mM final concentration of PMSF	Halt reaction with 1 mM final concentration of PMSF	Freeze bulk purified toxin at -80 °C	2nd Cation-exchange chromatography
	Freeze bulk purified toxin -80 °C	Freeze bulk purified toxin -80 °C	Freeze bulk purified toxin at -80 °C	**End**	Freeze bulk purified toxin at -80 °C
	End	**End**	**End**		Thaw, dilute sample and add excipients (HSA)
					Freeze bulk concentrated lot -80 °C
					End

Table 4.1 - BoNT production batch differences: 1 - Lysozyme (2 mg/ml), protease inhibitor cocktail (1:200 v/v) and benzonase (1500 units), 2 - Thrombin 1U/mg toxin at 22 °C for 1 hours, 3 - Thrombin 1U/mg toxin at 22 °C for 3 hours, 4 – Thrombin 4U/mg toxin at 22 °C for 4 hours, then at 8 °C for 20 hours, pH 6.